

Shun Hing Institute of
Advanced Engineering
信興高等工程研究所



Report and Research Highlights
2014 - 2015

June 2015

香 港 中 文 大 學
The Chinese University of Hong Kong



蒙民偉工程學大樓

William M. W. Mong
Engineering Building

Printed in July 2015, this report contains information known as June 2015.

Every effort has been made to ensure that the information contained in this report is correct at the time of printing. Shun Hing Institute of Advanced Engineering (SHIAE) – CUHK, reserves the right to make appropriate changes to the materials presented in this report without prior notice.

For further information, please visit our website: <http://www.shiae.cuhk.edu.hk>

Contents

信興高等工程研究所
Shun Hing Institute of Advanced Engineering

INTRODUCTION OF SHIAE	4
ORGANIZATION	6
COMPOSITION OF INTERNATIONAL ADVISORY BOARD	7
COMPOSITION OF MANAGEMENT COMMITTEE	9
SHUN HING VISITING SCHOLARS/ FELLOWS	10
FINANCIAL STATUS OF SHIAE	11
RESEARCH	13
<i>OUTSTANDING RESEARCH HIGHLIGHTS</i>	13
<i>ACADEMIC PUBLICATIONS</i>	13
<i>RENEWABLE ENERGY TRACK</i>	14
<i>Research Reports</i>	14
<i>BIOMEDICAL ENGINEERING TRACK</i>	39
<i>Research Reports</i>	39
<i>MULTIMEDIA TECHNOLOGIES TRACK</i>	73
<i>Research Reports</i>	73
SHUN HING DISTINGUISHED LECTURE SERIES	81

Introduction of SHIAE

Mission of SHIAE

The MISSION of the Institute is to spearhead, conduct, promote and co-ordinate research in advanced engineering. There is no end to the list of areas to be explored and the plan is to give priority to research topics that are both exciting and innovative. The Institute also aspires to transferring its research results to industry for practical application and to put across to the community at large the role of engineering as a driving force for human development through educational activities.

As a pioneering institute exploring the forefront of the engineering science, The Shun Hing Institute of Advanced Engineering will

- spearhead state-of-the-art advanced engineering research
- create and sustain synergy with world-class researchers
- develop with and transfer to industries cutting edge technologies
- promote appreciation of engineering in society through educational programmes

The Shun Hing Education and Charity Fund was founded by Dr. William Mong Man Wai with the aim of enhancing educational opportunities for the younger generations. The Fund has already sponsored numerous educational and research programmes in Hong Kong, the Mainland, and overseas educational institutions. Himself an engineer and a firm believer in advancing the quality of life through the development of science and technology, Dr. Mong had been there to support the establishment and growth of this Institute from the beginning.

Centre of Excellence at CUHK

The Chinese University of Hong Kong is an internationally renowned institution of higher learning devoted to quality teaching and both academic and applied research. The University has established 29 research institutes and a number of research centres with a view to pursuing up-front research endeavours with focused goals and objectives. The Shun Hing Institute of Advanced Engineering plays a crucial part in the research infrastructure of the Chinese University which is committed to exciting research programmes in advanced engineering areas.

As a strategic centre of excellence at The Chinese University of Hong Kong, the Institute supports greater regional and international research collaborations, and strives to attract talent from the world over to achieve greater internationalization, a vision strongly advocated by every member of the University.

Commitment of the Faculty of Engineering

The Faculty of Engineering was founded in 1991 and was built upon existing strengths with added talent from all over the world. The Faculty has been able to attract some of the best minds. Many received their training in leading universities in North America, Great Britain and Australia. Most of them have extensive experience in industry and many are leaders in their fields. This team of top-notch talent is gathered to nurture local talent through educational programmes, and break new frontiers in research through innovative and exciting research endeavours.

The positioning of The Shun Hing Institute of Advanced Engineering in the William M.W. Mong Engineering Building is deliberate as a key nucleating point to integrate research endeavours in the Engineering Faculty and its neighbours. Our members join hands with their counterparts from the Faculties of Science and Medicine in many interesting research collaborations. It is the ambitious goal of the Faculty of Engineering that the Institute should become a lighthouse for the local technology landscape to herald the migration towards high value-added technology and an information economy.

The mission of the Institute is to spearhead, conduct, promote and co-ordinate research in advanced engineering. There is no end to the list of areas to be explored and the plan is to give priority to research topics that are both exciting and innovative. The Institute also aspires to transferring its research results to industry for practical application and to put across to the community at large the role of engineering as a driving force for human development through educational activities.

Building on Strength and The Way Ahead

Many of the Institute's research projects are built upon areas in which the Faculty has already achieved outstanding performance. These are areas that have great potential for further technological advancement and in line with industrial development in Hong Kong. The Institute provides a vibrant R&D environment to spur new discoveries and speed up their translation into applications. Since 2012, we have expanded our scope to cover new frontiers in Renewable Energy striving to answer tomorrow's energy challenges.

Technology Transfer

Synergy with industry is the ultimate goal of research and development in Hong Kong. External experts have been brought in to the Institute to lead research projects that could benefit the industrial sector.

The technology transfer arm of the Faculty of Engineering plays an important role in the traffic between the Institute and industry. The Institute houses an array of top-notch research and development activities encompassing contract research, spin-off companies, and consultancies.

Contribution to Society

The Institute has been making contributions to the progress of Hong Kong through a wide range of educational activities like training courses, seminars, symposiums which disseminate the latest technologies to promote appreciation of engineering in society and arouse interest of the younger generations in engineering.

Organization of SHIAE

International Advisory Board

SHIAE Management Committee

**Multimedia
Technologies
Research
(MMT)**

– since 2005 –

**Biomedical
Engineering
Research
(BME)**

– since 2005 –

**Renewable
Energy
Research
(RNE)**

– since 2012 –

We also provide support and sponsorship to the Faculty of Engineering in organizing prestigious academic conference in Hong Kong so as to raise our international profile.

Composition of International Advisory Board

Chairman:

Mr. David T.Y. MONG 蒙德揚先生

*Chairman and Group CEO
Shun Hing Group
Hong Kong*



Members:

Professor Victor ZUE

*Delta Electronics Professor of Electrical Engineering and Computer
Science
Massachusetts Institute of Technology,
U.S.A*



Dr. Harry SHUM 沈向洋博士

*Executive Vice President, Technology and Research
Microsoft Corporation,
U.S.A.*



Professor Yongmin KIM

*President
POSTECH-Pohang University of Science and Technology,
South Korea*



Professor Chih-Ming HO 何志明教授

*Ben Rich-Lockheed Martin Professor in School of Engineering
University of California, Los Angeles,
U.S.A.*



Professor C.C. Jay KUO

*Professor of Electrical Engineering and Computer Science
University of Southern California,
U.S.A.*



Professor Tai Fai FOK 霍泰輝教授

*Pro-Vice-Chancellor
The Chinese University of Hong Kong
Hong Kong*



Professor Wing-shing WONG 黃永成教授

*Choh-Ming Li Professor of Information Engineering
The Chinese University of Hong Kong
Hong Kong*



Professor Ching Ping WONG 汪正平教授

*Dean of Engineering
The Chinese University of Hong Kong
Hong Kong*



Professor Pak Chung CHING 程伯中教授

*Director of Shun Hing Institute of Advanced Engineering
Choh-Ming Li Professor of Electronic Engineering
The Chinese University of Hong Kong
Hong Kong*



Composition of Management Committee

Director:

Professor Pak Chung CHING

Choh-Ming Li Professor of Electronic Engineering

Secretary:

Professor John C.S. LUI

Choh-Ming Li Professor of Computer Science and Engineering

Members:

Professor Ching Ping WONG (*ex-officio*)

Dean of Faculty of Engineering

Mr. Terrence CHAN

*Managing Director of Shun Hing Technology Co., Ltd
Hong Kong*

Professor Kwong-sak LEUNG

Department of Computer Science and Engineering

Professor Dennis Y.M. LO

*Associate Dean (Research) of Faculty of Medicine
Department of Chemical Pathology*

Professor Helen M.L. MENG

Chairman, Department of Systems Engineering & Engineering Management

Professor Max Qing Hu MENG

Department of Electronic Engineering

Professor Wei-Hsin LIAO

Department of Mechanical and Automation Engineering

Professor King-lap WONG

*Department of Mechanical and Automation Engineering
(till July 1, 2015)*

Professor Wing-shing WONG

Choh-Ming Li Professor of Information Engineering

Shun Hing Visiting Scholars/ Fellows

The Institute has launched a Shun Hing Distinguished Scholar Program with an aim to attract distinguished scholars to pursue research collaboration with our faculty and to strengthen our research profile. The following scholars visited to work either on a short term or on a longer term engagement with the Institute between 2014 and 2015.

Shun Hing Fellows and Research Associate:

(in alphabetical order)

Dr CHEN Zhong <i>The Sun Yat-sen University, China</i>	2014-2016
Dr LI Jinming <i>Nanyang Technological University, Singapore</i>	2014-2015
Dr LOU Yishan <i>The Chinese University of Hong Kong</i>	2014-2015
Dr SHANG Fanhua <i>The Chinese University of Hong Kong</i>	2015
Dr WALKER Steven L. <i>Johns Hopkins School of Medicine, Baltimore, USA</i>	2014-2015
Dr WEI Kongchang <i>The Chinese University of Hong Kong</i>	2014-2015

Financial Status of SHIAE

As at 30 June 2015
HK\$

INCOME

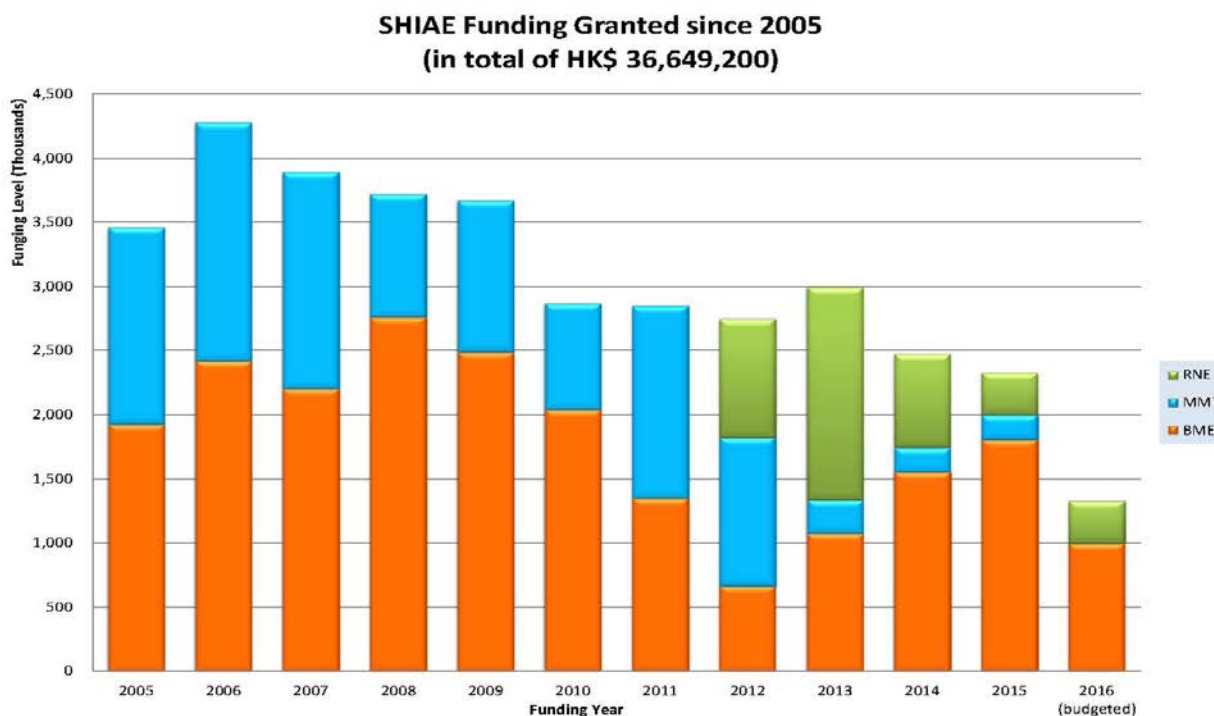
Start Up Seed Fund	34,500,000
Interest and investment income	6,762,903
Sub-total:	41,262,903

EXPENDITURE

Research funding granted since 2005-2015	(1)	35,321,200
Committed Research Budget in 2016	(2)	1,328,000
Unspent remaining fund from all completed projects		-2,963,360
Committed staff cost		658,271
Operating cost		3,678,332
Sub-total:		38,022,443

BALANCE as at 30 June 2015 **3,240,460**

(1) Annualized Research Funding to each research areas granted since 2005



This figure shows the distribution of the SHIAE funding granted to each track of research projects, namely Biomedical Engineering (BME), Multimedia Technology (MMT) and Renewable Energy (RNE) annually.

(2) Detail funding level on each batch of projects (in HK\$ '000)

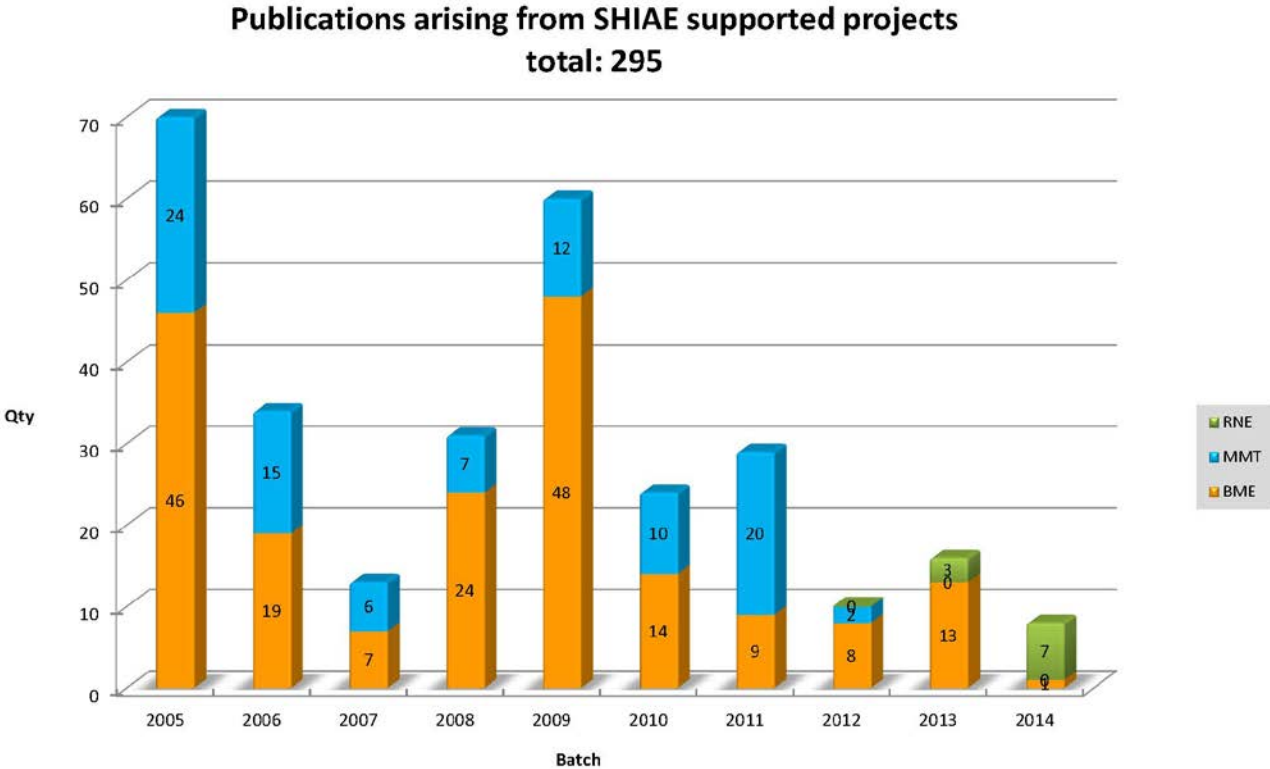
Funding Year/ No. of projects	<u>2016</u> <i>(budgeted)</i>	<u>2015</u>	<u>2014</u>	<u>2013</u>	<u>2012</u>	<u>2011</u>	<u>2010</u>	<u>2009</u>	<u>2008</u>	<u>2007</u>	<u>2006</u>	<u>2005</u>
Year 2005 Batch (6 Projects)	-	-	-	-	-	-	-	-	-	60	2,586	3,462
Year 2006 Batch (5 Projects)	-	-	-	-	-	-	-	-	-	1,480	1,695	-
Year 2007 Batch (7 Projects)	-	-	-	-	-	-	-	200	1,792	2,354	-	-
Year 2008 Batch (4 Projects)	-	-	-	-	-	-	-	1,848	1,928	-	-	-
Year 2009 Batch (5 Projects)	-	-	-	-	-	268	1,414	1,624	-	-	-	-
Year 2010 Batch (5 Projects)	-	-	-	-	-	1,334.6	1454.6	-	-	-	-	-
Year 2011 Batch (4 Projects)	-	-	-	-	1,228	1,248	-	-	-	-	-	-
Year 2012 Batch (5 Projects)	-	-	-	1,520	1,520	-	-	-	-	-	-	-
Year 2013 Batch (4 Projects)	-	-	1,474	1,474	-	-	-	-	-	-	-	-
Year 2014 Batch (3 Projects)	-	1,002	1,002	-	-	-	-	-	-	-	-	-
Year 2015 Batch (4 Projects)	1,328	1,328	-	-	-	-	-	-	-	-	-	-
WOSP2007 Workshop	-	-	-	-	-	-	-	-	-	25	-	-
Annualized total:	1,328	2,330	2,476	2,994	2,768	2,850.6	2,868.6	3,672	3,720	3,919	4,281	3,462
Accumulated Total	HK\$36,649.200											

This table shows the detail amount of SHIAE funding granted to each batch of research projects. The subtotal amount of 1.328 million budgeted for 2016 is committed to support research projects in July 2016.

Research - Outstanding Research Highlights

Academic Publications

So far 41 projects have been successfully completed and 295 articles arising from the results of these research projects have been published in international conference proceedings and journals. The other 11 on-going projects are also progressing well with encouraging results produced. All publications generated by each individual projects are kept in the archive of SHIAE office. The chart below shows the number of academic publications produced each year.



The list of publications can also be downloaded from the webpage of SHIAE at www.shiae.cuhk.edu.hk/research.htm

Renewable Energy Track

Research Reports In Renewable Energy

Newly Funded Projects

(2015-2017)

* Experimental and modeling study of biodiesel combustion

Continuing Projects

(2013-2015)

* Earth-Abundant Metal/Metal Oxide Nanostructures for Rechargeable Li-Air Batteries: Catalyst Design and Mechanistic Investigation

* Graphene-based asymmetric supercapacitors with high energy density for clean energy storage systems

Completed Projects

(2012-2014)

* Vibration Energy Harvesting Utilizing Multifunctional Phononic Meta-Materials and Structures

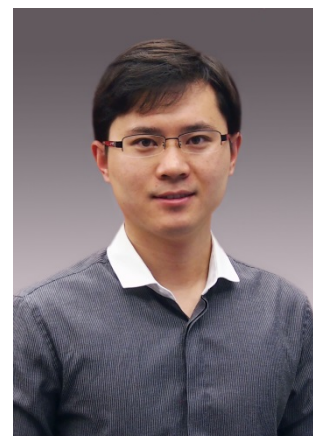
* Understanding Electron and Phonon Transport in Boron Carbide Nanowires for Thermoelectric Energy Conversion

* Ternary Hybrid Polymer/Nanocrystal Bulk Heterojunction Solar Cells with Cascade Energy-Level Alignment

EXPERIMENTAL AND MODELING STUDY OF BIODIESEL COMBUSTION

Principal Investigator: Professor Wei REN
Department of Mechanical & Automation Engineering
CUHK

Project Start Date: 1 July 2015



ABSTRACT

Liquid fossil fuels such as gasoline, diesel, and kerosene are the most popular choices for transportation. However, the burning of fossil fuels has led to serious environmental issues of air pollution and global warming. Biofuels offer an attractive alternative to fossil fuels and can contribute significantly to sustainable development in terms of economic and environmental concerns. Biodiesel, with its numerous desirable fuel properties, is among the best candidates to replace diesel fuel in engine systems. Considerable effort is currently being devoted to the development of quantitatively predictive mechanisms for biodiesel combustion, which are required by the design of new engines and fuel blends. However, the detailed biodiesel combustion chemistry is still far from completion. This research aims to understand the fundamental combustion kinetics of biodiesel surrogates and even real components. A novel aerosol shock tube is designed to allow measurements of the very-low-vapor-pressure biofuels. Ignition delay times, species time-histories, and elementary reaction rate constants will be measured to understand the chemical kinetics of three biodiesel surrogates and one particular biodiesel component, methyl oleate. The proposed study will result in new and valuable information to improve the existing understanding of biodiesel combustion.

PROJECT OBJECTIVES:

- To develop and test the new method of aerosol shock tube for studying combustion chemical kinetics of biofuels with very low vapor pressure.*** The necessity of gas-phase fuel loading in shock tubes is the most important limitation of conventional gas-phase shock tubes used for combustion research. However, the large fatty acid methyl esters (FAMES) composing biodiesel have so low vapor pressures (sub-Torr) that obtaining sufficient gas-phase fuel molecules in a shock tube is virtually impossible. We propose a novel design of Laval nozzle to be used in the CUHK shock tube to generate uniform fuel aerosol, making it suitable to study biodiesel combustion. This new design can be extended for studying chemical kinetics of all types of biofuels and even those of nanoparticle-laden combustion in the future.
- To investigate the influence of alkyl chain length and C=C bond on the combustion kinetics of methyl esters.*** Most of the previous biodiesel combustion research focused on the short-chain methyl esters containing <5 carbon atoms. Moreover, FAMES in biodiesel are mostly unsaturated containing C=C double bonds, while considerably less work has been reported on unsaturated methyl esters. We will systematically investigate the chemical kinetics of methyl esters with varied alkyl chain lengths and the existence of C=C bond in the molecular structure.

3. ***To measure the ignition delay times, species time-histories, and elementary reaction rate constants during the oxidation of methyl oleate.*** The biodiesel blends are usually composed of five FAMES with methyl oleate (MO, C₁₉H₃₆O₂) the largest constituent. The kinetic properties of MO is not yet well-understood, and especially no experimental data for MO currently exist in the literature. With the advanced aerosol shock tube/laser diagnostics technique, our research can provide such valuable shock tube data for the validation of reduced/detailed kinetic mechanisms for biodiesel fuels.

4. ***To understand and interpret the experimental data of methyl oleate pyrolysis and oxidation by detailed kinetic modeling.*** Detailed kinetic modeling using state-of-the-art quantum chemistry techniques will be performed to interpret the measured species time-history data during the pyrolysis and oxidation of methyl oleate. Meanwhile, individual reaction rate, the core parameter in the chemical kinetic model controlling the reaction pathways, can be directly measured by carefully selecting the reactive mixtures. Such reaction rates can be directly incorporated into kinetic mechanisms, yielding immediate improvements. These results assist further understanding of the mechanisms in terms of improving biofuel combustion efficiency and reducing emissions.

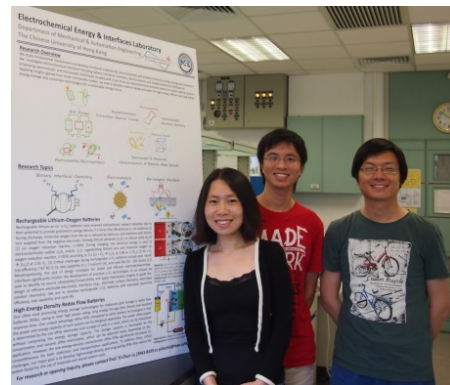
EARTH-ABUNDANT METAL/METAL OXIDE NANOSTRUCTURES FOR RECHARGEABLE LI-AIR BATTERIES: CATALYST DESIGN AND MECHANISTIC INVESTIGATION

Principal Investigator: Professor Yi-Chun LU
Department of Mechanical & Automation Engineering
 CUHK

Research Team Members: Yulin CAO, Research Assistant ⁽¹⁾,
 Zhuojian LIANG, Junior Research Assistant ⁽¹⁾

⁽¹⁾ Dept. of Mechanical and Automation Engineering, CUHK

Reporting Period: 01 August 2013 – 30 April 2014



ABSTRACT

Electrical storage technologies are of vital importance to enable effective utilization of intermittent renewable energy sources and the creation of sustainable electric transportation. Lithium-air (or Li-O₂) batteries have received extraordinary research attention owing to their potential to provide gravimetric energy density 3-5 times that of the conventional Li-ion batteries. However, the lack of fundamental understanding of the reaction mechanisms and materials design strategies has led to numerous critical challenges including poor round-trip efficiency, low rate capability, and poor cycle life. Here, we propose to develop earth-abundant metal/metal oxide nanostructures including nanoporous metal foams and mesoporous metal oxides as electrode materials to promote the rate capability, round-trip efficiency and cycle life of rechargeable Li-O₂ batteries. In addition, we will investigate the Li-O₂ interfacial chemistry and electrode reactivity via spectroscopic characterization techniques coupled with in situ and ex situ electrochemical characterizations. We seek to identify the source of instability/irreversibility and apply mechanistic insights to guide the design of efficient electrode-electrolyte interfaces (e.g., electrode surface chemistry, electrolyte solution chemistry). We intend to demonstrate rechargeable Li-O₂ batteries with improved round-trip efficiency, rate capability, and cycle life with minimum capacity loss.

1. OBJECTIVES AND SIGNIFICANCE

We aim to (1) develop earth-abundant nanostructured metal/metal oxide electrode materials to promote the rate capability and round-trip efficiency of rechargeable Li-O₂ batteries; (2) develop stable electrode-electrolyte interfaces to improve the cycle life of rechargeable Li-O₂ batteries; (3) unravel Li-O₂ reaction mechanisms, identify key processes that limit battery performance and develop design guidelines for stable and efficient electrode-electrolyte interfaces. These objectives will directly address the most critical challenges of rechargeable Li-O₂ batteries and are expected to enable transformative advances in rechargeable Li-air technology

2. RESEARCH METHODOLOGY

To improve the round-trip efficiency, rate capability and cycle life of rechargeable Li-O₂ batteries, we propose to (1) develop earth-abundant nanostructured metal/metal oxide electrode materials and (2) investigate Li-O₂ interfacial chemistry and identify battery degradation mechanism to guide the design of stable electrode-electrolyte interfaces. The overview of the proposed research plans is summarized in Fig.1.

2.1. Synthesis of nanostructured indium tin oxide/chromium oxide nano-composite

Indium tin oxide (ITO) is one of the most promising conducting oxides for electrochemical application and has been shown stable during Li-O₂ cycling environment by Li et al.¹ However, noble metal ruthenium (Ru)

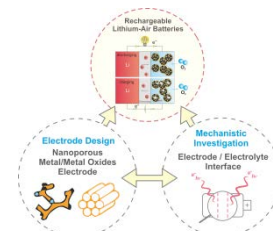


Fig.1. Overview of the research plans

was used in the work of Li et al.¹ as a catalyst to facilitate the Li-O₂ reactions due to the low catalytic activity of ITO. A recent work of the PI has revealed that chromium-containing oxide exhibit superior charging activity compared to carbon and exhibit similar catalytic activity as noble metals. Therefore, we here exploit chromium oxide (Cr₂O₃)/ITO nano-composite as cathode materials for rechargeable Li-O₂ batteries. Here we use a surfactant assisting method followed by a low-temperature heat treatment. 50 mg ITO is firstly dispersed in 50 ml distilled water by ultrasonication for 15 min. Then 250 mg triblock copolymer (HO(CH₂CH₂O)₁₀₆(CH₂CH(CH₃)O)₇₀(CH₂CH₂O)₁₀₆H) Pluronic® F127 is added under vigorous stirring for 24 h. Then 2 ml of K₂CrO₄ (10 mg/ml H₂O) is added to the above suspension under vigorous stirring for another 24 h. The resulting mixture is aged in air at 50 °C for 48 h in a Petri dish and then calcinated by heat treated at 500 °C for 1.5 h under H₂/Ar atmosphere.

2.2. Synthesis of nanostructured titanium carbide

Titanium carbide (TiC) has been recently reported to demonstrate superior cycling stability in rechargeable Li-O₂ batteries.² However, the TiC used in the reported literature only exhibits limited specific surface area (~15 m²/g),² which significantly limit the specific capacity of the Li-O₂ batteries. Here we aim to synthesize high surface area TiC using C₃N₄ as carbon source.³ Bulk C₃N₄ can be synthesized using melamine as precursor.⁴ We design a solid-state reaction assisted by carbothermal reduction process to synthesize fine TiC nanoparticles. The C₃N₄ acts as a precursor to react with another oxide TiO₂ at 1100-1200 °C. The C₃N₄ was firstly prepared by reaction of melamine under air at 500-600 °C according to the literature.⁴ For the fabrication of TiC, the as-synthesized C₃N₄ and oxide TiO₂ are mixed together. The mixed powder are then put on an alumina boat and inserted into a tube furnace. The furnace is evacuated to 10⁻² mbar. And then the furnace is heated to 1100-1200 °C at the rate of 5 °C/min and kept at high temperature for 1-2 hours. Finally, black powder sample is obtained and cooled down naturally to room temperature.

2.3 Synthesis of porous silicon nanowires

Porous materials have been used as supports for catalysts because of their large number of pores, large surface area, and ease of recycling compared with other nanomaterials. Porous Si nanowires (Si NWs) have high surface areas, good electrical conductivity and fine chemical stability, which make Si NWs interesting candidate as cathode materials for rechargeable Li-O₂ batteries. We synthesize Si NWs via a method involving the deposition of silver particles on the surface of bare Si substrates followed by wet chemical etching.⁵ Briefly, pieces of commercially available highly doped p-type Si(100) wafers are used as starting materials. The Si wafers are cleaned by sonication in DI water, acetone and isopropanol and dried by nitrogen blowing. The cleaned Si wafers are immersed on a buffered oxide etchant (BOE) for 2 minutes to remove the native oxide layer and then immersed in a solution containing 0.01-0.04 M AgNO₃ and 5 M HF for 1 minute at room temperature. The colorful surface of Si wafer indicates that Ag nanoparticles have been formed on Si surface. The Ag-deposited Si wafers are cleaned with DI water to remove the extra Ag⁺ ions and then immersed on the solution containing 4.8 M HF and 0.3 M H₂O₂ for different time. Finally the Ag particles are removed by immersing the Si wafers in the concentrated H₃NO₃ for one hour. The as-etched products are inspected with a scanning electron microscope (SEM) at 10 kV of electron acceleration voltage.

2.4. Lithium-air cell design and assembly

We have designed and fabricated an electrochemical Li-O₂ testing apparatus or Li-O₂ cells, as shown in Fig. 2. The cell design is modified upon on a model proposed by the PI in a previous work.⁶ Basic function of the cell is to enclose battery components and active material and protect them from exposing to the ambient environment. The cell composes mainly of stainless steel and polytetrafluoroethylene (PTFE). The cell is assembled by placing a lithium metal foil, a polymer separator (Celgard 2325), a cathode and a current collector in the center of the bottom plate, between two of which 100uL of electrolyte (0.1 M lithium perchlorate (LiClO₄) in dimethyl sulfoxide (DMSO)) is added, followed by installing bolts that hold the top plate, spacer and bottom plate together. Gas (i.e., pure O₂) is then purged through the valves and the gauge will

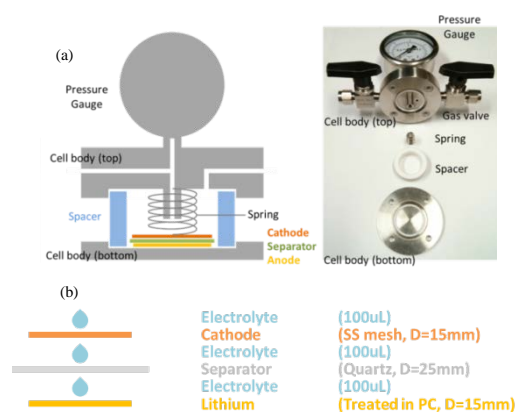


Fig. 2. (a) Illustration of the Li-O₂ cell; (b) Assembling of Li-O₂ cells

be used to indicate quality of the hermetic sealing. We have conducted a leakage test that successfully proved that the cell can be well-sealed. Therefore the fabricated cell is suitable for our future work on battery materials.

3. RESULTS ACHIEVED SO FAR

3.1. Materials characterization of as-synthesized $\text{Cr}_2\text{O}_3/\text{ITO}$ cathode material.

Cathode materials consisting Cr_2O_3 nanoparticles supported on ITO were synthesized by a soft template method followed by low temperature heat treatment. Fig. 3 shows the schematic of the synthesis process, SEM and energy-dispersive X-ray spectroscopy (EDS) of the as-synthesized $\text{Cr}_2\text{O}_3/\text{ITO}$. It is interesting to note that the original color of ITO was yellow and after the coating of Cr_2O_3 , the final $\text{Cr}_2\text{O}_3/\text{ITO}$ product is dark color, which might indicate improved electronic conductivity. The EDS result shows the major composition consists of In, Sn, and Cr. The atomic ratios of Cr and In elements are 19.08% and 54.12%, respectively.

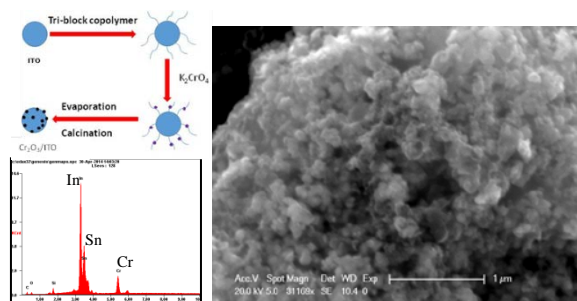


Fig. 3. Synthesis process of $\text{Cr}_2\text{O}_3/\text{ITO}$; SEM and EDS spectrum of the as-synthesized $\text{Cr}_2\text{O}_3/\text{ITO}$

3.2. Materials characterization of as-synthesized TiC cathode material.

Fig. 4 shows the SEM images and the XRD pattern of as-synthesized black product by the solid-state reaction assisted by carbothermal reduction method described earlier. SEM images show that the obtained product composed of irregular nanoparticles. The EDS spectrum (not shown here) shows that the as-synthesized product contains the Ti, O, and C elements. And the atomic ratios of Ti and C elements are 17.07% and 14.93%, respectively. The atomic ratio of Ti/C is close to 1:1. The XRD pattern demonstrate that the as-synthesized product was crystalline TiC. The index pattern basically agrees with JCPDS card no.32-1383. The XRD pattern of oxide precursor TiO_2 was also shown for comparison. It means that the TiO_2 precursor can be transformed into TiC after reaction with C_3N_4 by present method in this case. The results suggest that this route is effective in converting TiO_2 to TiC. The reaction mechanism can be expected to include two steps: Firstly, C_3N_4 decomposes into different carbon nitride species, such as C_2N_2^+ , C_3N_2^+ , and C_3N_3^+ , at temperature higher than 550°C . These species are highly reactive and easily bonded to oxygen atoms and reduce the titanium oxide into titanium metal. The subsequent carbonizing process between the titanium metal and the carbon-rich species will occur and finally lead to the formation of nanoparticles of TiC. We will evaluate the specific surface area of the as-synthesized TiC via the Brunauer, Emmett and Teller (BET) method.

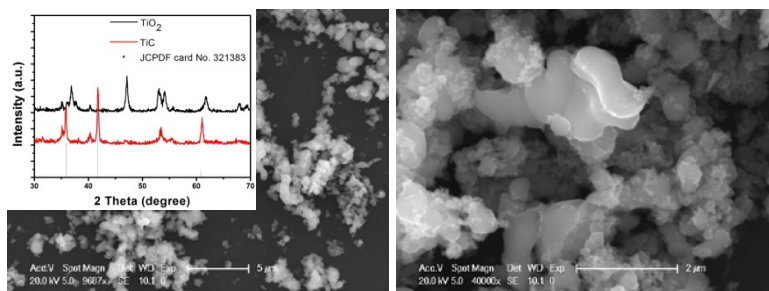


Fig. 4. SEM images and XRD pattern of as-synthesized TiC.

3.3. Materials characterization of as-synthesized porous Si NWs cathode material.

Fig. 5 shows the photograph (top left) and top view SEM image (top right) of the as-synthesized Si nanowires on highly doped Si substrate. In order to clearly reveal the Si NWs morphologies, the cross-section view of the Si substrate is shown in Fig. 5 (bottom). It is observed that surface of Si substrate is etched and morphology of these etched Si is nanowire arrays. The Si nanowire arrays have length of $10\ \mu\text{m}$ and width of $80\text{--}120\ \text{nm}$. The Si nanowire arrays have been successfully fabricated. The Si nanowires have crystalline crystal structures and large length-diameter aspect ratio and porous properties.⁷ The as-synthesized porous Si nanowires have large surface areas which may be a good candidate as catalyst supporter. We will

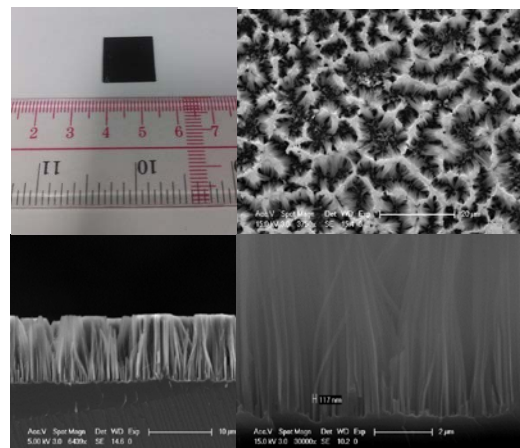


Fig. 5. Photograph and SEM images of Si NWs.

evaluate the specific surface area of the as-synthesized Si NWs via the BET method.

3.4. O₂-cathode fabrication and electrochemical characterization of select cathode materials

Oxygen-cathodes are fabricated by first mixing the cathode powder with PTFE binder in the ratio 95:5 (m/m) in isopropanol (Fig. 6a). The slurry is then drop casted onto a stainless steel mesh (0.6 mg/cm²). The coated mesh is dried in vacuum for over 12 hours at 150 °C. After this the electrodes are transfer to the glove box without exposure to air. As shown in Fig. 6b, the resulted electrode that the cathode material is evenly distributed across the mesh, both on and between the mesh wires. To establish our testing apparatus and methodology, we first select commercial available conducting metal carbide as cathode model systems due to its superior reaction stability reported recently.² We systematically select five metal carbides including TiC, vanadium carbide (VC), chromium (Cr₃C₂), molybdenum carbide (Mo₂C), and tungsten carbide (WC). The galvanostatic electrochemical characterizations of the five carbide nanoparticles are shown in Fig. 7. The rates for discharge and charge were 50mA/g_{cathode} and 10mA/g_{cathode}, respectively. We also limited the discharge process to a capacity of 100mAh/g_{cathode} to examine the discharge and charge behavior of Li-O₂ batteries without forming large/thick insulating Li₂O₂ particles. As shown in Fig. 7, the VC exhibits low discharge (i.e., poor discharge activity) but exceptionally low charge voltage (i.e., high charge activity). The low discharge voltage may be explained by its relatively small specific surface area, which further suggests that the VC exhibits the best catalytic activity for charging of the Li-O₂ batteries among the five carbides. In addition, TiC shows the highest charge potential, suggest that TiC exhibit lower charging activity compared with other four carbides. To quantitatively evaluate and compare the intrinsic catalytic activity of the five select cathode materials for discharge and charge reactions, we will perform comprehensive electrochemical characterizations including cyclic voltammetry (CV), Potentiostatic Intermittent Titration Technique (PITT) and Galvanostatic Intermittent Titration Technique (GITT) tests on these materials. Activity obtained from these measurements will be normalized by the true surface area of each material to be measured by the BET method.

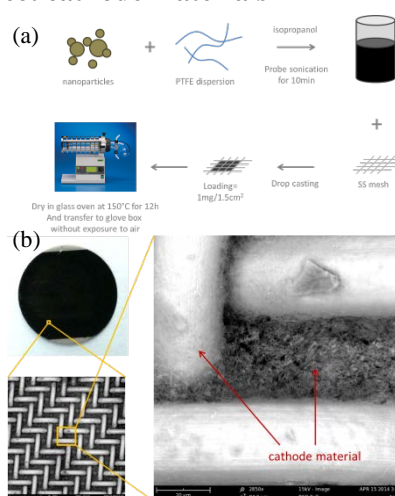


Fig.6. (a) Cathode fabrication (b) SEM image of O₂-cathodes on stainless steel.

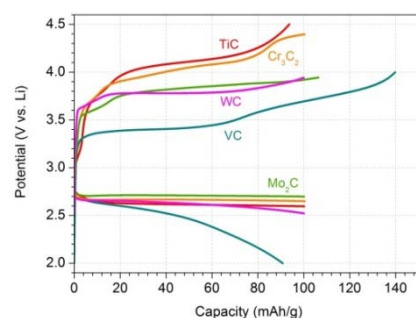


Fig. 7. First charge/discharge profile of Li-O₂ cells with cathode materials including TiC, Cr₃C₂, WC, VC and Mo₂C.

3.5. Design and setting up on-line electrochemical mass spectrometer

We designed and are developing an on-line electrochemical mass spectrometer (OEMS, Fig. 8)⁸ to identify and quantify the gas or volatile species formed in the cell during charge. It consists of an electrochemical cell, a sampling system and a mass spectrometer. A pressure transducer will be connected to the cell and measures during discharge the change of oxygen pressure, from which the amount of oxygen consumed can be determined. During charging, the gas and volatile species yield during charge will be sent to the vacuum chamber by the sampling system. The mass spectrometer can be used to analyze the composition of the gas.

References: (1) Li et al., *Nano Lett.* 2013, 13, 4702. (2) Ottakam Thotiyl et al., *Nat. Mater.* 2013, 12, 1050. (3) Li et al., *J. Alloys Compd.* 2007, 430, 237. (4) Zhang et al., *J. Am. Chem. Soc.* 2013, 135, 18. (5) Qu et al., *Nanoscale* 2011, 3, 4060. (6) Lu et al., *Electrochem. Solid State Lett.* 2010, 13, A69. (7) Qu et al., *J. Mater. Chem.* 2010, 20, 3590. (8) Tsiouvaras et al., *J. Electrochem. Soc.* 2013, 160, A471.

4. PUBLICATION AND AWARDS

To date, there is no publication arising from this funded project, but we expect 1-2 journal articles to be published upon the completion of the second year project period.

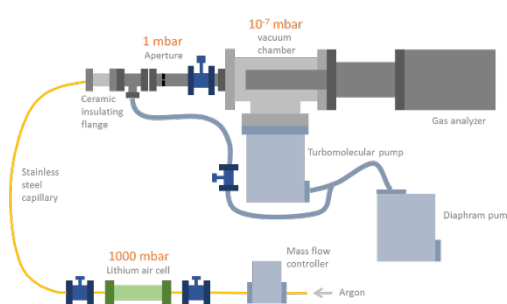


Fig. 8. Schematic of the OEMS design.

GRAPHENE-BASED ASYMMETRIC SUPERCAPACITORS WITH HIGH ENERGY DENSITY FOR CLEAN ENERGY STORAGE SYSTEMS

Principal Investigator: Professor ZHANG Li^(1, 2)
Department of Mechanical & Automation Engineering, CUHK

Research Team Members:

HAN Lijuan, Shun Hing Research Assistant^(1, 2)
WANG Feng, Shun Hing Research Assistant^(1, 2)

⁽¹⁾ Dept. of Mechanical and Automation Engineering

⁽²⁾ Shun Hing Institute of Advanced Engineering



Reporting Period: 1 July 2013 – 30 April 2014

ABSTRACT

The objective of the proposed research is to fabricate, characterize and optimize graphene-based supercapacitors with high performance for clean energy storage systems.

Supercapacitors have attractive properties such as high charge-discharge efficiency at high power densities, long cycling life, and pollution-free for clean energy storage; however, to date, their potential applications are hindered by the low energy density. Graphene is recently considered as an ideal electrode material for supercapacitors due to their 2-D single-atom-layer structure and excellent intrinsic physical properties such as ultra-high specific surface area (SSA), outstanding electrical conductivity and excellent mechanical and chemical stability. Though graphene-based supercapacitors are promising for practical applications, their energy and power densities are still need to be adequately improved to reach their best performance.

Taking advantage of novel synergistic effect of graphene nanosheets (GNS) and active nanostructured components, the PI proposes to design and prepare asymmetric supercapacitors using GNS-based nanocomposites as electrodes, and to characterize and optimize the microstructural and electrochemical properties of prototype supercapacitor devices having high energy and power densities. The ultimate goal is to develop high-performance and low-cost supercapacitors which can be scaled-up for future commercial applications.

This proposed research will result in fundamental understanding on the synergistic effect of the nanocomposites consisting of GNS and metal oxide/hydroxide nanostructures for the enhanced performance of the supercapacitors, thus, to pave the way for the development of next-generation energy storage devices and systems.

1. OBJECTIVES AND SIGNIFICANCE

1. To synthesize graphene oxide (GO) from expanded graphite using Hummers method. Since the surface of GO containing rich oxygen functional groups, it is an advantage to dispersively anchor metal ions for the nucleation of nanoscale metal oxides or hydroxides for the preparation of graphene-based nanocomposites.
2. To fabricate metal-oxide/reduced-graphene-oxide nanocomposites (MO/RGO, such as nanocomposite consisting of Mn_3O_4 and RGO) and metal hydroxide/graphene (MOH/RGO) nanocomposites using a one-step solution method, a facile and low-cost process. Their microstructural aspects will be investigated by SEM, high resolution electron microscopy (HRTEM), X-ray diffraction (XRD), infrared

spectrometer and thermogravimetric analysis (TG) to understand the formation mechanism of the nanocomposites.

3. To design and prepare prototype asymmetric supercapacitors using MO/RGO or MOH/RGO as positive electrodes and activated carbon as negative electrodes. These kinds of asymmetric supercapacitors are expected to have much higher working voltage and energy density than other type of supercapacitors.
4. To investigate the electrochemical properties of the as-fabricated supercapacitors using cycle voltammetry (CV), galvanostatic charge–discharge and electrochemical impedance spectroscopy (EIS) to determine their capacitance properties.
5. To conduct systematic optimization from both the composition of the hybrid materials and the design of the asymmetric electrodes to enhance the capacitor performance.

Long-term impact: Graphene-based nanocomposites are considered as one of the most suitable candidates for preparing supercapacitors, however, several crucial problems remain challenging: i.e., how to fabricate massive and high-quality graphene-based nanocomposites in low-cost for the high-performance supercapacitors, and how to effectively enhance their energy and power densities for future commercial applications. In this research, a facile one-step method will be developed, where the reduction of graphene oxide and formation of nanocomposites can be realized simultaneously. Based on this strategy, the high specific surface area of graphene will be effectively utilized through the sandwiched nanostructures and the chemical structure of metal-oxides/hydroxide nanostructures would be significantly stabilized upon their rooting on the graphene substrate. Thus, both the double layer capacitance of graphene and pseudocapacitance of metal-oxide/hydroxide can be gained to significantly enhance the performance of supercapacitors owing to the synergy of the hybrid materials. Moreover, asymmetric prototype supercapacitors will be designed, assembled, tested and then optimized, in order to reach the best working voltage and the energy density of the devices. The proposed study will impact scientific and technological development through providing high-performance supercapacitors for future low-cost and environmental-friendly commercial energy storage systems.

2. RESEARCH METHODOLOGY

Supercapacitor is promising for energy storage applications, in particular for the systems which require high power density, such as energy back-up systems and electrical/hybrid vehicles [1]. According to the different energy storage mechanism there are two types of supercapacitors: electrochemical double-layer capacitors (EDLC) and Faradic pseudocapacitors. Their performance can be quantified by the energy and power density respectively, i.e. $E=1/2(C_s U^2)$ and $P=E/t$, where C_s is the specific capacitance, U is the working voltage window and t is the time to discharge. Apparently, to enhance the E and P , large specific capacitance and voltage window with high electrical conductivity are required. Graphene is a single layered carbon material with ultra-large SSA (2675 m²/g), high electrical conductivity and mechanical strength (~1 TPa), showing great potential applications in EDLC, however, it remains a great challenge to fully utilize its SSA due to the re-stacking and agglomeration of the graphene nanosheets. By contrast, metal-oxides/hydroxides such as RuO₂ and Ni(OH)₂ show much higher pseudocapacitance than EDLCs, but their low electrical conductivity and power density, poor structural stability are still the drawback for practical applications. Therefore, to improve the performance of supercapacitors, an effective strategy is to design, synthesize and optimize advanced nanocomposites using the synergy between graphene and other active nanoscale structures.

Work done by us before the project: The PI was engaged in electrochemical capacitor researches from 2006 (Tao *et al.*, Carbon, Vol. 44, 1425-1428, 2006), and he has noticed that hybrid/nanocomposite materials have great potential for high-performance supercapacitors and other green energy systems.

The research was started from the fabrication of supercapacitors using carbon-based nanocomposites as electrode materials. Initially, nanocomposites of goethite nanorods and reduced graphene oxide (RGO) was synthesized and investigated, which showed an electrochemical capacitance of 165.5 Fg⁻¹, promising for electrochemical capacitors [7]; the electrode material we prepared from *in situ* construction of

potato-starch-based carbon nanofiber/AC hybrid structure also exhibited good performance for EDLC [8]. Recently, the PI conducted some experiments of synthesizing graphene-based nanocomposites, such as $\text{Co}_3\text{O}_4/\text{RGO}$ (inserted figure, upper one) and $\text{CoAl}(\text{OH})_2/\text{RGO}$, as electrode materials of supercapacitors, and the preliminary results are striking [9, 10]. The prototype asymmetric electrochemical capacitors we assembled using $\text{CoAl}(\text{OH})_2/\text{RGO}$ nanocomposite as positive electrode and activated carbon as negative electrode showing an improved electrochemical properties with higher energy density and working voltage (1.75 V in 6 M KOH aqueous electrolyte) in comparison to the traditional ones, which are capable of lighting a red LED with 1.5 V on-voltage (inserted figure, below one). As the PI proposed in this proposal, to further develop the graphene-based supercapacitors with higher performance for the new clean energy storage systems, great efforts on systematic investigation and optimization of the nanocomposites are still required.

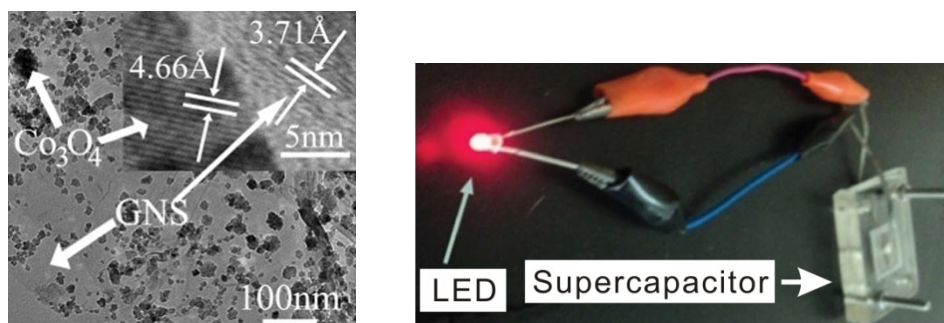


Fig. 1: The left image shows the microstructural properties of the nanocomposite consisting of GNS and Co_3O_4 . The right photograph shows a LED connected with a supercapacitor.

3. RESULTS ACHIEVED SO FAR

In order to design and prepare asymmetric supercapacitors with optimized performance, nanocomposites with varied materials and architectures as well as thin graphene paper are investigated in parallel.

Hierarchical core-shell-shell nanowire arrays based on metal oxide-conductive polymer-metal oxide were successfully developed using hydrothermal synthesis and electrode position (Fig. 2). The key to fabricate one-dimensional hierarchical architecture, $\text{Co}_3\text{O}_4@\text{PPy}@\text{MnO}_2$ “core-shell-shell” nanowires, was to introduce a PPy intermediate layer on the surface of Co_3O_4 nanowire, which could enhance the conductivity of nanowire arrays and act as a reactive template to induce a coating of amorphous MnO_2 . The device based on the ternary composite $\text{Co}_3\text{O}_4@\text{PPy}@\text{MnO}_2$ nanowire arrays exhibited prominent electrochemical performance with a high energy density of 34.3 Wh kg^{-1} at a power density of 80.0 W kg^{-1} and it is notable that the device exhibits a superior cycling behavior with 100.4% retentions of initial capacitance after 11,000 charge/discharge cycles because the elastic thin PPy shell can provide facile strain relaxation during long cycling, enhancing structural stability.

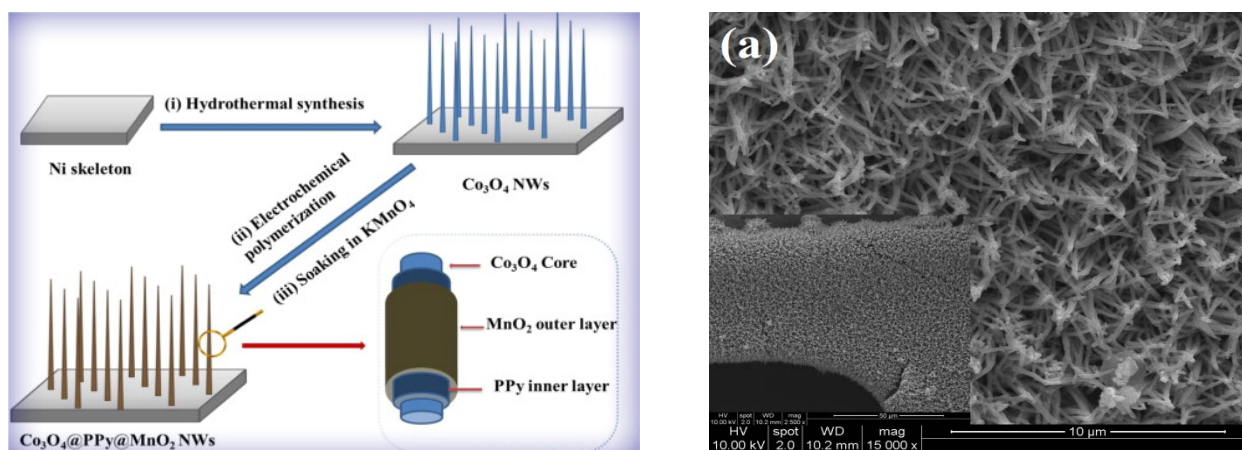


Fig. 2: (left) Schematic illustration of the fabrication process for $\text{Co}_3\text{O}_4@\text{PPy}@\text{MnO}_2$ core-shell-shell nanowire arrays. (right). SEM micrograph of ternary $\text{Co}_3\text{O}_4@\text{PPy}@\text{MnO}_2$ hybrid nanowire arrays.

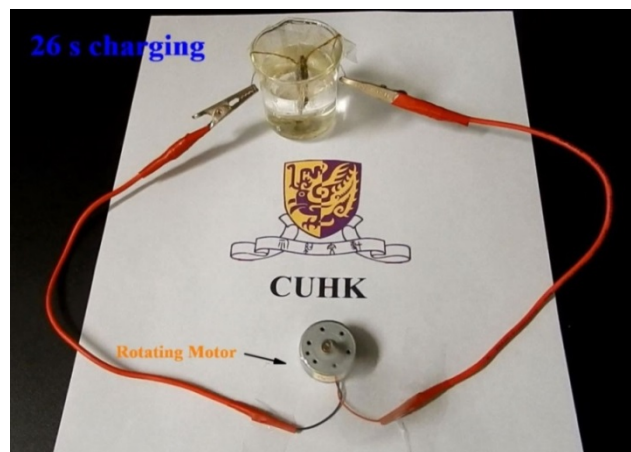


Fig. 3: A DC motor is powered by an AC//Co₃O₄@PPy@MnO₂ aqueous supercapacitor device in 1.0 M NaOH solution which was charged for 26 s. The mini-motor was able to rotate approximately 30 seconds by the charged supercapacitor. The length and the width of the device is ca. 1cm × 1 cm.

The performance of as-assembled asymmetrical supercapacitor was demonstrated using a DC motor (Fig. 3), in which the device can drive a mini-motor rotating robustly for approximately 30 s after charging at 17.4 mA cm⁻² for 26 s. The results were published in *Nano Energy* in 2014 (see Section 4). In the second year of this project, we plan to replace the conductive polymer layer, i.e. PPy, with graphene using chemical vapor deposition (CVD) or chemical solution methods. The goal is to achieve freestanding 3D networked structures based on graphene materials as the electrode of high-performance supercapacitors. It is also notable that, inspired by the paper published by Ajayan *et al.*, (*Nano Letters*, Vol. 11, 1423-27, 2011), we are also developing planar graphene-paper-based supercapacitors for ultrathin flexible electronic devices. In the first year, r-GO papers were successfully prepared with a varied thickness from nano- to micro-scale.

In addition, nanocomposites of carbon nanotubes (CNTs) coated with Ni-Co oxide nanoparticles were also synthesized using electroless plating in the first year with the collaboration with Zhejiang University, which were then applied as the conductive agents of activated carbon (AC) electrode for supercapacitors. Our results showed the specific surface, porosity, electrical conductivity, as well as electrochemical activity can be tuned by adjusting the molar ratio of nickel and cobalt in the electroless plating process. More importantly, the modification of the conductive agent for the electrode can improve the electrochemical performance of supercapacitors. The results indicate that the nanocomposite of carbon-based material/metal oxide have potential to act as additive materials in AC for the improvement of performance of supercapacitors. This part of results was published in *IEEE Transactions on Nanotechnology* in 2014 (see Section 4), and was presented in the conference IEEE NANO 2013.

4. PUBLICATION AND AWARDS

[1] Q. Li, J. Cheng, and **L. Zhang**, “Nickel-cobalt Oxide Coated CNTs as Additives of Activated Carbon Electrode for High-performance Supercapacitors”, *Proc. of the 13th IEEE International Conference on Nanotechnology (IEEE NANO 2013)*, Beijing, China, pp. 348-351, 2013.

[2] L. J. Han, P. Y. Tang, and **L. Zhang**, “Ternary Hierarchical Co₃O₄@PPy@MnO₂ Core-Shell-Shell Nanowire Arrays for Enhanced Electrochemical Energy Storage”, *Nano Energy*, Vol. 7, pp. 42-51, 2014.

[3] Q. Li, J. Cheng, B. Wang, and **L. Zhang**, “Activated Carbon Modified by CNTs/Ni-Co Oxide as Hybrid Electrode Materials for High Performance Supercapacitors”, *IEEE Transactions on Nanotechnology*, Vol. 13, 3, pp. 557-562, 2014.

VIBRATION ENERGY HARVESTING UTILIZING MULTIFUNCTIONAL PHONONIC META-MATERIALS

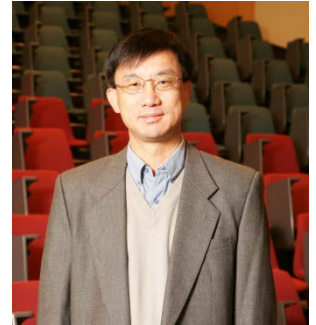
Principal Investigator: Professor Michael Yu WANG
Department of Mechanical & Automation Engineering, CUHK

Research Team Member:

Xiaoming WANG, Shun Hing Research Fellow ⁽¹⁾
Feifei Chen, Research Assistant ⁽¹⁾

⁽¹⁾ Dept. of Mechanical and Automation Engineering

Project Start Date: 1 July 2012
Completion Date: 30 June 2014



ABSTRACT

Our project focuses on a class of multifunctional, microstructured materials (meta-materials) and structures for vibration energy harvesting. The meta-materials have superior mechanical wave handling properties and energy conversion capabilities. These abilities of meta-materials can inhibit elastic waves from propagating within specific frequency ranges known as phononic bandgaps. By utilizing the multi-functional meta-materials and structures, vibration energy can be localized (or trapped); the vibration wave can be guided (or channeled) to a specific location; and multi-frequency waves can be separated (or filtered) into single-frequency parts. Consequently, the vibration energy can be collected, filtered, and finally channeled to and accumulated at converting locations, where it is converted into electrical power by piezoelectric harvesters with tuned resonances.

1. OBJECTIVES AND SIGNIFICANCE

Energy harvesting has become the talk of the engineering world. Generating electrical energy from natural or environmental sources, such as ambient vibrations and heat, would give self-powered capability to a sea of portable electronic devices, wireless sensors and MEMS systems. Vibration energy harvesting holds a great potential, as vibrations are omnipresent in machines and structures, scattering energy over wide space and in a wide frequency range. The challenge is to collect vibrations effectively and convert them efficiently into electricity, allowing energy harvesting on a continuous basis and employed in hostile and inaccessible environment.

The aim of this research project is to develop the multifunctional structures whereby meta-materials with desired bandgap functions are integrated as building blocks to form the structures for efficient energy harvesting. The proposed approach is hierarchical and is physically driven. The overall goal of the project is to develop the hierarchical design method and to demonstrate the applicability of the proposed vibration energy harvesting system. The proposed system is also scalable for microscale applications. It is expected that this investigation would yield a novel vibration energy harvesting technique that would significant advance the state-of-the-art.

The objectives of the project include:

1. Development of an optimization-based approach that employs level set methods to provide complex designs of bandgap meta-materials of multiple frequency-dependent dispersive dynamic characteristics;
2. Systematic explorations of unit cell optimization of meta-materials to optimize the three desired functional materials crucial to the proposed vibration energy harvesting structure: (1) trapping, to localize elastic waves of a specified frequency range, (2) channeling, to guide vibration waves to a specific location, and (3) filtering, to separate or select multi-frequency waves into single-frequency parts;

3. Hierarchical design for energy harvesting structures: (1) synthesizing the topology of bandgap structure with a layout of regions of the required multifunction meta-materials, and (2) employing the designed materials to form a bounded structure with bandgap functions that correlate with those of the materials in the structure;

4. Demonstration of the proposed approach with design cases where ambient vibration energy of a structure is filtered, accumulated and channeled for harvesting, showing the feasibility of the concept and the efficiency of the proposed phononic structure.

2. RESEARCH METHODOLOGY

A key contribution of our approach stems from a complete understanding of the dynamics of periodic bandgap materials and structures. We embark upon the difficulties of ambient vibration sources characterized by their spatial distribution (location) and time distribution (frequency), as they are often generated from multiple sources, propagated throughout the structure and distributed over a large surface area. Their energy might be scattered over a range of frequency spectrum. Fortunately, phononic bandgaps can have multiple functions. A phononic material can disperse different wavelengths, stopping or letting pass a selected frequency and, thus, acting as a wave trap. We intend to utilize these fundamental dynamical properties and to construct bounded structures from bandgap materials such that they are to be used as basic functional building blocks for our novel multiscale multifunctional system for vibration energy harvesting.

3. RESULTS ACHIEVED SO FAR

During the project, we focus on vibration energy harvesting with phononic bandgap structures. First, we study benchmark problems of bandgap materials and optimization. The problems include bandgap mechanisms for broadband frequency wave attenuation in low frequency range. We studied flexural beams with multi-DOF resonators attached, which generate locally resonant wave trapping. With the innovative use of different configurations of 2-DOF resonators, we have found very interesting properties of wave dispersion. Particularly, our preliminary results indicate that we can achieve super-wide frequency bandgaps at low frequency range. This is a scenario suited for harvesting the energy of the vibration wave with two piezoelectric harvesters with tuned resonance frequency. We further examined another arrangement of the resonators such that the 2-DOFs are not co-located. This arrangement is shown to have an effect to further widen the bandgap. While the physics principles are still under investigation, the observations and simulation results are very exciting and they will need to be verified with experimental testing.

4. PUBLICATION AND AWARDS

Our research findings arising from the funded project are published in the following publications. All these publications have directly acknowledged the SHIAE funding support.

[1] Xiaoming Wang and Michael Y. Wang, "Band Gaps in Periodic Flexural Beams With Multi-DOF/Continuum Local Resonators," PHONONICS 2013: 2nd International Conference on Phononic Crystals/Metamaterials, Phonon Transport and Optomechanics, June 2-7, 2013. <http://phononics2013.org>

[2] Michael Y. Wang and Xiaoming Wang, "Wide-Band Low Frequency Gaps in Periodic Flexural Beams With Nonlinear Local Resonators," PHONONICS 2013: 2nd International Conference on Phononic Crystals/Metamaterials, Phonon Transport and Optomechanics, June 2-7, 2013. <http://phononics2013.org>

[3] Michael Y. Wang and Xiaoming Wang, "Broadband Wave Attenuation in Locally Resonant Periodic Flexural Beams With Force-Moment Resonators," 25th Conference on Mechanical Vibration and Noise, ASME IDETC/CIE 2013, August 5-8, 2013. <http://www.asmeconferences.org/idec2013>

[4] M. Y. Wang and X. Wang, "Frequency band structure of locally resonant periodic flexural beams suspended with force-moment resonators," *Journal of Physics D: Applied Physics*, (46)25, 255502, June 2013. DOI: [10.1088/0022-3727/46/25/255502](https://doi.org/10.1088/0022-3727/46/25/255502)

[5] M. Y. Wang and H. Lv, Numerical and Experimental Study of Flexural Wave Band Gaps of Periodical LR Beams with Suspended Force-Moment Resonators, Paper IMECE2014-36730, ASME 2014 International Mechanical Engineering Congress and Exposition, November 14-20, 2014, Montreal, Canada.

UNDERSTANDING ELECTRON AND PHONON TRANSPORT IN BORON CARBIDE NANOWIRES FOR THERMOELECTRIC ENERGY CONVERSION

PI: Professor Dongyan XU

Department of Mechanical and Automation Engineering, CUHK

Research Team Members:

Juekuan Yang, Visiting Scholar, Shun Hing Fellow⁽¹⁾

Aijun Zhou, Visiting Scholar, Shun Hing Fellow⁽¹⁾

Xiaomeng Wang, Postgraduate Student⁽¹⁾

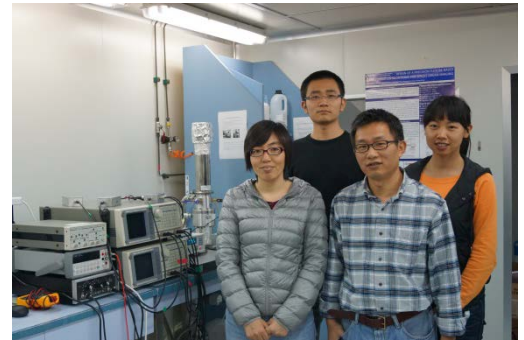
Qiang Fu, Postgraduate Student⁽¹⁾

Yucheng Xiong, Postgraduate Student⁽¹⁾

⁽¹⁾ Dept. of Mechanical and Automation Engineering

Project Start Date: 1 July 2012

Completion Date: 30 June 2014



ABSTRACT

The objective of the proposed research is to study the structure and transport property relation of boron carbide nanowires for thermoelectric energy conversion applications. Thermoelectric devices show a great potential for waste heat recovery by directly converting heat into electricity; however, to date their practical applications have been limited by their low efficiency. Recently, several reports demonstrated significantly improved thermoelectric efficiency by engineering thermoelectric materials into nanostructures, such as nanowires, primarily through thermal conductivity reduction. Despite boron carbides have been projected as a promising class of high-temperature thermoelectric materials, so far, no one has studied thermoelectric transport properties of one-dimensional boron carbide nanowires yet. The PI proposes to study transport properties of boron carbide nanowires for high-temperature thermoelectric applications. The approach is to integrate systematic transport property measurement on individual boron carbide nanowires and detailed structure and composition characterization for each measured wire. The ultimate goal is to develop the structure-transport property relations for boron carbide nanowires.

1. OBJECTIVES AND SIGNIFICANCE

The objectives of the proposed research are

- To measure thermoelectric properties (thermal conductivity, electrical conductivity, and Seebeck coefficient) of individual boron carbide nanowires in a wide temperature range (10 – 800 K). Since these properties are determined on the same nanowire sample, we can construct thermoelectric figure-of-merit for each boron carbide nanowire.
- To thoroughly characterize the structure and composition of each measured nanowire.
- To construct the relations between composition, structure, and transport properties of boron carbide nanowires upon the completion of the first two objectives.
- To clarify the effects of many important factors, including nanowire diameter, carbon concentration, planar defect, and doping level, on thermoelectric properties of boron carbide nanowires.

Significance: Boron carbides are promising high-temperature thermoelectric materials whose transport properties are not well understood yet especially for one-dimensional nanostructures. The proposed research will provide previously unavailable data to answer the following two fundamental scientific questions: (1) Can we correlate the structure-transport property relation of boron carbide nanowires? (2) To

what extent boron carbide nanowires can enhance thermoelectric performance compared to bulk materials? Answering these questions will not only enhance our understanding on electron and phonon transport in boron carbide nanowires but also lead to materials design rules to achieve better thermoelectric performance. The proposed study will impact technology development through providing better materials for high-temperature thermoelectric energy conversion applications.

2. RESEARCH METHODOLOGY

2.1. Microdevices for Properties Characterization

To characterize thermoelectric properties of an individual nanowire, we designed and fabricated a unique microdevice as shown in Figure 1. The device consists of two suspended $25\ \mu\text{m} \times 15\ \mu\text{m}$ silicon nitride (SiN_x) membranes separated by a gap of 2 to $6\ \mu\text{m}$. A 30 nm thick Platinum (Pt) coil and two separate Pt electrodes are patterned on each membrane. Each coil is electrically connected to four contact pads via metal lines on suspended beams, enabling four-probe measurement of electrical resistance of the coil. The Pt coils serve as a heater to increase the temperature of the suspended membrane, as well as a resistance thermometer to measure the temperature of each suspended membrane. An individual boron carbide nanowire can be placed bridging two membranes using a micromanipulator. The design of the microdevice enables us to determine thermal conductivity, electrical conductivity, and Seebeck coefficient of an individual nanowire in one measurement. Thus, thermoelectric figure-of-merit of individual boron carbide nanowires can be calculated.

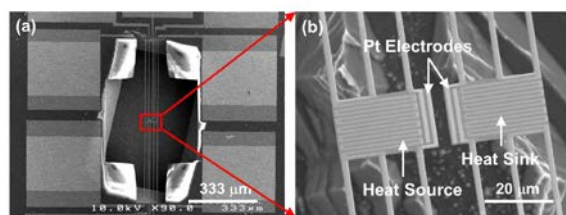


Figure 1 SEM images of the microdevice used to characterize thermoelectric properties of an individual nanowire.

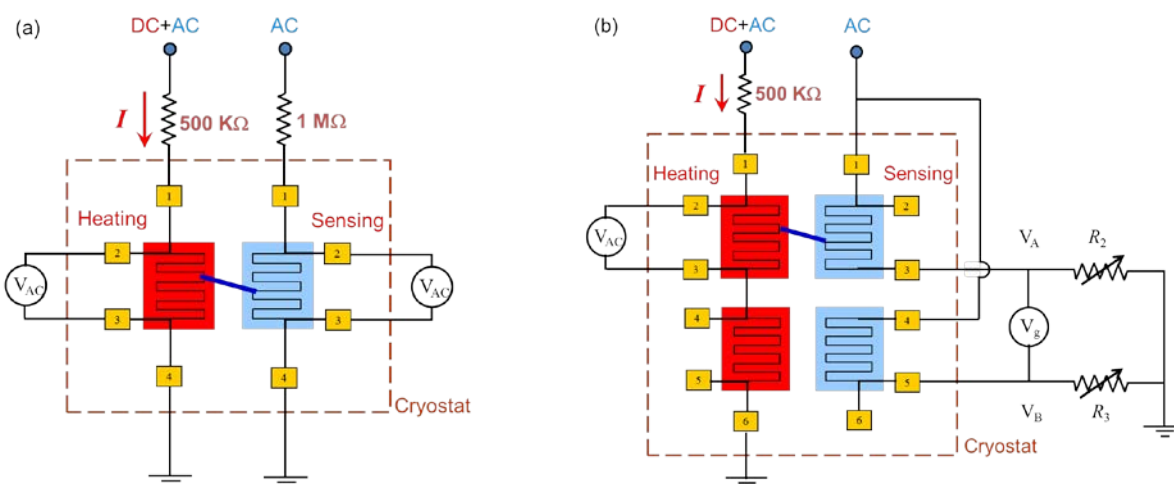


Figure 2 Schematics of traditional measurement method (a) and cancelling bridge method (b).

2.2. Thermal Conductivity Measurement

The measurement technique we used in this project was invented by Kim et al in 2001, and has been widely used to characterize thermal properties of various nanowires, nanoribbons, carbon nanotubes, and graphene sheets. The schematic of traditional measurement method is shown in Figure 2(a). During the measurement, a DC current is applied to one Pt coil and generates Joule heating, and accordingly increases the temperature of the heating membrane. Part of the generated heat will flow through the nanowire to the sensing membrane and raise its temperature. A small AC current will be applied to the Pt coil on each membrane to measure the coil resistance using a four-probe method and then the temperature rise of each membrane can be calculated from the coil resistance change. The thermal conductance of the nanowire can be determined by solving the heat transfer equation for the whole system. Then thermal conductivity of the nanowire can be extracted after its length and cross sectional information are obtained.

The traditional method has a sensitivity of approximately 1 nW/K. Therefore it is applicable for samples with a thermal conductance much higher than 1 nW/K. On the other hand, in the traditional method, radiation between the heating membrane and the sensing membrane also contribute to the total thermal conductance, which may result in an overestimation on thermal conductivity of the nanowire. The radiation conductance is also on the order of 1 nW/K at room temperature. In order to measure thermal properties of one-dimensional nanostructures with thermal conductance less than 1 nW/K, recently, Wingert et al introduced a Wheatstone bridge into the sensing side circuit to improve the sensitivity (cancelling bridge method), as shown in Figure 2(b). In this method, a reference device without the nanostructure is used to cancel the contribution of radiation to the total thermal conductance. Their experiments show that the cancelling bridge method can achieve a measurement sensitivity of 10 pW/K. In this project, we implemented both traditional measurement method and cancelling bridge method to measure thermal properties of boron nanoribbons and the contribution of radiation to the measurement is evaluated by comparing the measurement results from both methods.

3. RESULTS ACHIEVED

Our major achievement in this project is given as follows.

3.1. Design and Fabrication of Microdevices

In this project, we have designed and fabricated a series of suspended microdevices on silicon wafers through standard microfabrication processes. Devices with different spacings between two suspended membranes are obtained for different applications. To prepare samples, a micromanipulator with a sharp probe tip is used to place individual nanowires or nanoribbons bridging two membranes under an optical microscope.

3.2. Implementation of Traditional Measurement Method and Cancelling Bridge Method

We have built an experimental system for thermal conductivity measurement of one-dimensional nanostructures as shown in Figure 3. Both traditional measurement method and cancelling bridge method have been implemented and calibrated and experimental results are given in next section. In order to determine the temperature dependence of thermal conductivity, the sample is mounted in a cryostat system, which is capable to change the environmental temperature rapidly from 10 K to 800 K. Before the measurement, the cryostat chamber will be pumped down to a pressure lower than 10^{-6} torr to minimize the convective heat loss.



Figure 3 Experimental setup

3.3. Thermal Conductivity Measurements of Boron Nanoribbons

Before characterizing boron carbide nanowires, we first calibrated our experimental system by measuring thermal conductivities of boron nanoribbons. Boron nanoribbons are chosen for calibration mainly for two reasons: 1) Thickness of our boron nanoribbon samples is very uniform, normally within 20 ± 2 nm, and their thermal conductivities are found very repeatable; 2) Prof. Deyu Li's group at Vanderbilt University has measured boron nanoribbon samples with traditional measurement method. Their results can serve as a reference for our measurements. Moreover, one-dimensional boron nanostructures are promising materials for nanoscale electronic devices due to their superior physical properties. However, thermal transport in this complex material has not been well understood yet. On the other hand, thermal conductivity of boron nanoribbons at high temperature (>500 K) has not been

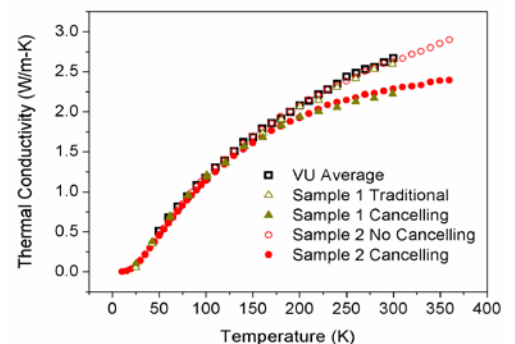


Figure 4 Thermal conductivity of boron nanoribbons.

studied so far, which will be one of our research focuses in this project.

Two boron nanoribbon samples have been measured and thermal conductivity results are shown in Figure 4. Sample 1 has been measured by using both traditional measurement method and cancelling bridge method. The thermal conductivity result of traditional measurement method (open triangles) agrees well with the average data (open squares) obtained by Prof. Deyu Li's group at Vanderbilt University, which indicates that our traditional measurement system works properly. In order to calibrate the cancelling bridge setup, a DC current is applied only to the heating coil on the device with a nanoribbon but not to the counterpart on the reference device. Since the reference device is not heated up, the radiation conductance cannot be cancelled in this case and the cancelling bridge method is essentially degraded to the traditional measurement method. As seen in Figure 4, thermal conductivity result of sample 2 measured with degraded cancelling bridge method (Sample 2 No Cancelling) agrees well with the results of traditional measurement method, confirming that our cancelling bridge setup also works well.

Thermal conductivity results of these two boron nanoribbon samples measured with cancelling bridge method are also shown in Figure 4. As we can see in this figure, thermal conductivity results obtained by cancelling bridge method overlap with the results of traditional measurement method when temperature is below 100 K, and are lower than the results of traditional method above 100 K due to the contribution of radiation conductance. As temperature increases, the difference between two methods also increases, indicating that the contribution of radiation to the measurement error will be significant at high temperature, especially for samples with a low thermal conductance. Since we will characterize thermal properties of boron carbide nanowires from 10 K to 800 K in this project, we will adopt cancelling bridge method for thermal conductivity measurements.

In order to study the temperature dependence of radiation conductance, we measured a bare device with no nanoribbon bridging two membranes by using the degraded cancelling bridge method (no cancelling mode) and the result is shown in Figure 5. On the other hand, we calculated radiation conductance by subtracting thermal conductance results of sample 2 measured with no cancelling and cancelling modes and the result is also given in Figure 5. As seen in Figure 5, two results agree well with each other, further confirming that our cancelling bridge setup works properly. The radiation conductance approximately changes with temperature as a function of T^2 .

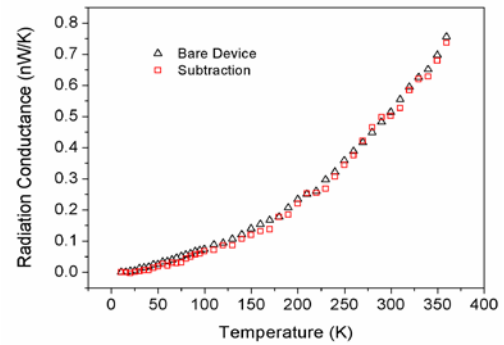


Figure 5 Radiation conductance obtained by measuring a bare device with degraded cancelling bridge method (open triangle) and by subtracting thermal conductance results of sample 2 measured with no cancelling and cancelling modes (open squares).

3.4. High Temperature Measurement

To date, thermal conductivity characterization of various one-dimensional nanostructures has been conducted in the relatively low temperature range (lower than 500 K) in the literature, although it is very important to characterize thermal properties of certain materials at high temperature, such as boron carbide nanowires, silicon nanowires, and silicon/germanium nanowires, for thermoelectric power generation applications. In order to successfully measure thermal properties of one-dimensional nanostructures at high temperature, we first need to solve a few technical difficulties.

As mentioned above, radiation heat transfer from the heating membrane to the sensing membrane may result in an overestimated thermal conductivity for one-dimensional nanostructures, which can be cancelled by adopting the cancelling bridge method. On the other hand, it is worth noting that two radiation shields have been installed in the vacuum chamber to reduce the radiation loss from the device to surroundings so that we can assume that the temperature of the membranes is the same as the substrate temperature when the heating current is zero.

Moreover, we carefully calibrated the substrate temperature of the measurement device by mounting a type E thermocouple on the device during the measurement and the calibration result is shown in Figure 6. In this figure, y axis is the temperature difference between the substrate temperature and the setting temperature of the cryostat ($\Delta T = T_{\text{sub}} - T_{\text{set}}$), and x axis is the setting temperature. As seen in Figure 6, below 300 K, the substrate temperature is close to the setting temperature and ΔT is smaller than 5 K. However, above 300 K, the substrate temperature could be substantially lower than the setting temperature and ΔT could be as large as -40 K at 800 K. In this project, we have used the calibrated substrate temperature for all the data analysis.

Another challenge we are facing for the high temperature measurement is that the microfabricated platinum thermometers are not stable above 650 K. Figure 7 shows the electrical resistance of the platinum coil on the heating membrane for an as-fabricated device (black squares). It is observed that electrical resistance of the platinum coil is decreasing with the temperature above 650 K which indicates that annealing of the platinum thermometer is taking place during the measurement. In order to stabilize the platinum thermometers before the measurement, we tried to pre-anneal the bare suspended devices in an argon environment at 700 °C for 5 mins in a rapid thermal annealing furnace. The platinum thermometer after the pre-annealing treatment is found much more stable and its electrical resistance increases with the temperature linearly.

We also conducted thermal conductivity measurement of boron nanoribbons with the annealed device up to 800 K and results are shown in Figure 8. Although we have pre-annealed the platinum thermometers, we still observed a large scatter for thermal conductivity of boron nanoribbons at high temperature, which might be attributed to the following two factors:

- 1) Thin platinum coils might not be continuous strips after the annealing treatment. The platinum coils are fabricated by the sputtering process with a thickness of 30 nm. We speculate that platinum particles might migrate and form partially connected islands during annealing, which might result in non-uniform heating of the heating membrane and the increased noise level during the measurement.
- 2) Thermal conductance of boron nanoribbons is very low especially at high temperature, which is only around 2-3 nW/K. Due to the low thermal conductance, temperature rise of the sensing membrane is also small (less than 0.3 K). We expect that the temperature fluctuation in our cryostat is larger at high temperature which might cause relatively large measurement errors for low thermal conductance samples.

In the future, to further improve the stability of the high temperature thermal property measurement, we will

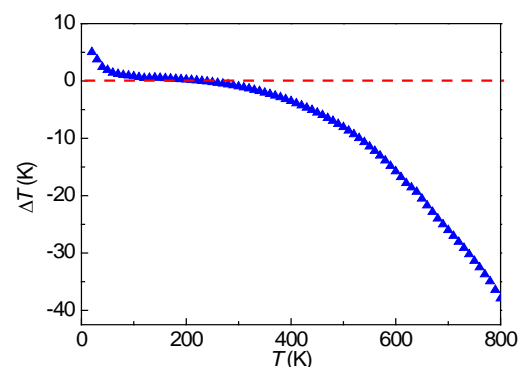


Figure 6 Temperature difference between the substrate temperature and the setting temperature vs. the setting temperature of the cryostat system.

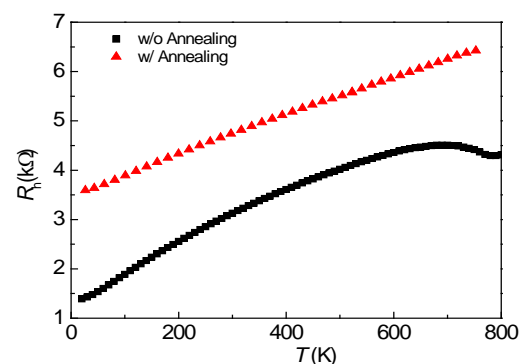


Figure 7 Electrical resistance of the platinum coil on the heating membrane with and without the pre-annealing treatment.

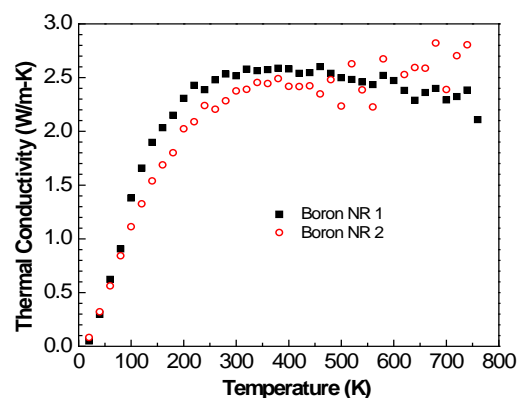


Figure 8 Thermal conductivity of boron nanoribbons measured with the annealed suspended devices.

revise the microfabrication procedure of the suspended devices and incorporate the annealing process into the device fabrication. Meanwhile, we will also quantify temperature fluctuations in our cryostat.

4. PUBLICATION AND AWARDS

Journal Publication

- [1] J. Wu, X. Wang, M. Chen, D. Xu, and J. Yang, "Estimation of Temperature Coefficient of Resistance for Microfabricated Platinum Thermometers in Thermal Conductivity Measurements of One-dimensional Nanostructures," *Measurement Science and Technology*, **25**, 025008, 2014.

Conference Presentations

- [2] J. Yang, X. Wang, Y. Yang, Y. Chen, Z. Ni, T. Xu, D. Li, and D. Xu, "Intrinsic Thermal Conductivity Characterization of 20-nm-thick Boron Nanoribbons at Low Temperature," Presented in *ASME 2013 4th Micro/Nanoscale Heat & Mass Transfer International Conference*, Hong Kong SAR, China, December 2013.
- [3] J. Yang, X. Wang, Y. Yang, Y. Chen, Z. Ni, T. Xu, D. Li, and D. Xu, "Thermal Conductivity Characterization of Individual Boron Nanoribbons at High Temperature," Presented in *2013 ASME International Mechanical Engineering Congress & Exposition*, San Diego, CA, USA, November 2013.

Awards

1. Best Poster Award (First Prize), "Thickness-dependent Cross-plane Thermal Conductivity of Thin Graphite Flakes," The 2nd International Conference on Phononics and Thermal Energy Science (PTES2014), 26-31 May, 2014, Shanghai, China.
2. Best Poster Award (Third Prize), "Thermoelectric Transport in Individual Bismuth Selenide Nanoribbons," The 2nd International Conference on Phononics and Thermal Energy Science (PTES2014), 26-31 May, 2014, Shanghai, China.

TERNARY HYBRID POLYMER / NANOCRYSTAL BULK HETEROJUNCTION SOLAR CELLS WITH CASCADE ENERGY-LEVEL ALIGNMENT

Principal Investigator: Professor Ni ZHAO
Department of Electronic Engineering, CUHK

Co-Investigator: Baoquan Sun ⁽²⁾

Research Team Members:

Feng Wang (research assistant) ⁽¹⁾,
Haihua Xu (research associate) ⁽¹⁾,
Hui Yu (PhD student) ⁽¹⁾, Xiaojing Wu (PhD student) ⁽¹⁾,
Ting Xiao (PhD student) ⁽¹⁾, Mengyu Chen (PhD student) ⁽¹⁾



(1) Dept. of Electronic Engineering, CUHK

(2) Institute of Functional Nano & Soft Materials, Soochow University

Project Start Date: 1 July 2012

Completion Date: 30 June 2014

ABSTRACT

This proposal aims to develop ternary hybrid organic/inorganic heterojunction solar cells with cascade energy-level alignment. Semiconductor nanocrystals, polymers and organometal halide perovskites are attractive photoactive materials due to their solution processability, high absorption coefficient and wide spectral tunability. Hybrid solar cells combine the mechanical flexibility of organic materials with the morphological stability of inorganic components and therefore have the potential to offer superior solar cell properties. In this project we propose to create a cascade of energy levels (Figure 1) in the photoactive layer of hybrid solar cells by utilizing a ternary heterojunction structure. We have developed solution-based methods to fabricate two ternary hybrid structures, polymer/nanoshell/nanorod and polymer/perovskite/compact nanocrystalline TiO₂; the latter has yield a solar cell efficiency of more than 17%. The properties of these structures are investigated via morphological, electrical and spectroscopic characterizations. The technological know-hows and the fundamental understanding gained from this project will contribute to the efforts towards realizing the next generation solar cell technology.

1. OBJECTIVES AND SIGNIFICANCE

1. To develop solution-based processes for scalable fabrication of ternary hybrid bulk and planar heterojunction solar cells with cascade energy-level alignment.
2. To establish a versatile testing platform, consisting of spectroscopic, optoelectronic and microscopic characterization methods, with which the optimal condition for producing photovoltaic effects can be identified for various cascade hybrid systems.
3. To demonstrate high-efficiency ternary hybrid organic/inorganic solar cells via a multi-pronged approach consisting of material selection, processing optimization and device design.

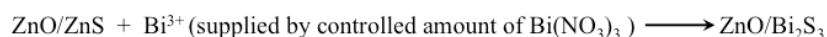
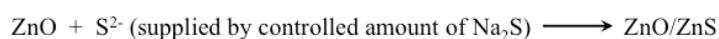
Significance: In this project we developed two novel approaches that enable fabrication of heterojunction solar cells with great uniformity and high reproducibility, both are key to the realization of large-scale production of solar panels. One of the approaches to make AMX₃ (A: CH₃NH₃⁺ (MA) or HC(=NH)NH₃⁺ (FA); M: Pb; X: Cl or I) perovskite solar cells has resulted in power conversion efficiencies of >17%, exceeding those of commercialized silicon solar cells. The work demonstrates the importance of precursor

design and engineering. Furthermore, the fundamental understanding gained through the spectroscopic, optoelectronic and microscopic characterizations provide guidelines on the design of photoactive materials with new functionalities.

2. RESEARCH METHODOLOGY

1. Materials:

(i) polymer/nanoshell/nanorod structure: Polymer materials were purchased from Lumtec Corp. ZnO nanorods were prepared according to the method reported in Refs [1, 2]. In brief, potassium hydroxide solution (in methanol) was added drop by drop into zinc acetate solution (in methanol mixed with water) under constant magnetic stirring. The reaction was then held at 60 °C for several hours until nanorods with desired dimension were produced. Before use, the nanorods were washed with ethanol for three times. The nanoshell/nanorod structures were fabricated via a surface ion-exchange method we developed. The reactions involved are briefly described below:



Importantly, we placed the reaction apparatus in ice-water bath to achieve a slow reaction rate. In this way the shell thickness can be well controlled.

(ii) polymer/perovskite/compact nanocrystalline (nc) TiO₂ structure: This work introduced a new Pb-based precursor, HPbI₃, to synthesize formamidium lead iodide (FAPbI₃) perovskite. The HPbI₃ powders were prepared by mixing PbI₂ (Sigma-Aldrich, 99%) and 57% w/w hydroiodic acid (molar ratio is 1:1.5) in DMF. After stirring the solution for 1 h, HPbI₃ could be collected by evaporating the solvent at 80°C under reduced pressure. The powders were washed with copious diethyl ether until the supernatant turns to colorless. The collected powders are stored in an oven at 40°C. Formamidinium iodide (FAI) powders were synthesized according to a previously reported method [3]. Briefly, formamidinium acetate (Sigma-Aldrich, ≥98.0%) was dissolved in 57%w/w hydroiodic acid in a molar ratio of 1:2. The precipitate was recovered upon evaporating the solvent at 60°C under reduced pressure. After washing with diethyl ether and recrystallized with ethanol, FAI powders were obtained. The FAPbI₃ is prepared by a simple one-step spin-coating process of FAI/HPbI₃ mixture, followed by thermal annealing of the perovskite films.

2. Device fabrication: Solar cells were fabricated on patterned ITO and FTO substrates. The photoactive layer was fabricated via spin-coating; other interlayers and top electrodes were deposited via spin-coating and thermal evaporation.

3. Characterization: The nanoshell/nanorod structures were examined using transmission electron microscopy (TEM). The perovskite films were examined using scanning electron microscopy (SEM), X-ray diffraction (XRD) and X-ray photoelectron spectroscopy (XPS). The current-voltage and impedance characteristics of the solar cells were measured using an I-V source meter and electrochemical impedance spectroscopy, respectively. To achieve a fundamental understanding of the device performance, spectroscopic methods, such as steady-state and time-resolved photoluminescence spectroscopy, electroabsorption spectroscopy (EA), charge modulation spectroscopy (CMS) and photoinduced absorption (PIA) spectroscopy, were used to probe the charge- and energy-transfer processes in the cascade structure as well as the photo-induced change in the dipole property in the active materials.

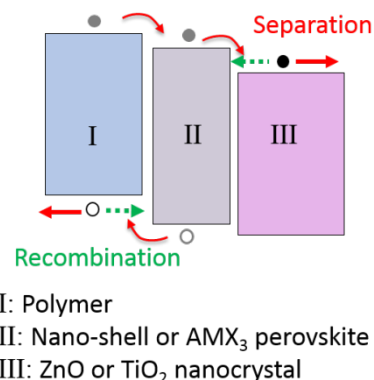


Figure 1 Energy-level diagram of a cascade structure and the material systems studied in this project. The energetic offset favors the charge separation (red arrows) and suppress the charge recombination (green arrows).

3. RESULTS ACHIEVED

3-A. polymer/nanoshell/nanorod structure

We have synthesized ZnO nanorods with controllable aspect ratio. The relatively uniform size distribution of the nanorods was confirmed by TEM, as shown in Figure 2a. A two-step ion-exchange process is developed to grow ZnO/Bi₂S₃ and ZnO/PbS core-shell nanorods. This reaction process is simple and well controlled; furthermore, the whole process is held in aqueous solutions, thus minimizing the use of toxic solvents. The shell thickness can be tuned by controlling the excess amount of Bi³⁺ and S²⁻ ions. Figure 2b shows an extreme case that the ZnO core almost completely be turned in to Bi₂S₃ nanoparticle shell. This new synthesis process via sequential cation and anion exchange reaction offers a very simple way of producing colloidal nanoparticles without ligands. TEM images show that Bi₂S₃ nanoparticles have a diameter of around 5 nm and can self-assemble to form nanowires, which may serve as the charge transport pathways in the hybrid solar cell structures.

Photoluminescence spectroscopy was used to investigate the impact of the shell passivation on the optical properties of ZnO nanorods. It is shown that the defect emission of ZnO at ~530 nm is greatly decreased after the growth of Bi₂S₃ nanoshell (Figure 2a), suggesting that we have successfully passivated the surface defect states on ZnO nanorods by Bi₂S₃. This is an important step towards reducing the charge recombination loss in the solar cells. We also note that the intrinsic emission of ZnO at ~440 nm is reduced after shell growth, due to the photogenerated holes partially transferred from ZnO to Bi₂S₃. The charge transfer properties between a donor polymer, P3HT, and the ZnO nanorods are also investigated by photoluminescence spectroscopy. As shown in Figure 2c, the fluorescence intensity of P3HT drops 34% after mixing with ZnO and 70% after mixing with ZnO/Bi₂S₃. This result proves that our proposed cascade energy level alignment (P3HT/Bi₂S₃/ZnO) indeed benefits the charge separation between P3HT and ZnO. Since the photogenerated electrons are funneled from P3HT to ZnO via Bi₂S₃, the chance of charge recombination is greatly reduced. This has been confirmed by the low charge recombination rate constant measured via transient photovoltage measurement (Data not shown here).

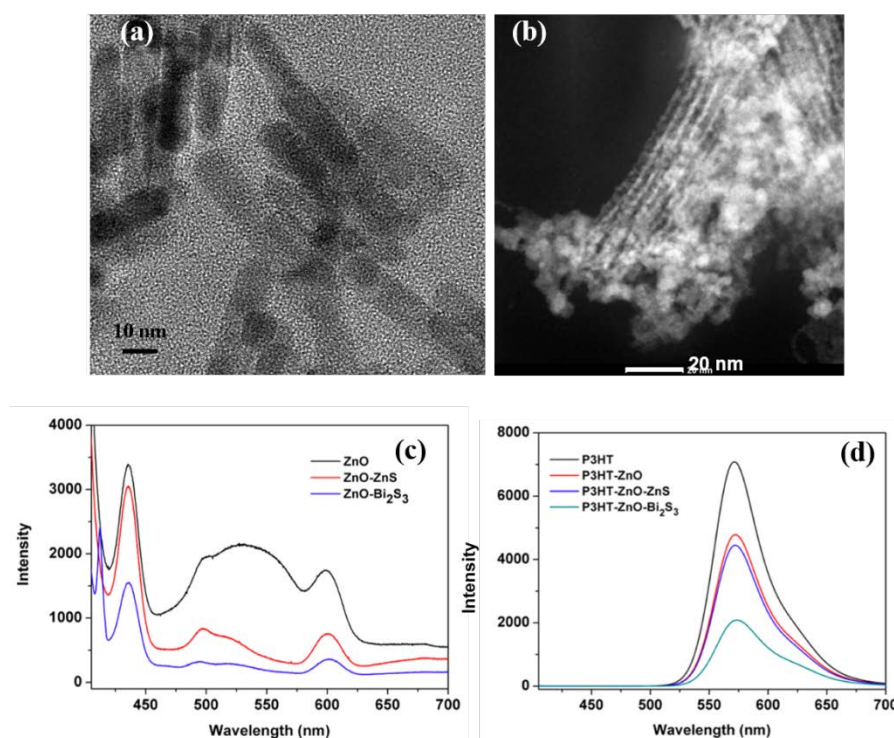


Figure 2 (a) TEM images of ZnO nanorods. (b) TEM image of assembled Bi₂S₃ nanoparticle shells on ZnO. (c) Photoluminescence spectra of ZnO, ZnO/PbS and ZnO/Bi₂S₃ nanocrystal solution (Excitation wavelength: 380 nm). (d) Photoluminescence spectra of P3HT films before and after mixing with ZnO, ZnO/ZnS and ZnO/Bi₂S₃ nanocrystals. (Excitation wavelength: 380 nm).

We have fabricated solar cell devices to evaluate the performance of the material systems we developed. Our testing results show that the open-circuit voltage (V_{oc}) of the ternary P3HT/Bi₂S₃/ZnO solar cells is up to 0.6 V, significantly higher than 0.47 V for the binary P3HT/ZnO solar cells. The short-circuit current density (J_{sc}) and fill factor (FF) are still low, mainly due to the low loading ratio of the nanorods. We also implemented a Bi₂S₃ nanocrystal/P3HT bulk heterojunction (BHJ) into the testing solar cell structure. The cells exhibit a short-circuit current density (J_{sc}) up to 2.2 mA/cm². This value is about 7 times higher than those reported for

the same material system [4, 5]. The origin of the high photogenerated current could be related to the ligand-free process during the synthesis of Bi_2S_3 nanocrystals. We expect further improvement in the device performance through optimization of the fabrication parameters. In summary, our device characterization results suggest that Bi_2S_3 could act as an n-type semiconductor with suitable electronic properties for hybrid BJJ solar cells. Using ion-exchange method we can control the loading ratio of Bi_2S_3 in the BJJs. *We are currently preparing manuscript to describe this part of the work.*

3-B. polymer/perovskite/compact nc- TiO_2 structure

Although the polymer/nanoshell/nanorod structure has conceptually proves the advantages of combining organic and inorganic components in a ternary heterojunction, the material system yields low solar cell efficiencies (< 2%). We therefore explored another hybrid system – organometal halide perovskites. Firstly, we studied the formation mechanism of perovskites through a proto-type material, $\text{CH}_3\text{NH}_3\text{PbI}_{3-x}\text{Cl}_x$. Despite the rapid improvement in the PV efficiency of $\text{CH}_3\text{NH}_3\text{PbI}_{3-x}\text{Cl}_x$, the fundamental question regarding the role of Cl in determining the properties of the perovskite remains unclear. Our work addresses this question through investigating the reaction mechanism that leads to the formation of the perovskite. Commonly, the $\text{CH}_3\text{NH}_3\text{PbI}_{3-x}\text{Cl}_x$ films are prepared by spin-coating a precursor solution of $\text{CH}_3\text{NH}_3\text{I}$ and PbCl_2 in dimethylformamide (DMF) at a 3:1 molar ratio, followed by thermal annealing at around 100°C. By monitoring the annealing products with XRD and energy-dispersive X-ray spectroscopy we found that the slow formation of the $\text{CH}_3\text{NH}_3\text{PbI}_{3-x}\text{Cl}_x$ perovskite is likely driven by release of gaseous $\text{CH}_3\text{NH}_3\text{Cl}$ (or other organic chlorides in a similar form) through an intermediate organolead mixed halide phase. Furthermore, by comparing the perovskite films produced from $\text{CH}_3\text{NH}_3\text{I}/\text{PbCl}_2$ and $\text{CH}_3\text{NH}_3\text{I}/\text{PbI}_2$ precursor combinations with different molar ratios, we demonstrated that the initial introduction of a CH_3NH_3^+ rich environment is critical to slow down the perovskite formation process and thus improve the growth of the crystal domains during annealing; accordingly, the function of Cl is to allow the removal of excess CH_3NH_3^+ at a relatively low annealing temperature. Our study reveals the importance of controlling the formation reaction of perovskites through precursor engineering. *The work has been published on Advanced Functional Materials this year [6], and we have already received many positive comments from research groups that are working on hybrid solar cells.*

Based on the findings on $\text{CH}_3\text{NH}_3\text{PbI}_{3-x}\text{Cl}_x$, we proceeded to develop another perovskite material, FAPbI_3 , due to its extended absorption range and excellent charge transport properties. While most previous studies focused on optimizing the deposition processes of the perovskite films, the selection of the precursors is rather limited to the PbI_2 / FAI combination. In this work we developed a new precursor, HPbI_3 , to replace PbI_2 . The HPbI_3 compound shows excellent solubility (up to ca. 2.5 M) in DMF at room temperature, and can react with FAI to produce FAPbI_3 perovskite films with high uniformity and excellent thermal stability. As compared to the previously reported FAPbI_3 films produced from the PbI_2 based precursor combinations, the HPbI_3 based FAPbI_3 films exhibit much purer crystalline phase with strong (110) preferred orientation. Such

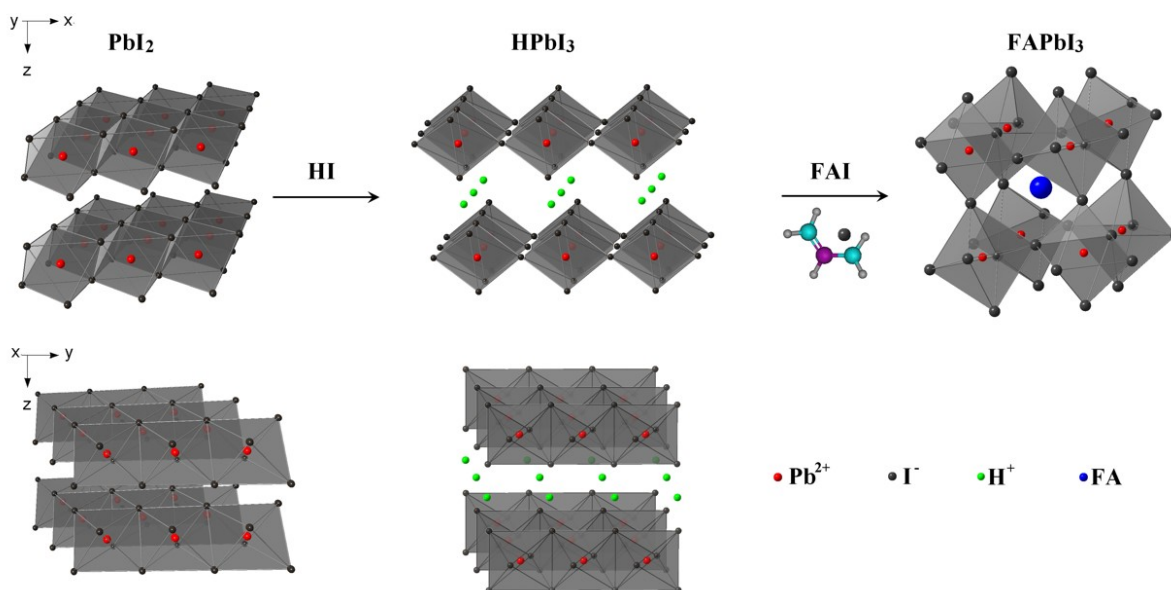


Figure 3. Schematic illustration of the configurations of PbI_2 , HPbI_3 and FAPbI_3 .

high crystallinity benefits from a slow crystallization process involving exchange of H^+ and FA^+ ions in the PbI_6 framework (Figure 3). Our work represents the first attempt to develop alternative lead-based precursors for perovskite photovoltaic materials. The new precursor, HPbI_3 , can be applied to other perovskite materials to produce high quality films through a simple one-step solution-coating process. Using a spiro-MeOTAD/perovskite/compact nc-TiO_2 cascade heterojunction structure, we demonstrate a solar cell efficiency of 17.5% (so far the world record for FAPbI_3 cells). The high performance results from the excellent film uniformity (Figure 4) as well as the efficient cascade structure, where holes and electrons are effectively transferred to the spiro-MeOTAD and compact nc-TiO_2 layers, respectively, and collected by the electrodes. *The work has been submitted to Advanced Functional Materials [7], and we are currently revising the manuscript based on the reviewers' comments.*

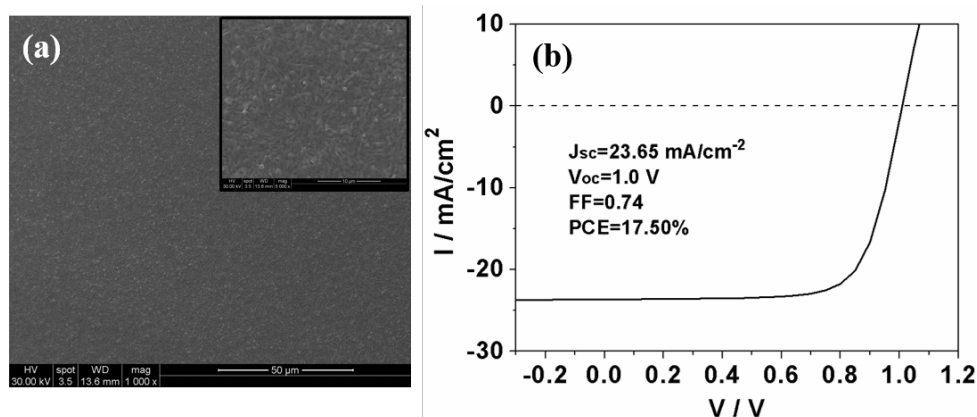


Figure 4 (a) SEM images of FAPbI_3 fabricated from FAI/HPbI_3 on compacted TiO_2 substrates (inset shows the film morphology at high magnification). (b) Current density-voltage characteristic measured under AM 1.5 simulated sun light for the champion FAPbI_3 device.

3-C. Testing Platform

Throughout the execution of this project, we have set up various characterization equipment including electroabsorption (EA) spectroscopy, charge modulation spectroscopy, photoinduced absorption spectroscopy and transient photovoltage measurement unit. These tools have helped us to study a variety of

photoactive materials, ranging from polymers, nanocrystals to perovskites [8-10]. For instance, we carried out the first quantitative analysis on the composition-dipole moment correlation in AMX_3 perovskite materials using the EA spectroscopy. We show that the A and M cations could both largely affect the dielectric and dipolar property of the perovskite materials, but through different mechanisms, such as ionic polarization, rotation of molecular dipoles and charge migration. These processes occur at different time scales and thus result in a frequency-dependent dipole response. This spectroscopic study, together with theoretical calculations, can help to improve the understanding on the remarkable electronic properties of the AMX_3 perovskites and provide guidelines on the design of perovskite materials with new functionalities. *The work has been submitted to Journal of Physical Chemistry C [8], and we are currently revising the manuscript based on the reviewers' comments.*

References:

- [1] C. Pacholski; A. Kornowski; H. Weller, *Angew. Chem., Int. Ed.* **2002**, 41, 1188-1191.
- [2] B.Q. Sun; H. Sirringhaus; *Nano Lett.* **2005**, 5, 2408-2413.
- [3] G. E. Eperon; S. D. Stranks; C. Menelaou; M. B. Johnston; L. M. Herz; H. J. Snaith, *Energy Environ. Sci.* **2014**, 7, 982
- [4] Y.Q. Li; Y.Z. Zhang; Y. Lei; P.J. Li; H.M. Jian; H.W. Hou; Z. Zheng, *Mater. Sci. Eng. B*, **2012**, 177, 1764-1768.
- [5] H.C. Liao; M.C.Wu; M.H. Jao; C.M. Chuang; Y.F. Chen; W.F. Su, *CrystEngComm*, **2012**, 14,3645-3652.
- [6] H. Yu; F. Wang; F. Xie; W. Li; J. Chen; N. Zhao, *Adv. Funct. Mater.* **2014**, DOI: 10.1002/adfm.201401872.
- [7] F. Wang; H. Yu; H. H. Xu; N. Zhao, *Adv. Funct. Mater.* Under revision
- [8] X.J. Wu; H. Yu; L. L. Li; F. Wang; N. Zhao, *J Phys Chem C*. Under revision
- [9] H.H. Xu; Y.Q. Jiang; J. Li; B.S. Ong; Z.G. Shuai; J.B. Xu; N. Zhao, *J Phys Chem C*, **2013**, 117, 6835–6841
- [10] L. Ye; H.H. Xu; H. Yu; W.Y. Xu; H. Li; H. Wang; N. Zhao; J.B. Xu, *J Phys Chem C*, **2014**, 118, 20094–20099.

4. PUBLICATION AND AWARDS

Journal publications:

1. F. Wang; H. Yu; H. H. Xu; N. Zhao, “HPbI₃: a New Precursor Compound for Highly Efficient Solution-Processed Perovskite Solar Cells”, *Advanced Functional Materials*; Under revision
2. X.J. Wu; H. Yu; L. L. Li; F. Wang; N. Zhao, “Composition-Dependent Electric Dipole Moment in Organometal Halide Perovskites”, *Journal of Physical Chemistry C*; Under revision
- 3.H. Yu; F. Wang; F. Xie; W. Li; J. Chen; N. Zhao, “The Role of Chlorine in the Formation Process of “CH₃NH₃PbI_{3-x}Cl_x” Perovskite”, *Advanced Functional Materials* **2014**, DOI: 10.1002/adfm.201401872.
4. H.H. Xu; Y.Q. Jiang; J. Li; B.S. Ong; Z.G. Shuai; J.B. Xu; N. Zhao, “Spectroscopic Study of Electron and Hole Polarons in a High- Mobility Donor - Acceptor Conjugated Copolymer”, *Journal of Physical Chemistry C*, **2013**, 117, 6835–6841

Award:

H. Yu and F. Wang, “Precursor Engineering for High Efficiency Organometal Halide Perovskite Solar Cells” **Best Poster Award**, CU Energy Day 2014

Biomedical Engineering Track

Research Reports In Biomedical Engineering

Newly Funded Projects

(2015-2017)

- * Development of a Novel flexible Surgical Robot with Haptic Sensation
- * Development of injectable supramolecular hydrogels for regenerative medicine
- * Developing Optomechanical Devices based on Layered Nanomaterials for Single-Biomolecule Mass Spectrometry

Continuing Projects

(2014-2016)

- * Development of High-speed Laser Scanning Microscope for In Vivo Deep Brain Imaging
- * Mechanism for the transcytosis of targeted nanoparticles across the blood-brain barrier

(2013-2015)

- * Development of the Next Generation Neurosurgical Assistant System Based on Functional Brain Mapping
- * Biomimetic scaffold for stem cell based cartilage regeneration and drug delivery

Completed Projects

(2012)

- * Dielectrophoresis Nano-separator for Precision Manufacturing of Polymeric Nanoparticles for Tumor-Targeted Drug Delivery

The following reports are enclosed in “Research Highlights” printed in June 2014

Completed Projects

- (2011) * Viewing Biomolecules at the Right Site by Plasmonic Tweezers and Surface Enhanced Raman Scattering

The following reports are enclosed in “Research Highlights” printed in 2013

Completed Projects

- (2010) * An inexpensive functional finger prosthesis with rebounded type progressive hinge lock
- * Diffusion Tensor MRI Predictors of Cognitive Impairment in Confluent White Matter Lesion
- * Lanthanide-impregnated molecularly imprinted polymer microspheres as antibody mimics on an optofluidic platform for the detection of disease biomarkers
- (2009) * Terahertz probe for in vivo imaging
- * Signal Processing Strategies on Cochlear Implant Devices for Effective Speech Perception of Tonal Languages
- * Development of A Robotic Endoscope Holder for Nasal Surgery

The following reports are enclosed in “General Report and Research Highlights 2009-2011” printed in October 2011.

Completed Projects

- (2008) * Development of highly sensitive and large throughput surface enhanced Raman scattering (SERS) substrates for molecular diagnosis
- * Research on Language and Brain Waves
- * Development of an Efficient Locomotion Mechanism for Wireless Active Capsule Endoscope
- (2007) * Bio-electromagnetic Modeling and Experiment Setup for Medical Electronics RF Safety Assessment
- * Medical Applications of Terahertz Imaging
- * Hybrid Assistive Knee Braces with Smart Actuators
- (2006) * RF Radiation Effect and Efficiency of Wireless Medical Devices on Human Body
- * Photonic biosensor micro-arrays for screening of common cancers

The following reports are enclosed in “Research Highlights 2005-2007” printed in January 2008.

Completed Projects

(2005)

- * Cochlear Implants
- * Virtual Anatomy and Dexterous Simulators for Minimal Access Cardiothoracic and Neuro-endoscopic Surgeries
- * Systematic Synthesis of Nano-informatics Chips by Nano-Robotics Manipulation

DEVELOPMENT OF A NOVEL FLEXIBLE SURGICAL ROBOT WITH HAPTIC SENSATION

Principal Investigator: Professor Zheng LI
*Division of Biomedical Engineering and
Institute of Digestive Disease, Faculty of Medicine, CUHK*

Project Start Date: 1 July 2015



ABSTRACT

This project aims to develop a novel tele-operated flexible surgical robot for general minimally invasive surgery (MIS). In the proposed robot, key drawbacks in existing surgical robots will be addressed. The performance of the robot will be evaluated systematically in the CUHK Jockey Club Minimally Invasive Surgical Skills Center and the Chow Yuk Ho Technology Center for Innovative Medicine by ex vivo mockup surgeries and animal (pig) tests.

Robot assisted MIS brings to patient multiple benefits, including shorter hospital stay, less post-operative pain, less blood loss, better cosmesis, etc. In the market, the da Vinci robot is the dominant player in MIS. It is equipped with slender rigid arms and lacks of tactile sensation which is crucial in surgical interventions. The rigid arms pivot about the trocar and lack of dexterity inside the body. Also, the pivoting creates a large sweeping motion, which may cause damages to vital structures. Flexible robot is intrinsically safer. However, their payload capacity is small due to the low stiffness. The sweeping motion generated by the arm bending remains significant. Also, the workspace and dexterity are limited due to the lack of control in either the length or the curvature of the bending section. In this project, a novel constrained tendon-driven serpentine mechanism (CTSM) will be employed to design the proposed flexible surgical robot. In the CTSM both the length and curvature of the bending section are controllable, which gives the robot much improved dexterity and larger workspace. A shape reconstruction based force sensing method will be developed to enable the robot's tactile sensation. What's more, a tension based stiffness control method will be implemented to endow controllable stiffness to the flexible robot. Therefore, the payload capability can be actively adjusted based on the surgical task. As a summary, the developed robot will integrate the following advantages: tactile sensation, much reduced sweeping motion, controllable stiffness, enhanced dexterity, and expanded workspace.

The success of this project will advance the research of robotics in surgery and finally lead to a market ready surgical robot, which can bring to patients a safer, less invasive, less time consuming and cost effective surgery. This will also strengthen CUHK's leading position in innovation and development of medical technologies.

PROJECT OBJECTIVES:

1. Development of a novel tele-operated flexible surgical robot with the following advantages or performances without sacrificing the surgical robot arm's dimensions:

- (a) Tactile sensation with a force sensing resolution of finer than 0.1 N.
 - (b) Controllable stiffness: the robot can work with at least two stiffness options, i.e. stiff-floppy.
 - (c) Reduced sweeping motion than existing rigid/flexible surgical robot arms at same dimensions.
 - (d) Improved dexterity than existing rigid/flexible surgical robot arms at same dimensions and same end effector condition.
 - (e) Larger reachable workspace than existing rigid/flexible surgical robot arms at same base movement.
 - (f) Tele-operation: the slave flexible robot can be controlled stably with the master input device.
2. For ex vivo mockup tests and animal tests, we'd like to achieve the following:
- (a) Build a test platform for ex vivo mockup surgery, which can be used for the developed flexible surgical robot as well as other similar surgical instruments for MIS.
 - (b) Verify the aforementioned advantages of the developed flexible surgical robot, and find its possible limitations for future improvement.
 - (c) Prove the feasibility of the developed flexible surgical robot in live animal surgery. By applying targeted nanoparticles to a non-contact blood-brain barrier (BBB) model, examine the mechanism for their transcytosis across brain endothelial cells *in vitro*. Determine how the choice of targeting ligands dictates a nanoparticle's route of transcytosis, including the intracellular compartments and specific proteins within brain endothelial cells.

LONG TERM IMPACT

Every upgrade in surgical tools can bring multitude benefits to patients and surgeons, as shown by the da Vinci robot system. The successful completion of this work will yield a surgical robot much more capable than the existing da Vinci robot, including restored tactile sensation, controllable stiffness, reduced sweeping motion, enhanced dexterity, and expanded workspace inside the body. The tactile sensation is not possessed by the da Vinci robot yet. It gives surgeons an additional sense, therefore more comprehensive intraoperative decisions can be made. The improved dexterity and expanded workspace enable the surgeons fulfilling operations in an easier way and new operations that is less invasive and less time consuming is predictable. The reduced sweeping motion and controllable stiffness enable the robot avoiding damages to vital structures during the operation. Thus, safety can be improved. The controllable stiffness can suits the robot arm to variable surgical tasks. Therefore less surgical tools are needed during the surgery and the cost can be reduced.

We envision our flexible surgical robot will lead to a market ready surgical robot in the near future. The wide adoption of the robot will bring to patients a safer, less invasive and less expensive surgery and will bring to surgeons operations that are simpler and less time consuming. What's more, the success of this project will strengthen CUHK's leading position in innovation and development of medical technologies as well as enhance the position of Hong Kong as the innovation center and the medical hub in Asia and worldwide. The technologies developed in this work will also advance the research in robotics, especially in mechanism design, force sensing and control.

DEVELOPMENT OF INJECTABLE SUPRAMOLECULAR HYDROGELS FOR REGENERATIVE MEDICINE

Principal Investigator: Professor BIAN Liming
*Department of Mechanical and Automation Engineering,
CUHK*

Project Start Date: 1 July 2015



ABSTRACT

Objectives: to develop self-healing, bioadhesive, and mechanically resilient supramolecular gelatin hydrogels for articular cartilage repair.

Motivation: hydrogels are ideal carrier material for the delivery of therapeutic cells (like stem cells) and drugs to enhance the healing and regeneration of damaged biological tissues/organs. However, conventional chemically crosslinked hydrogels have a number of limitations that hinder the clinical translation of these hydrogels. In this project, we aim to develop novel supramolecular hydrogels, which are free of chemical crosslinking and have an array of unique features that are desirable for potential clinical applications.

Methodology: supramolecular hydrogel are generally mechanically weak. We have developed a novel “Host-guest macromer” (HGM) approach to fabricate supramolecular hydrogels with enhanced mechanical properties. Briefly, premixing the free diffusing crosslinkable host molecules with the polymer containing guest motifs significantly enhance the host-guest complexation efficiency due to the low steric hindrance. The subsequent polymerization of the obtained “HGM” produces the supramolecular hydrogels that are highly stretchable and self-healable. Furthermore, the residual hydrophobic cavities of the host molecules in the hydrogels afford the potential for facile modular modifications such as incorporation of hydrophobic drugs and tethering of bioactive molecules.

Impact & benefit: the advantages of the proposed HGM supramolecular hydrogels compared to existing products include mechanical resilience, tissue adhesiveness, self-healing, ease of use, and capability of delivering hydrophobic drugs. These benefits make the proposed hydrogels ideal vehicles for delivering therapeutic cells and drugs to assist treatments of human cartilage defects and a variety of other diseases including spinal cord injury, intervertebral disc herniation, etc.

Clinical demand for effective medical intervention of cartilage degeneration

Osteoarthritis (OA) is characterized by progressive degradation of articular cartilage in limb joints such as knees and hips. A recent study in Hong Kong found that among men aged 50 years and older, 17% had persistent knee pain and 7% can be diagnosed to have osteoarthritis of the knee. Among women aged 50 years and older, 24% had persistent knee pain and 13% can be diagnosed to have osteoarthritis of the knee [1]. This showed that osteoarthritis is one of the major causes of disability among Hong Kong population as observed in the developed western countries. The total annual cost of treating all OA patients in Hong Kong was estimated to be 3.5 billion (HKD) representing 0.28% of Hong Kong GNP (gross national product) and this economic burden is largely placed on the government [2].

Early articular cartilage injury is a major cause of the osteoarthritis. Therefore, early effective intervention to repair the injured cartilage is essential to preventing or delaying the occurrence of osteoarthritis. The latest clinical solution, autologous chondrocyte transplantation (ACI), is based on the tissue engineering principles (Figure 1)[3]. This new therapy has rapidly evolved to the third generation. The third-generation ACI innovatively employs a three-dimensional biomaterial carrier to protect and support the cells delivered to cartilage defects, thus effectively improving the therapeutic outcome of the ACI. However, three-dimensional cell carrier materials still have a number of limitations (Table 1).

Table 1. the limitations of the biomaterials used in the current ACI therapy

<i>Brand</i>	<i>Cell carrier biomaterials used</i>	<i>Manufacturer</i>	<i>Limitations</i>
MACI®	Type I/III collagen membrane	Genzyme , US	1 , 2 , 3 , 4 , 5 , 6 , 8 , 10 , 11
Hyalograft®	Porous hyaluronic acid scaffold	Fidia Advanced Biopolymers , Italy	1 , 2 , 3 , 4 , 5 , 6 , 8 , 9 , 10 , 11
Novocart®3D	Porous collagen scaffold	TETEC , Germany	1 , 2 , 3 , 4 , 5 , 6 , 8 , 10 , 11
Novocart®Inject	Injectable polymeric hydrogels	TETEC , Germany	3 , 4 , 5 , 6 , 7 , 8 , 9 , 10 , 11

1. not-injectable, not suitable for minimally invasive surgery.
2. not able to fit the irregular cartilage defects tightly
3. poor bio-adhesion on cartilage
4. difficult to prepare in operation room, requiring experienced users to prepare
5. not able to load and control release small molecule drugs
6. weak mechanical properties
7. poor biocompatibility
8. no self-healing capacity
9. hinders the recruitment of endogenous cells
10. not suitable for the delivery of stem cells
11. costly (US \$ 20-35 k USD per patient)

PROJECT OBJECTIVES:

1. To fabricate and characterize the supramolecular gelatin hydrogels.
2. To examine the hMSC chondrogenesis in the physically crosslinked supramolecular hydrogels.
3. To assess the controlled release of hydrophobic chondrogenic small molecules from the supramolecular hydrogels.
4. To evaluate the efficacy of the supramolecular hydrogels as the carrier material of stem cells and drug to repair cartilage defects in an animal model.

LONG TERM IMPACT

The findings from this project will help guide the design and promote the clinical translation of injectable hydrogels for cartilage repair. Hydrogels developed in this study will not only enhance cartilage repair but will also be instrumental to the development of minimal invasive therapies for repairing connective tissues including bone, meniscus and intervertebral disc.

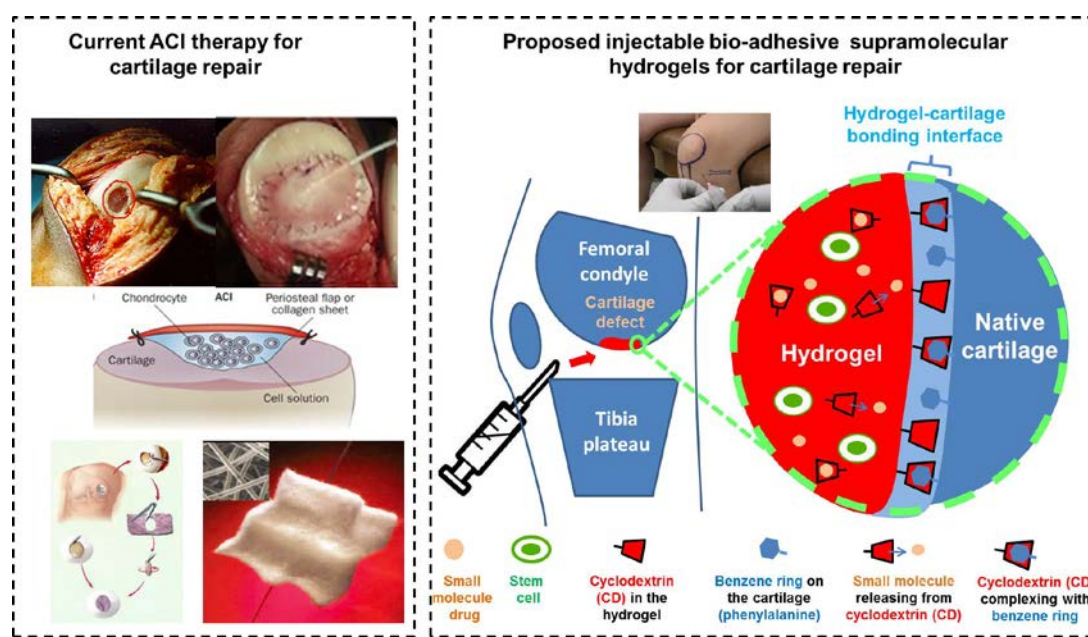


Figure 1 current autologous chondrocyte transplantation (ACI) and the proposed strategy to treat cartilage defects in knee joints.

DEVELOPING OPTOMECHANICAL DEVICES BASED ON LAYERED NANOMATERIALS FOR SINGLE-BIOMOLECULE MASS SPECTROMETRY

new

Principal Investigator: Professor Xiankai SUN
*Department of Electronic Engineering and
Division of Biomedical Engineering, CUHK*

Project Start Date: 1 July 2015



ABSTRACT

The capability of determining the mass of biomolecules with high accuracy and fast speed has been playing a crucial role in proteomics for the development of molecular and cellular biology. Conventional mass spectrometers suffer from high cost, relatively large sample consumption, and low sensitivity. Nanoelectromechanical-system-based mass spectrometers can measure the proteins' mass directly. Landing of analyte (e.g., a protein) onto the device results in a variation of the resonator mass and thus shifts its resonant frequency. By tracking the frequency shift in real time, one can measure the mass variation, so as to determine the analyte species and quantity. However, the large parasitic capacitance and impedance mismatch inherent with the electrical transduction scheme limit the operation bandwidth and detection sensitivity.

Here we propose to develop nano-optomechanical devices based on layered nanomaterials (e.g., graphene, MoS₂, and black phosphorus) to obtain the ultimate sensitivity. The mass of the mechanical resonator is greatly reduced from that made in a traditional material, thus enabling a much higher resolution for detecting the analyte mass. By using optical methods for mechanical actuation and detection, we can obtain theoretically unlimited operation bandwidth and, more importantly, the ultimate detection sensitivity that is capable for resolving a single biomolecule..

PROJECT OBJECTIVES:

1. To design and simulate an optomechanical structure based on layered nanomaterials that is capable of detecting a single biomolecule for mass spectrometry
2. To establish an on-chip integration platform for single-biomolecule mass spectrometry that involves simultaneous measurements of photonic, electronic, and mechanical properties
3. To experimentally investigate the schemes of monolithic integration of nanophotonic circuits and nanomechanical resonators with layered nanomaterials
4. To fabricate an optomechanical device based on a layered nanomaterial and demonstrate its capability for single-biomolecule mass detection

LONG TERM IMPACT

Mass spectrometry has been playing a crucial role in proteomics for the development of molecular and cellular biology. Its capability to identify and precisely quantify proteins from complex samples has broad impact on biology and medicine. Conventional mass spectrometers measure electromagnetic properties of ionized biomolecules to determine their mass-to-charge ratios. However, this technique suffers from high cost, relatively large sample consumption, and low sensitivity.

Nanoelectromechanical system (NEMS)-based mass spectrometers measure mass of the proteins directly. Fabricated on an all-integrated platform, such spectrometers serve as an efficient interface between the frontend analyte and the backend outside world with the aid of CMOS integrated electronics. Landing of analyte (e.g., a protein) onto the device results in a variation of the resonator mass and thus shifts its resonant frequency. By tracking the frequency shift in real time, one can measure the analyte mass, so as to determine its species and quantity. However, the large parasitic capacitance and impedance mismatch inherent with NEMS limit the operation bandwidth and detection sensitivity.

To overcome this difficulty, we propose to develop nano-optomechanical devices based on layered nanomaterials (graphene, transition metal dichalcogenides, and black phosphorus) to obtain the ultimate sensitivity that a nanomechanical resonator could ever achieve. With a layered nanomaterial being the nanomechanical element, the mass of the mechanical resonator is greatly reduced from that made in a traditional material, thus enabling a much higher resolution for detecting the analyte mass. By using optical methods for mechanical actuation and detection, we can obtain theoretically unlimited operation bandwidth and, more importantly, the ultimate detection sensitivity that is capable for resolving a single biomolecule. The ability to detect single proteins in real time will eventually lead to the possibility of single-cell proteome profiling, an important milestone in both areas of biology and medicine.

DEVELOPMENT OF HIGH-SPEED LASER SCANNING MICROSCOPE FOR IN VIVO DEEP BRAIN IMAGING

Principal Investigator: Professor Shih-Chi CHEN

Department of Mechanical and Automation Engineering, CUHK

Co-Investigator (if any):
YUNG, Wing-Ho ⁽²⁾

Research Team Members:
WALKER, Steven ⁽²⁾, JIANG, Jun ⁽¹⁾
CHENG, Jiyi ⁽¹⁾, ZHANG, Dapeng ⁽¹⁾

⁽¹⁾ Dept. of Mechanical and Automation Engineering, CUHK

⁽²⁾ School of Biomedical Science, CUHK



Reporting Period: 1 July 2014 – 30 April 2015

ABSTRACT

This proposal aims to develop new imaging techniques for custom-designed laser scanning confocal and two-photon excitation (TPE) microscopes, including (1) tunable frame rate and (2) omnidirectional imaging. Current microscopes typically run at a fixed frame rate with a flat imaging plane. However, all biological subjects are “3-dimensional (3-D)” in nature and various biological events, e.g. blood flow or neuron signaling, occur at different time scales. Accordingly, a versatile microscope with capabilities of frame-rate tuning and a 3-D programmable imaging plane is highly desirable. The frame-rate tuning function can be achieved by a new synchronization circuit and related software development. Omnidirectional imaging, i.e. 3-D programmable imaging plane, is achieved by the introduction of a high-speed piezoelectric objective scanner. During the in-plane raster scan procedure, the objective lens can be moved to any arbitrary position in the Z axis, thus enabling the “omnidirectional scan”. These new functions will be used to investigate deep regions in brain in vivo and enable many new studies that cannot be realized in the past. Specifically, we will follow neuron axons (not in the same plane) in a mouse brain and identify their related neural circuits and simultaneously observe their signaling processes at high frame rate, e.g. 30 -1000 fps. We will perform deep brain calcium imaging of visual and motor cortical columns (400-800 μ m deep) and record from multiple hypercolumns in a single scan. Lastly, we will study and image dendritic spines and track the formation and disappearance of individual spines. These results will generate significant impact by elucidating the learning processes involved in visuomotor tasks.

1. OBJECTIVES AND SIGNIFICANCE

The objectives of this project include the development of new imaging modalities and functions for the confocal and TPE microscopes as well as the in vivo imaging and study of mice using the new microscope functions. For the new imaging techniques, we aim to achieve the following performance specs:

- (a) Tunable frame rate between 30 – 17, 280 frames per second with a constant pixel dwell time.
- (b) A 3-D programmable imaging plane that can follow different biological structures in space in vivo, e.g. blood vessels/neurons, and work with different frame rates.
- (c) The microscope can be operated in both fluorescence and reflectance modes and in both upright and inverted configurations.
- (d) A microscope system suitable for deep brain high-speed imaging, i.e. 0.8-1.2mm (depth).
- (e) The microscope should achieve 0.2/0.6 μ m lateral/axial resolution.

For in vivo deep brain imaging and study on mice, we like to achieve the following:

- (a) Develop an adaptive algorithm to identify neurons and related neural circuits based on calcium imaging.
- (b) Perform deep brain calcium imaging of visual and motor cortical columns to depths of 0.8mm, and record from hypercolumns, 0.5mm across, in a single scan.
- (c) Image dendritic spines and track the formation and disappearance of individual spines, as well as overall spine density, as a measure of the plastic changes in neural connectivity.
- (d) Correlate the circuit activity and dendritic spine morphological changes to elucidate the learning processes involved in visuomotor tasks.

Most breakthroughs in biology and medicine are driven by the advancement of new diagnostic tools and novel instrumentations. The successful completion of this work will enable scientists to image, discover, and study new biological phenomena that have never been seen; for example, to image and follow neuron axons in a mouse brain in vivo and observe their signaling processes at ultra-high frame rate, e.g. 1000 fps, or to image cancer cell trafficking in vivo. For the proposed brain imaging experiments, visuomotor coordination is a central component of human interaction with the environment. It enables an individual to manipulate objects, defend against physical threat and is vital for survival. However, to date little is known about them due to limited instrumentation performance. Our new microscope system enables an unprecedented ability to identify and record neurons/circuits of interest over an arbitrary path/plane and large effective volume, at high temporal and spatial resolution. Elucidation of such circuits and the corresponding neural computation may reveal strategies for visuomotor training, as well as rehabilitation or compensatory therapies in disorders such as brain trauma or visuomotor ataxia. Successful demonstration of this system will have a wider impact in neuroscience research, in which many other higher mammalian functions mediated by other areas of the neocortex can be investigated beyond existing capabilities.

2. RESEARCH METHODOLOGY

1. Development of the (1) frame rate tuning and (2) omnidirectional imaging modalities.

2. A head-fixated 2-dimensional forelimb lever manipulation task: *To address the computational function of the motor cortex (M1), we first develop a behavioral test in which the extrinsic parameters, e.g. forelimb kinematics and kinetics, are precisely controlled. Accordingly, we custom-built a two degrees of freedom planar robotic lever with which mice could interact using a single forelimb while head-fixated under the imaging system. A pair of quadrature rotary encoders is used to sense the lever joint angles and then solved for the end effector position in real-time using MATLAB software. Two servomotors are used to perturb the limb motion and/or provide physical resistance. Together, this system enables precise acquisition of both intrinsic and extrinsic limb parameters, which we hypothesize to be encoded within the circuits of the motor cortex.*

3. In vivo imaging of M1 during motor performance and learning: *Mice undergo surgery for AAV viral injection and implantation of a cranial window and head-fixation plate. The mice are allowed to recover for 3-4 weeks while the transgene is expressed in neurons. We use the genetically encoded calcium indicator GCaMP6 to report calcium transients during neuronal action potential. GCaMP6 is also expressed in dendritic spines; the formation and elimination of which is a form of morphological plasticity and associated with motor learning. We perform chronic imaging of the motor cortex as the mice are trained to perform the above tasks, and thus be able to dissect neuronal population activities in terms of its immediate computation as well as its spatiotemporal changes over the duration of training.*

3. RESULTS ACHIEVED SO FAR

The project has been progressing well and hitting all the milestones. Following, we describe the major results in three sub-sections:

3.1. Progress on microscope imaging modality development

We have successfully developed the frame rate tuning module and installed it on the two-photon microscope for in vivo experiments. The module enables flexible frame rate tuning ranging from 30Hz to 17,280Hz. In our approach, the higher frame rates are obtained at the expense of reduced field of view (instead of adjusting the scanning speed of polygonal scanner). Hence, the number of photons from each pixel/point is the same as

it runs at lower frame rates. In other words, the pixel dwell time does not change when frame rate is adjusted. This is important as in our system higher frame rates can be obtained without sacrificing the signal to noise ratio. However, it is worthy to note that as the same area is scanned more frequently at higher frame rates, specimens/tissue samples can be photo-bleached in a shorter amount of time. We have also carefully measured the point spread function of the multiphoton microscope to ensure the lateral and axial resolution achieves 0.2 and 0.6 μm respectively.

For omnidirectional imaging, we have successfully demonstrated the function using a high-speed piezoelectric objective scanner (400 μm stroke) with feed-forward control; the piezo-scanner is synchronized with the high-speed scanner (polygon mirror) and the secondary scanner (galvanometer). The custom-developed feed-forward controller is critical to solve the resonance problem introduced by the weight of the objective lens, which lowers the natural frequency of the piezo-scanner to around 60 Hz. The controller effectively improves the dynamic performance of the objective piezo-scanner and increases the cut-off frequency and decreases the phase lag. Figure 1 shows an example of real time omnidirectional imaging. The result of the work has led to the 2015 SPIE Photonic West poster competition award in the Multiphoton Microscopy session.

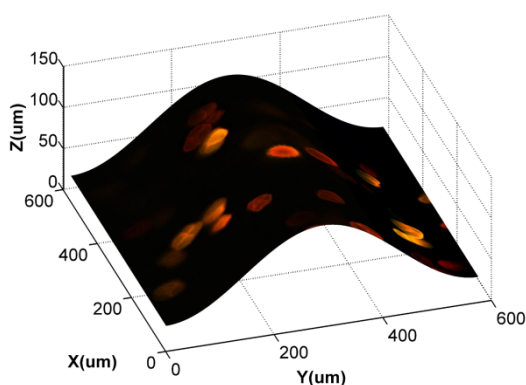


Figure 1: Pollen sample: An imaging plane is programmed to be sinusoidal

3.2. Progress on forelimb manipulation system & mouse training

We tested the forelimb manipulation system (described in Section 2.2) in a cue-response paradigm with no force feedback. A blue LED presented a cue for up to 30 seconds, during which a mouse must move the lever in both X and Y directions above a fixed distance, e.g. 5mm. The successful completion of the task led to the delivery of a 25 μL sucrose reward. Over four training days, the mice were acclimatized to the test, exhibiting a greater range of motion on the last day compared to the first day of training. We also observe a substantial increase in the mean travel per trial as well as overall performance. The results are shown in Figure 2.

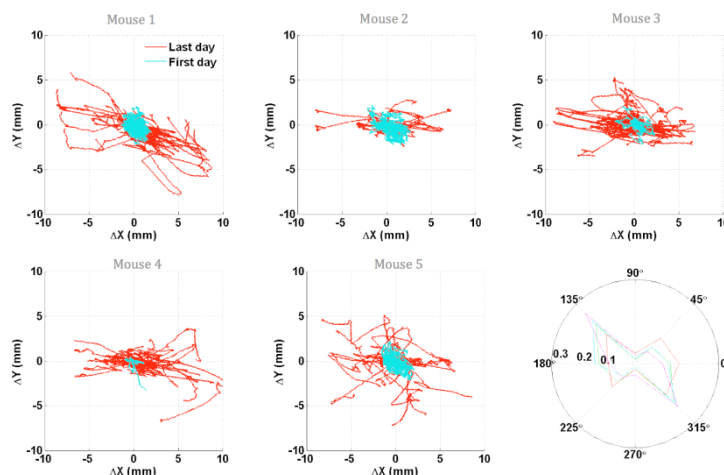


Figure 2: Training statistics of five mice over 4 training days, showing substantially improved success rate

To confirm the validity of our approach, we first recorded from the mouse M1 using a well-established in vivo extracellular recording system. By sorting the electrophysiological signal and aligning them with the onset of movements, we have identified neurons with firing phases that correspond to the movement in a particular direction (135°), as shown in Figure 3 below.

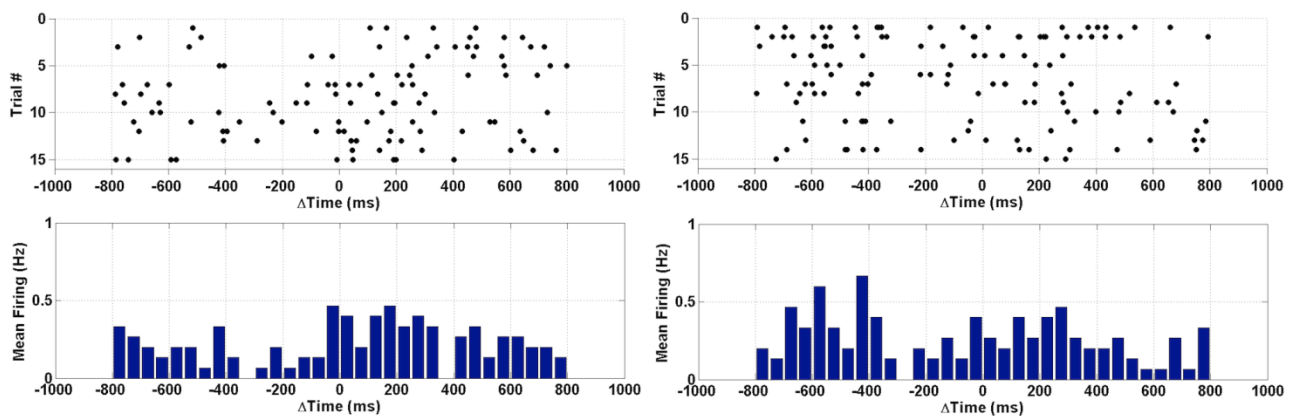


Figure 3: Raster and histogram plots for two neurons

3.3. Progress on in vivo deep brain imaging

We successfully injected the fluorescent calcium indicator Oregon Green Bapta-1 (OGB-1) into M1 of lever-trained mice, along with the astrocyte label sulforhodamine 101 (SR101). We obtained real-time two-photon images of the area, as shown in Figure 4. The green fibers indicate the apical dendrites of pyramidal neurons, and the red cell bodies are the labelled astrocytes. This work has established the viability of the behavioral test paradigm and its association with the region of interest in the brain, and can readily be studied using our custom-built in vivo two-photon microscope system in the next year.

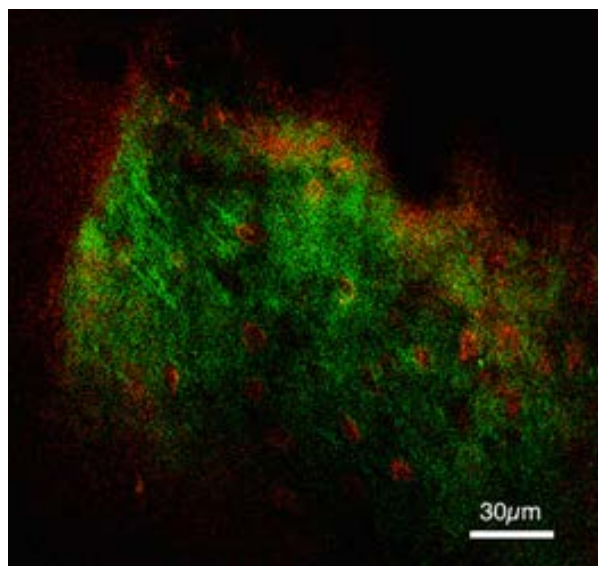


Figure 4: A real-time two-photon image of M1 using OGB-1 and SR101

4. PUBLICATION AND AWARDS

[1] J. Cheng, D. Zhang, and S. Chen, “Multi-photon Laser Scanning Omnidirectional Imaging with Tunable Frame Rate”, *2015 SPIE Photonic West*, San Francisco, USA. (Poster Competition Award)

MECHANISM FOR THE TRANSCYTOSIS OF TARGETED NANOPARTICLES ACROSS THE BLOOD-BRAIN BARRIER

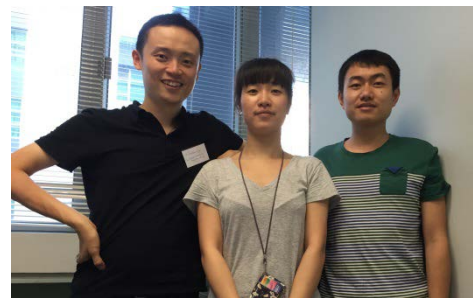
Principal Investigator: Professor CHOI Chung Hang, Jonathan ⁽¹⁾
Dept. of Electronic Engineering (Biomedical Engineering), CUHK

Research Team Members:

Dr. CHEN Zhong and Dr. ZHANG Lei ⁽¹⁾

⁽¹⁾ Dept. of Electronic Engineering (Biomedical Engineering), CUHK

Reporting Period: 1 September 2014 – 30 April 2015



ABSTRACT

In vivo delivery of therapeutics to the brain represents a significant challenge. Unlike small molecules such as nutrients or metabolic wastes, nanoparticles cannot easily penetrate through the blood-brain barrier (BBB), a layer of tightly packed endothelial cells that separates the brain from circulating blood, and accumulate in the brain in clinically relevant amounts. One non-invasive approach to directing intravenously administered nanoparticles across the BBB involves the attachment of ligands on the surface of nanoparticles for engaging receptors on the surface of brain endothelial cells. Such targeted nanoparticles are believed to enter, traverse, and exit the BBB by a process called “receptor-mediated transcytosis”. Unfortunately, transcytosis suffers from very limited delivery. To shed light on this delivery bottleneck, we seek to examine the fundamental interactions between targeted nanoparticles and the BBB *in vivo* at both cellular and subcellular levels.

1. OBJECTIVES AND SIGNIFICANCE

In this progress report, our team will focus our efforts on achieving the following two objectives.

Objective 1: Fabrication of targeted nanoparticles

- Preparation of ligands for engaging the receptors of brain endothelial cells (e.g., transferrin, DNA)
- Physicochemical characterization of inorganic nanoparticles (e.g., gold, iron oxide) that contain targeting ligands on their surface

Objective 2: Probing the cellular uptake properties of targeted nanoparticles *in vitro*

- Tuning the expression levels of tight-junction proteins
- Monitoring the uptake of nanoparticles by mouse brain endothelial cells

Armed with the preliminary data presented below, we will investigate how targeted nanoparticles can cross the BBB using a non-contact *in vitro* model in the next phase of the project. Ultimately, our results will guide the design of more effective nanoparticle-based agents to non-invasively treat and image diseases arisen from the central nervous system, such as cancer, stroke, and other neurodegenerative or psychiatric diseases.

2. RESEARCH METHODOLOGY

Synthesis of HS-PEG-transferrin (Tf)

HS-PEG-COOH (MW:5000; JenKem) was reacted with 5 molar excess of 1-(3-Dimethylaminopropyl)-3-ethylcarbodiimide hydrochloride (EDC) and 5 molar excess of *N*-hydroxysuccinimide (NHS) in 1 mL dichloromethane (DCM) at room temperature (RT) for 2 h. After

evaporating away the excess DCM, the product (HS-PEG₅₀₀₀-NHS) was washed with cold ether and stored at -20 °C. Next, different molar amounts of human holo-transferrin (Sigma) were reacted with HS-PEG₅₀₀₀-NHS in phosphate-buffered saline (PBS). The reaction proceeded for 1 h under gentle mixing at RT. HS-PEG₅₀₀₀-Tf was purified by dialyzing against a 50 kDa MWCO centrifugal filter (Millipore) and washed by Nanopure water at least three times.

Preparation of transferrin-targeted gold nanoparticles (Tf-PEG-AuNPs)

Gold nanoparticles (AuNPs) of 35 nm in diameter were prepared by following previously published methods¹. 50 molar excess of HS-PEG₅₀₀₀-Tf was added to a solution of 0.6 nM AuNPs. After stirring for 1.5 h, excess methoxy-PEG₅₀₀₀-SH (JenKem) was added to the reaction mixture and left to stir for another 1.5 h. The resultant Tf-targeted nanoparticles (Tf-PEG₅₀₀₀-AuNPs) were pelleted at 8,000×g for 10 min and re-suspended in 1 mL PBS to remove the free Tf-PEG₅₀₀₀-SH. The washing process was repeated twice.

Preparation of DNA-coated gold nanoparticle conjugates (DNA-AuNPs)

DNAs were synthesized on an Oligo-800 oligonucleotide synthesizer (Azco Biotech) using standard solid-phase synthesis and reagents (Azco Biotech). All DNAs were purified using an Agilent 1260 high performance liquid chromatography (HPLC) instrument with a Microsorb C18 column (Varian). Thiol-modified DNA oligonucleotides and AuNPs were incubated in 0.5×TBE buffer for at least 8 h at RT. Small aliquots of concentrated NaCl (5 M) was slowly added to the reaction solution till the final concentration of NaCl reaches 0.5 M. The DNA-AuNPs were purified by centrifuging them at 8,000×g for 10 min to remove the excess DNA. The washing process repeated twice, and the solution was re-suspended in 1 mL PBS.

Preparation of DNA-coated superparamagnetic iron oxide nanoparticles (DNA-SPIONs)

Carboxylate-terminated, PEG-coated SPIONs (PEG-SPIONs) were synthesized by thermal decomposition of ferric acetyl-acetonate (Fe(acac)₃)², and later purified to remove the excess PEG. Amine-modified DNA oligonucleotides were attached to PEG-SPIONs via DCC/NHS chemistry. Typically, 5 mg PEG-SPIONs was dissolved in 0.5 mL DMSO and activated with 20 μmol DCC and NHS for 2 h. Next, 6 nmol DNA was added to the mixture and left to stir overnight. The DNA-coated SPIONs (DNA-SPIONs) were dialyzed against Nanopure water by a centrifugal filter (MWCO: 50000) for at least three times.

Cell culture

bEnd.3 mouse endothelial cells (ATCC) were grown in a 10 cm tissue culture dish (BD Biosciences) at 37 °C with 5% CO₂. The growth medium consists of Dulbecco's Modified Eagle's Medium (DMEM) supplemented with 10% v/v fetal bovine serum (FBS) and 1% v/v penicillin–streptomycin.

3. RESULTS ACHIEVED SO FAR

Synthesis of DNA oligonucleotides

Our research team is capable of preparing DNA oligonucleotides of defined length or sequence and with special chemical modifications. Here, we show the synthesis and purification of DNA oligonucleotides of 30 bases long chemically conjugated with a fluorophore called FITC. Shown in Fig. 1 are typical HPLC and gel electrophoresis data for the preparation of fluorescent DNA oligonucleotides, which will prove to be useful when we move to the confocal immunofluorescence experiments in the next stage. In this progress report, we have utilized bioconjugate chemistry to prepare targeted nanoparticles that contain DNA oligonucleotides on their surface and subsequently investigated their ability to interact with brain endothelial cells (Fig. 5).

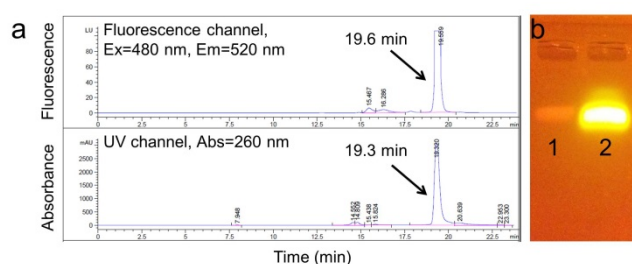


Fig 1. (a) HPLC chromatograms of FITC-modified oligonucleotides. Modified DNA that elute out of the HPLC column around 19 min show fluorescence emission at 520 nm (top) and UV absorbance at 260 nm (below), confirming modification of DNA with FITC. (b) Gel electrophoresis of non-fluorescent DNA (Lane 1) and FITC-modified DNA (Lane 2).

Synthesis of inorganic nanoparticles

Our group possesses the synthetic expertise of controlling the architecture (e.g., size, shape) of inorganic nanoparticles. Shown in Fig. 2 are typical methods for characterizing gold nanoparticles (AuNPs).

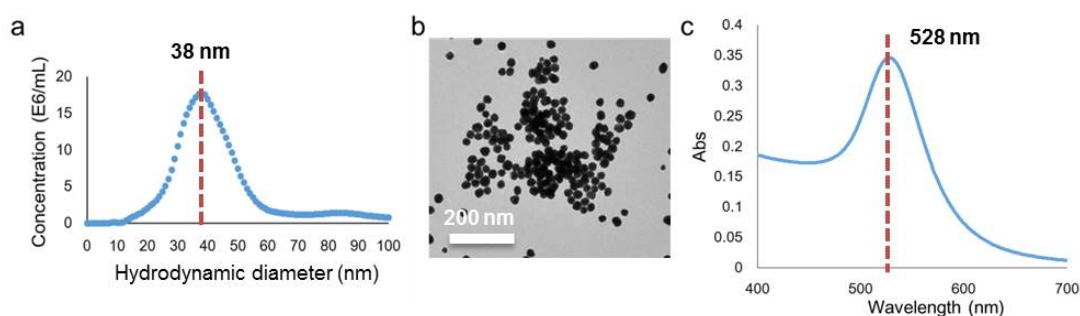


Fig 2 (a) Nanoparticle tracking analysis (NTA) shows that the unmodified AuNPs possess a hydrodynamic size of ~38 nm. (b) Representative TEM images reveal the near-spherical geometry of AuNPs. (c) The UV-Vis absorption data of AuNPs (with peak absorption at 528 nm) also agree with the NTA and TEM data.

Cellular uptake of transferrin-targeted nanoparticles

We have evaluated the potential of our as-synthesized targeted nanoparticles to enter brain endothelial cells *in vitro*. Here, we have used transferrin (Tf) as a model targeting ligand to engage the Tf receptors expressed on the surface of the brain endothelium. In particular, we have prepared AuNPs with varying amounts of Tf to engage Tf receptors on the surface of mouse brain endothelial cells (bEnd.3) *in vitro*. To probe the effect of Tf-mediated targeting, we have examined the cellular uptake properties of AuNPs coated with either bovine serum albumin (BSA) or Tf on the surface (Fig. 3a). Clearly, Tf-coated AuNPs can enter bEnd.3 cells more robustly than BSA-coated AuNPs, as evidenced by the intense red color indicative of the surface plasmon resonance of AuNPs. In addition, as the Tf amount increases, more AuNPs can enter bEnd.3 cells (Fig. 3b). In summary, our Tf-targeted nanoparticles are ready for delineating their transcytosis pathway in the next phase.

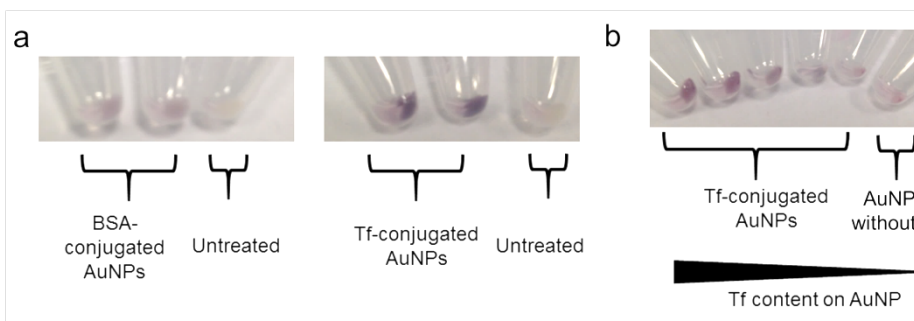


Fig 3 (a) AuNPs coated with can enter bEnd.3 cells more significantly than AuNPs coated with BSA. (b) The amount of AuNPs that enter bEnd.3 cells matches with the amount of Tf displayed on the surface of AuNPs.

Cellular uptake of DNA-targeted nanoparticles

DNA-coated nanostructures have received widespread attention due to their superior ability to enter multiple mammalian cell types. The PI previously showed that a dense, three-dimensional DNA shell on the surface of

inorganic nanoparticles allows for targeting of cell-surface Class A scavenger receptors (SR-A)³. Our team is now exploring whether this DNA shell will facilitate the nanoparticles to cross the BBB.

We have prepared AuNPs coated with either polyethylene glycol (PEG) or DNA (Fig. 4a). We expect that DNA-coated AuNPs can interact with SR-A on the surface of bEnd.3 cells whereas PEG-AuNPs cannot. By gel electrophoresis, DNA-AuNPs move along the applied electric field but not PEG-AuNPs, indicating that the AuNPs do contain the requisite DNA shell to interact with SR-A. Besides DNA-AuNPs, we have prepared superparamagnetic iron oxide nanoparticles (SPIONs) that are coated with DNA on their surface (Fig. 4b-c). By TEM imaging and gel electrophoresis, we have demonstrated that these DNA-SPIONs are near-spherical and negatively charged (~-32 mV), confirming the attachment of the DNA shell to the surface of SPIONs. By applying a magnetic field, we have demonstrated that these SPIONs exhibit superparamagnetic properties at RT (Fig. 4d), paving the way for performing *in vivo* MRI of the brain in the next phase of the project.

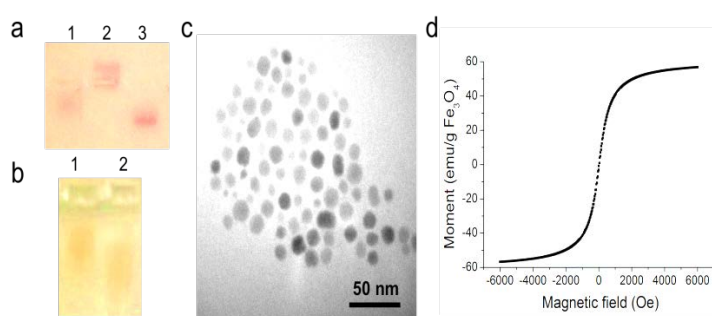


Fig. 4 (a) Gel electrophoresis of (1) citrate-capped AuNPs, (2) PEG-coated AuNPs, and (3) DNA-coated AuNPs. (b) Gel electrophoresis of (1) PEG-coated SPIONs and (2) DNA-coated SPIONs. The downward movement of AuNPs and SPIONs confirms successful conjugation of DNA. (c) TEM images of PEG-SPIONs show a near-spherical geometry. (d) The SPIONs exhibit superparamagnetic magnetization behavior.

Adenosine-mediated targeting: A new approach to crossing the BBB

Adenosine receptors (ARs) can influence the permeability of the BBB. When their ligands, adenosine, are presented to the BBB at high concentrations, the tight-junction proteins that constitute the BBB will become down-regulated, causing transient increase in the permeability of macromolecules across the BBB. Here, we hypothesize that enhancement in the concentration of adenosine near the BBB (e.g., in the form of NPs) can facilitate permeation across the BBB. As a proof-of-concept, we have chosen claudin-5 as a model tight junction protein. Shown in Fig. 5 are immunofluorescence data on the expression level of claudin-5 in bEnd.3 cells treated with DNA-AuNPs of different nucleobase compositions. Strikingly, the expression levels of claudin-5 was drastically reduced when bEnd.3 cells were incubated with poly A coated AuNPs, but not poly T (thymine) coated AuNPs. In addition, claudin-5 levels were reduced only when these cells were treated with poly A coated AuNPs but not single-stranded polymer of A, underscoring the effect of the nanoparticle architecture on modulating the response of AR. Our team is excited about these novel findings and will investigate the potential of using poly A AuNPs to cross the BBB *in vivo* in the next phase of the project.

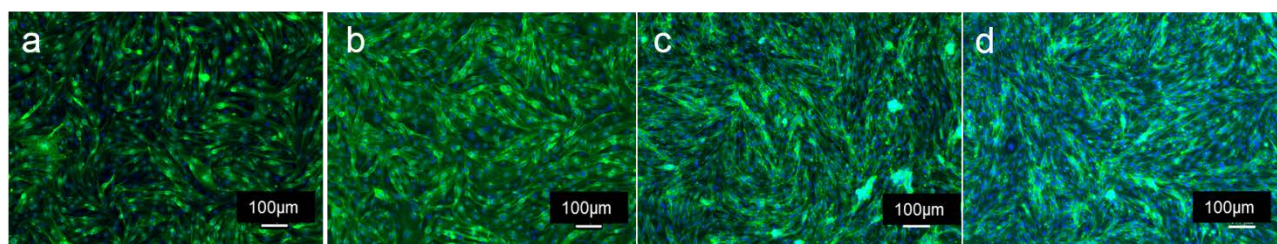


Fig 5 bEnd.3 cells incubated with (a) poly A AuNPs have noticeably reduced expression of claudin-5 than the (d) untreated cells. By contrast, cells incubated with (b) poly T AuNPs express similar levels of claudin-5 as the (d) untreated cells. Intriguingly, when these cells were incubated with single-stranded polymer of A, the level of expression of bEnd.3 cells did not reduce appreciably. Legend: Green = claudin-5; Blue = nucleus.

References:

1. N. G. Bastús, J. Comenge and V. Puntes, *Langmuir*, 2011, **27**, 11098-11105.
2. Q. Jia et al., *J. Am. Chem. Soc.*, 2011, **133**, 19512-19523.
3. C. H. J. Choi et al., *Proc. Natl. Acad. Sci. USA*, 2013, **110**, 7625-7630

DEVELOPMENT OF THE NEXT GENERATION NEUROSURGICAL ASSISTANT SYSTEM BASED ON FUNCTIONAL BRAIN MAPPING

Principle Investigator: Professor Defeng WANG ^(1,4)
Department of Imaging and Interventional Radiology, CUHK

Co-Investigator: Winnie Chiu-wing CHU ⁽¹⁾, Kwok Chu WONG ⁽²⁾, Lin SHI ^(1,3)
 Research Team Members: LIU Kai, PhD Student ^(1,4), SUN Xiaofei, MPhil Student ^(1,4)

⁽¹⁾ Department of Imaging and Interventional Radiology, CUHK

⁽²⁾ Department of Neurosurgery, CUHK

⁽³⁾ Department of Medicine and Therapeutics, CUHK

⁽⁴⁾ Department of Biomedical Engineering and Shun Hing Institute of Advanced Engineering, CUHK



Reporting Period: 1 July 2013 – 30 April 2014

ABSTRACT

Functional magnetic resonance imaging (fMRI) has become a promising approach to accurate function mapping for neurosurgery plan. However, children and patients suffering from developmental brain disorders have difficulties in performing high demand tasks but an alternative approach of resting state fMRI (rsfMRI) without any task required. Several research efforts were dedicated to develop assistant systems based on rsfMRI, which however, still cannot achieve the clinically acceptable efficiency and reliability. Besides, existed methods are developed for adults, which are not suitable for children with the changes of functional connectivity across the developmental age. Our objective is to develop a new generation neurosurgical assistant system based on functional brain mapping. We will propose an efficient and robust approach to determine the correlated functional regions with the advanced sparse representation model. Functional network templates will be constructed for several functions in multiple age stages. The functional mapping result will be integrated to build an efficient navigation system with the electromagnetic tracking device for neurosurgery plan. The developed technology will help to provide optimal plan and precise navigation to improve the efficiency and safety of the clinical neurosurgery, which decrease the risk of functional deficits after neurosurgery.

1. OBJECTIVES AND SIGNIFICANCE

- To identify the functional areas before neurosurgical removal of brain lesion to prevent the risk of functional deficits but the current gold standard approach is in a way of invasive cortical mapping. rsfMRI would be an alternative approach to gather functional information of brain areas;
- The purpose of this proposal is to develop a computational system based on functional brain mapping to guide neurosurgical planning and provide a precise navigation in clinical neurosurgery;
- The proposed navigation system would determine the correlated functional regions with the advanced sparse representation model;
- A functional network templates will be constructed for several functions in multiple age stages;
- The system will be able to perform data acquisition and preprocessing procedure for young children. Detailed data sampling parameters and scanning time will be tested to obtain proper data acquisition procedure;
- The functional correlated regions will be determined from the high dimensional rsfMRI
- The navigation system would provide information for better surgical planning and navigation during the surgery.
- The navigation system would increase the accuracy in removing brain lesion and avoid unnecessary removal to retain the maximum brain function as much as possible.

2. RESEARCH METHODOLOGY

The technology to be developed in this project will enable precise localization of functional areas to aid practical uses in clinical neurosurgical planning and surgical navigation. This novel technology includes data acquisition and preprocessing, detection of correlated regions, network templates construction, automatic identification of functional networks, development of navigation system, system validation and testing.

2.1 Data acquisition and preprocessing

The resting state functional magnetic imaging (rsfMRI) will be acquired at the Shanghai Huashan Hospital and the Prince of Wales Hospital. The optimal parameters will be obtained after several tests of scanning. An effective method will be adopted to preprocess the acquired data for subsequent analysis using the SPM8 tool. Considering the fact that head motion during long acquisition time may cause misalignment across the scans at the different time, images alignment is important for subsequent analysis. In order to enable the subsequent voxel-wise data analysis, the aligned images will be registered to a standard template. Besides, due to the low signal-to-noise ratio of the rsfMRI data, image smoothing will be leveraged to remove the random noises. The strategy of data acquisition and preprocessing will be completed in the first 2 months.

2.2 Detection of functional correlated regions

We will introduce an efficient and robust approach for detection of functional correlated regions from the high dimensional rsfMRI dataset by incorporating the prior knowledge of the brain function of young children. Several detection models have been proposed to identify the correlated regions. Commonly used methods are independent component analysis (ICA) method and seed ROI base approach. The ICA method is time consuming and depends on the number of orders. Therefore, the seed ROI model will be utilized as the basic model.

2.3 Network templates construction

We will construct multiple functional network templates to guide the precise selection of functional areas. To enable automatic identification of functional networks, templates of each function should be first constructed. An effective template construction algorithm will be first advanced to generate templates. Since there are changes of functional connectivity of the young children across the developmental ages, multiple templates will be computed at different ages. The default mode, visual, auditory, language and motor will be investigated for young children in six age stages: 0-2, 3-4, 5-6, 7-8, 9-10 and 11-12 years of age. Initial templates will be chosen with the prior knowledge from the neuroscience research.

2.4 Identification of functional networks

An automatic method will be developed to identify the corresponding functional networks from extracted multiple networks. With a given individual subject, templates will be chosen considering the age and type of function. A similarity measurement method will be developed to compute the similarity values between all the components and the templates. The components with the highest similarity values will be chosen as the function network. This algorithm and its implementation will be accomplished within the 12 months.

2.5 Development of navigation system

The developed components will be integrated to build an efficient navigation system. The electromagnetic tracking device will be utilized to measure the real-time position of surgical tools and fiducials attached to the patient's anatomy. The functional mapping results will be coded with different color and then visualized by overlaying on the high-resolution anatomical T1 MRI data. The diffusion tensor images and magnetic resonance angiography will also be integrated to make more precise location. The key modules of location, tracking, and registering processing will be implemented using the Image-Guided Surgery Toolkit (IGSTK). All the developed modules will be integrated into the framework of the Medical Imaging Interaction Toolkit (MITK) to establish a system with a high degree of interaction. The software will be compatible with commonly used OS of Windows, Macintosh, and Linux. The system will be validated on 200 subjects, including 100 normal and 100 patients.

3. RESULTS ACHIEVED SO FAR

We have published 5 peer-reviewed journal articles and 2 conference articles. In these publications, we have developed a new technique to enhance MR image quality using feature-preserving denoising method, a new technique to perform DTI segmentation, a brain atlas based on Chinese pediatric population and a fractional anisotropy and mean diffusivity analysis on adolescents.

Magnetic resonance imaging (MRI) is an outstanding medical imaging modality. To improve the signal to noise ratio is always a great challenge due to images suffer from noise pollution during image acquisition and transmission. Our publication presents a new technique to enhance image quality using feature-preserving denoising method. Most existing MRI denoising methods have not simultaneously take the global image prior and local image features into account. The denoising method in this publication is implemented based on an assumption of spatially varying Rician noise map. It takes full advantage of the global MR image prior and local image features. Numerous experiments have been conducted on both synthetic and real MR data sets to compare our model with some state-of-the-art denoising methods. The experimental results have demonstrated the superior performance of our proposed model in terms of quantitative and qualitative image quality evaluations [1]. This technique enhances the image quality and completed the task on section 2.1.

DTI scanning is one of the most reliable scanning to reveal the white matter fiber tracks and spinal cord. Results from previous studies demonstrated that some kind of diseases such as adolescent idiopathic scoliosis (AIS) affects the spinal cord, and the connectivity and morphology of the brain included cerebellum. To further study the physiology, morphology, and connectivity of the fiber track in human brain and spinal cord, we have developed a new technique to improve the performance of DTI segmentation. To overcome the disadvantages of requiring adequate prior knowledge and tuning parameters in other techniques, our new method automatically learns an adaptive distance metric by a graph based semi-supervised learning model [2]. Besides DTI segmentation, we have also developed a new technique on GPU-accelerated image registration based on the FLIRT Algorithm [10].

An accurate and representative brain atlas could help in neurosurgery. We have developed a high quality representative brain atlas based on Chinese pediatric population using Intensity and sulci landmark. It is important on medical image analysis and could also be useful for image guide surgeries. The newly constructed atlas can better represent the size and shape of brains of Chinese pediatric population [3]. We have constructed a probabilistic atlas of default mode network (DMN) from resting-state fMRI [5]. We have also developed a brain template based on Chinese children and adolescent [7] and measured the structural network on Chinese Children with Developmental Dyslexia [9]. These works have partially completed tasks in section 2.2 and 2.3.

From our previous studies, we know that the tonsil level in AIS was more negative than that in normal and the somatosensory evoked potentials (SSEP) was disturbed in AIS at above the vertebral C5-6 level. We postulated that the integrity of the spinal cord would have been affected and could be demonstrated by measuring the mean diffusivity (MD) or fractional anisotropy (FA) using DTI. Our recent publication has verified our hypothesis, which we found significantly decreased FA values and increased MD values at the medulla oblongata and C1-2, C2-3, C3-4, and C4-5 segments in patients with AIS compared with healthy subjects [4]. We have also predicted the occurrence of cerebral hyperperfusion syndrome (CHS) using pre- and post-operative change in cerebral blood flow (CBF) on patients with Moyamoya disease after surgery [6, 11], and have mapped the visual functions of dorsal and ventral Stream [8]. These works have partially completed section 2.4.

For section 2.5, we have started to build a navigation system using non-rigid registration to transform preoperative images into intraoperative space for functional data visualization in Image-Guided neurosurgery [12]. We have submitted our preliminary work and it be continued in the next few months to finalize the navigation system.

4. PUBLICATION AND AWARDS

Peer-reviewed journal articles:

- [1] Liu RW, Shi L, Huang W, Xu J, Yu SC, Wang D, Generalized total variation-based MRI Rician denoising model with spatially adaptive regularization parameters. *Magnetic Resonance Imaging*, Elsevier Science Inc, Amsterdam, 2014 Mar 18. pii: S0730-725X(14)00086-1. doi: 10.1016/j.mri.2014.03.004. [Epub ahead of print]
- [2] Kong Y, Wang D, Shi L, Hui SC, Chu WC, Adaptive distance metric learning for diffusion tensor image segmentation. *PLOS One*, Public Library of Science, San Francisco. 2014 Mar 20;9(3):e92069. doi: 10.1371/journal.pone.0092069. eCollection 2014.
- [3] Luo Y, Shi L, Weng J, He H, Chu WC, Chen F, Wang D, Intensity and sulci landmark combined brain atlas construction for Chinese pediatric population. *Human Brain Mapping*, Wiley-Blackwell, New Jersey. 2014 Jan 17. doi: 10.1002/hbm.22444. [Epub ahead of print]
- [4] Kong Y, Shi L, Hui SCN, Wang D, Deng M, Chu WCW, Cheng JCY, Variation in Anisotropy and Diffusivity Along Medulla Oblongata and the Whole Spinal Cord in Adolescent Idiopathic Scoliosis: A Pilot Study Using Diffusion Tensor Imaging, *American Journal of Neuroradiology*, American Society of Neuroradiology, Oak Brook. 2014 Aug; vol. 35 (In press)
- [5] Defeng Wang, Youyong Kong, Winnie CW Chu, Cindy WC Tam, Linda CW Lam, Yilong Wang, Georg Northoff, Vincent CT Mok, Yongjun Wang, Lin Shi, Generation of the Probabilistic Template of Default Mode Network Derived from Resting-State fMRI, *IEEE Transactions on Biomedical Engineering* (accepted)

Conference articles:

- [6] Defeng Wang, Ka Ming Fung, Lin Shi, Fengping Zhu, Ying Mao. Evaluation of Surgical Outcome of Moyamoya Disease Patients after Revascularization using Atlas-based Magnetic Resonance Brain Perfusion Analysis. European Congress of Radiology. Mar. 6-10, 2014. Vienna Austria. DOI: 10.1594/ecr2014/C-0192
- [7] Wong Kok Cheung, Luo Yishan, Shi Lin, Chen Feiyan and Wang Defeng, "Template Building For Chinese Children And Adolescent And Comparison With Western Standard Template", The Conjoint Congress of 18th Convention of Academia Eurasiana Neurochirurgica (AEN) 11th Asia Pacific Multidisciplinary Meeting for Nervous System Diseases (Brain Symposium), Hong Kong, Mar 5-8, 2014

Submitted articles:

- [8] Yan-Jia Deng, Lin Shi , Vincent Mok, Winnie Chu, Defeng Wang, Anil T. Ahuja. Mapping the Visual Functions in Dorsal and Ventral Stream using Activation Likelihood Estimation. (Under review at Human Brain Mapping)
- [9] Kai Liu, Lin Shi, Feiyan Chen, Mary MY Waye, Vincent CT Mok, Winnie CW Chu, Defeng Wang. Increased Local Segregation of Brain Structural Network in Chinese Children with Developmental Dyslexia (Under review at Cortex)
- [10] Defeng Wang, Ping Liu, Lin Shi, Ang Li, Wen-Hua Huang, Jing Qin, Pheng-Ann Heng, Anil T., Ahuja. GPU-accelerated Image Registration based on the FLIRT Algorithm. (Under review at Journal of Medical Systems)
- [11] Defeng Wang, Fengping Zhu, Ka Ming Fung, Wei Zhu, Yishan Luo, Winnie CW Chu, Vincent CT Mok, Jinsong Wu, Lin Shi, Ying Mao. Predicting Cerebral Hyperperfusion Syndrome Following Superficial Temporal Artery to Middle Cerebral Artery Bypass based on Intraoperative Perfusion-Weighted Magnetic Resonance Imaging (Under review at Neurosurgery)
- [12] Defeng Wang, Yishan Luo, Junfeng Lu, Winnie CW Chu, George KC Wong, Vincent CT Mok, Lin Shi, Jinsong Wu. Non-rigid Registration of Preoperative Images with Intraoperative Images for functional data visualization in Image-Guided Neurosurgery. (Under review at Human Brain Mapping)

BIOMIMETIC SCAFFOLD FOR STEM CELL BASED CARTILAGE REGENERATION AND DRUG DELIVERY

Principal Investigator: Professor BIAN Liming ⁽¹⁾
Department of Mechanical and Automation Engineering, CUHK

Co-Investigator:
Arthur MAK ⁽¹⁾

Research Team Members:
ZHU Meiling, FENG Qian, WEI Kongchang, LI Jinming ⁽¹⁾

⁽¹⁾ Dept. of Mechanical and automation Engineering

Reporting Period: 1 July 2013 – 30 April 2014



ABSTRACT

Osteoarthritis (OA) is symptomized as progressive degeneration of articular cartilage in human diarthrodial joints. A recent study in Hong Kong found that about 10% of the Hong Kong population aged 50 years and older can be diagnosed with knee osteoarthritis [1]. This showed that osteoarthritis is one of the major causes of disability among the Hong Kong population just as in the rest of the world. Current treatments including arthroplasty and mosaicplasty have various major limitations such as limited life span, lack of donor tissue, etc.

hMSCs (human mesenchymal stem cells) have gained increasing popularity as a cell source for cartilage repair, due to their multipotency and easy availability. However, after firstly differentiating (chondrogenesis) into chondrocytes (cartilage cells) like cells, hMSCs continue to differentiate toward a hypertrophic phenotype, resulting in extensive mineralization of the neocartilage formed, which should be free of mineralization. This problem, which motivates this proposed work, is now being recognized as a major obstacle to the widespread adoption of hMSCs as a clinically viable cell source for cartilage repair.

Glycosaminoglycan (GAG) is a key component of the cartilage extracellular matrix (ECM). Sulfated glycosaminoglycans have been shown to maintain the activity of growth factors. Sulfated glycosaminoglycans also attract cations including calcium ions with their negative charges, thereby changing the calcium concentration in the intercellular tissue environment and potentially influencing tissue mineralization. The project proposes to chemically incorporate the sulfate groups into biomaterial scaffold to emulate the biochemical properties of the native cartilage cellular microenvironment. This will allow us to investigate the role of sulfation in regulating hMSC chondrogenesis and subsequent hypertrophic tissue mineralization.

The results of the project will not only help the development of new stem cell therapies for cartilage repair, but will also guide the design of novel scaffold materials for repairing defects in interfacial regions including ligament/tendon to bone insertions and cartilage to bone interfaces.

1. OBJECTIVES AND SIGNIFICANCE

Objective 1: synthesize crosslinkable sulfated glycosaminoglycan biopolymers for the fabrication of hydrogel scaffold.

Objective 2: investigate the effect of sulfated hydrogel scaffolds made of sulfated glycosaminoglycan on the

retention of chondrogenic growth factors.

Objective 3: examine the effect of sulfated hydrogel scaffolds made of sulfated glycosaminoglycan on chondrogenic differentiation of hMSCs.

Objective 4: examine the effect of sulfated hydrogel scaffolds made of sulfated glycosaminoglycan on hypertrophic differentiation of hMSCs and resulting matrix mineralization.

Impact and novelty

The findings from this study will shed light on the influence of scaffold sulfation on drug delivery from biomaterial scaffold. Furthermore, it will also provide guidance on the design of biomaterial scaffold to better control hMSC differentiation and cartilage mineralization. Moreover, mineralization is found in many other connective tissues including bone, menisci and intervertebral discs either as a required developmental process or as a pathological condition. Therefore, the findings from this study will not only enhance hMSC-based cartilage repair but will also be instrumental in developing stem cell based therapies to regenerate or repair other musculoskeletal tissues including bone, menisci and intervertebral discs.

The novelty of this work lies in three aspects. Firstly, the retention and stability of chondrogenic growth factors in sulfated hydrogels has not been thoroughly investigated before; secondly, few previous studies have examined the effects of sulfation of hyaluronic acid on chondrogenesis. Lastly, no prior studies have studied the effect of hydrogel sulfation on hMSC hypertrophy and matrix mineralization following chondrogenesis.

2. RESEARCH METHODOLOGY

Methacrylation of hyaluronic acid (HA)

Methacrylated hyaluronic acid (molecular weight 70kD) (MeHA) will be synthesized as previously reported [23, 34-36] (**Figure 1**). Briefly, methacrylic anhydride (methacrylic anhydride, Sigma) is added to a solution of 1 wt% HA or CS in deionized water, adjusted to a pH of 8 with NaOH, and left to react on ice for 24 hours. The macromer solution will be purified via dialysis (MW cutoff 6–8kD) against deionized water for a minimum of 48 hours with repeated changes of water. The final product will be obtained by lyophilization and stored at -20 °C prior to use. The degree of methacrylation of final macromer products will be evaluated by ¹H NMR.

Preparation of MeHA Sulfates (S-MeHA)

Since chondroitin sulfate is a sulfated glycosaminoglycan, no additional sulfation of CS is needed. The sulfation of MeHA (HA is a nonsulfated glycosaminoglycan) will be carried out based on an adapted protocol describe previously. Briefly, MeHA will be dissolved in deionized water to produce 1% w/v solution. The solution will be stirred with 3 gram of Dowex-100 ion exchanger added for each gram of MeHA (tetrabutylammonium-form) for 8 hours. After filtration, the polymer solution will be lyophilized and dissolved in DMF at 1% w/v under N₂. Sulfur trioxide/dimethylformamide complex (SO₃-DMF) dissolved in DMF will be added to the TBA-MeHA solution in DMF (molar polymer/SO₃ ratio 1:20) under N₂ at room temperature. The reaction solution will stirred for 60 min. The sulfated products will be purified by precipitation into acetone and neutralized using ethanolic NaOH solution. The formed S-MeHA will be washed several times with acetone and purified by dialysis against distilled water, followed by lyophilization. The degree of sulfation of the S-MeHA will be determined using an automatic elemental analyzer.

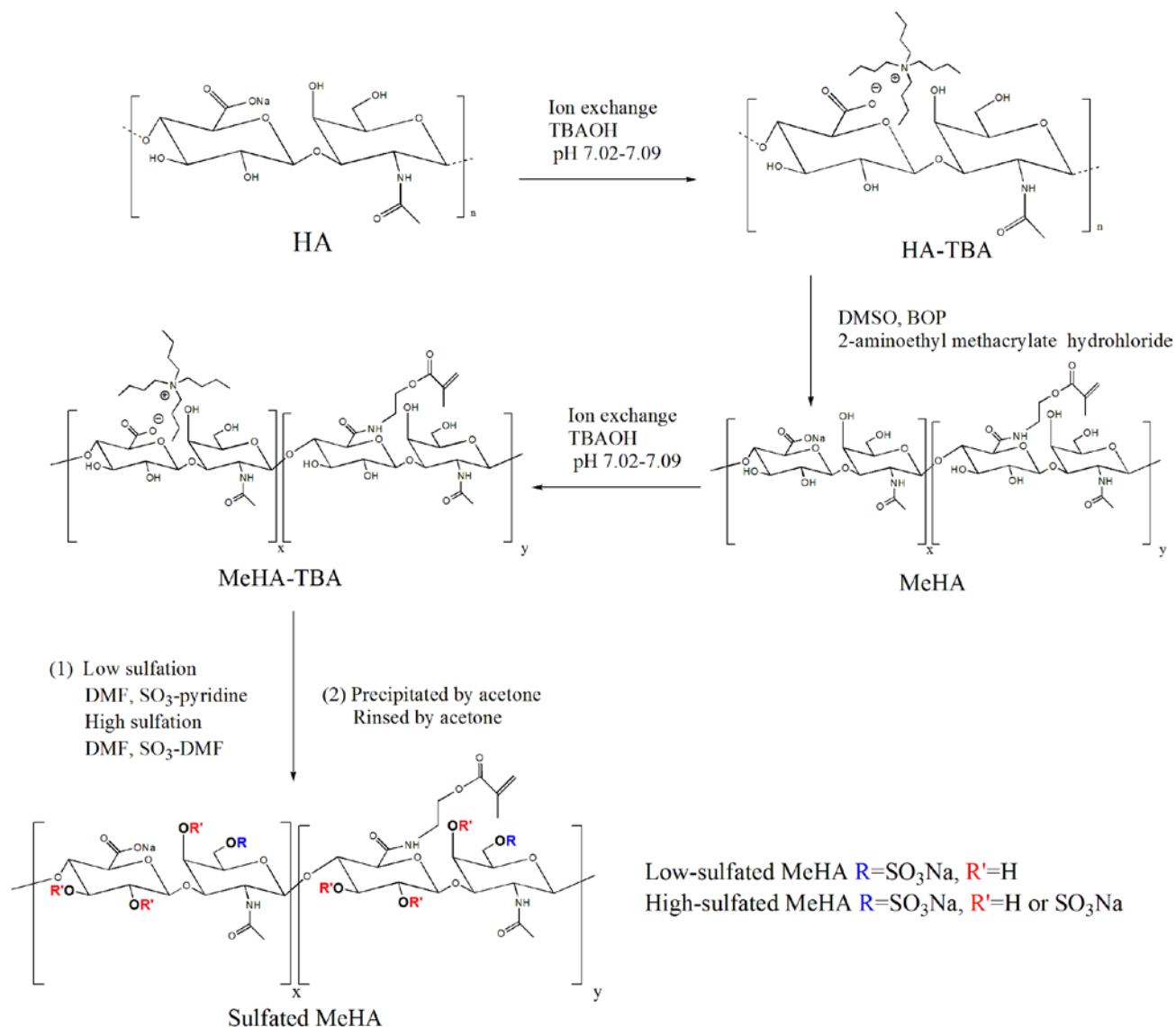


Figure 1. Synthesis of MeHA and S-MeHA

Objective 2

Quantification of the release of encapsulated molecules form hydrogels

Acellular hydrogels will be fabricated by photopolymerization of precursor solutions comprised of MeHA, S-MeHA dissolved in phosphate buffered saline (PBS) containing 0.05 wt% of the photoinitiator I2959 (2-methyl-1-[4-(hydroxyethoxy) phenyl]-2-methyl-1-propanone, Ciba) to allow for UV-mediated polymerization (**Figure 2 A without cells**). The precursor solutions will be exposed to ultra-violet light (UV time: 12 minutes, wavelength: 360nm; intensity: 1.2mW/cm²) for gelation. Gelation will be assessed by monitoring the storage (G') and loss (G'') modulus using a rheometer in a cone and plate geometry. Standard protein molecules used in release studies including bovine serum albumin (BSA, FITC tagged) will be mixed with the precursor solutions and subsequently encapsulated in the hydrogel upon gelation. The hydrogels samples will be incubated in PBS at 37 ° C. The release of the fluorescently tagged BSA will be quantified by a fluorescence microplate reader.

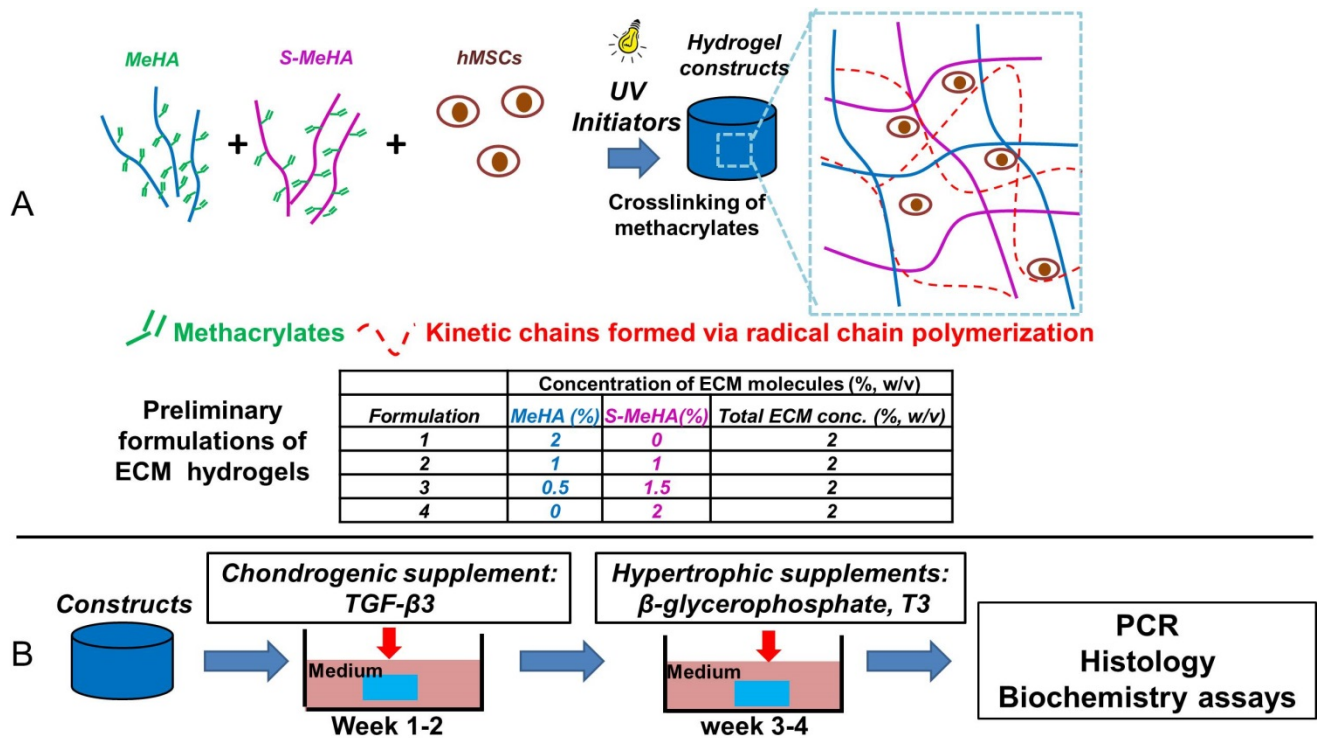


Figure 2. (A) Fabrication of sulfated ECM hydrogels via photocrosslinking. (B) *in vitro* culture of hMSC-seeded hydrogels for chondrogenic and hypertrophic differentiation.

Objective 3 & 4

hMSC encapsulation in hydrogels and chondrogenic and hypertrophic induction

Human MSCs (Lonza) will be expanded to passage 3 in a growth media consisting of α -MEM with 16.7% FBS (fetal bovine serum). MSCs (20 million/ml) will be encapsulated in hydrogel disk constructs as described above (\varnothing 5mm, 2.6 mm thickness) (Figure 2 A). Formed constructs will be cultured in chondrogenic media (DMEM, 1% ITS+Premix, 50 μ g/ml L-proline, 0.1 μ M dexamethasone, 50 μ g/ml ascorbate, antibiotics) supplemented with transforming growth factor (TGF- β 3, 10ng/ml)(Figure 2 B)[37]. To evaluate hypertrophy and resulting mineralization by hMSC, a previously established *in vitro* culture model will be employed. Briefly, constructs will be first cultured in chondrogenic media for 2 weeks. Media will be then switched to hypertrophic induction media (1nM dexamethasone, 1nM triiodothyronine/T3 and 10mM β -glycerophosphate/ β -gly) from week 3 through week 4 (Figure 2 B)[38].

Gene expression analysis

Gene expression of chondrogenic (type II collagen, Aggrecan, Sox9) and hypertrophic markers (type X collagen, MMP13, ALP/alkaline phosphatase) at selected time points will be analyzed by real time PCR. Sequences of the primers and probes are listed in a previous publication [31]. The relative gene expression will be calculated using the $\Delta\Delta$ CT method, where the fold difference will be calculated using the expression $2^{\Delta\Delta C_t}$. Each sample will be internally normalized to GAPDH and the expression levels of MSCs at the time of encapsulation.

Biochemical analysis

The PicoGreen assay (Invitrogen) will be used to quantify the DNA content of the constructs. The GAG content will be measured using the dimethylmethylene blue (DMMB) dye-binding assay. The overall collagen content will be assessed by measuring the orthohydroxyproline content via the dimethylaminobenzaldehyde and chloramine T assay. Calcium content will be quantified using a commercial kit (BioVision).

Histological analysis

Constructs will be fixed in 4% formalin, embedded in paraffin, and processed using standard histological

procedures. Immunohistochemical staining will be performed on histological sections (8 μm thick) for targets of interest using the Vectastain ABC kit and the DAB Substrate kit for peroxidase (Vector Labs).

Statistical and power analysis

Statistica (Statsoft) will be used to perform statistical analyses using two-way ANOVA, followed by Tukey's HSD post hoc testing to allow for comparison between groups. Statistical significance will be set at $p < 0.05$. A statistical power analysis indicates that $n=8$ samples per group should be sufficient for obtaining a study power of 0.85 with significance set at $p < 0.05$.

3. RESULTS ACHIEVED SO FAR

Objective 1: we have successfully synthesized sulfated methacrylated hyaluronic acid (HA) with varying degree of sulfation. The synthesis protocols have been established for modifying hyaluronic with both methacrylate groups and sulfate groups sequentially. The synthesis products were evaluated using NMR to confirm and quantify these two modifications on hyaluronic acid. The results show that both methacrylate and sulfate groups were successfully conjugated to hyaluronic acid backbone (Figure 1). For the sulfation, low and high level of sulfation was successfully achieved by controlling the reaction parameters during synthesis (Figure 2).

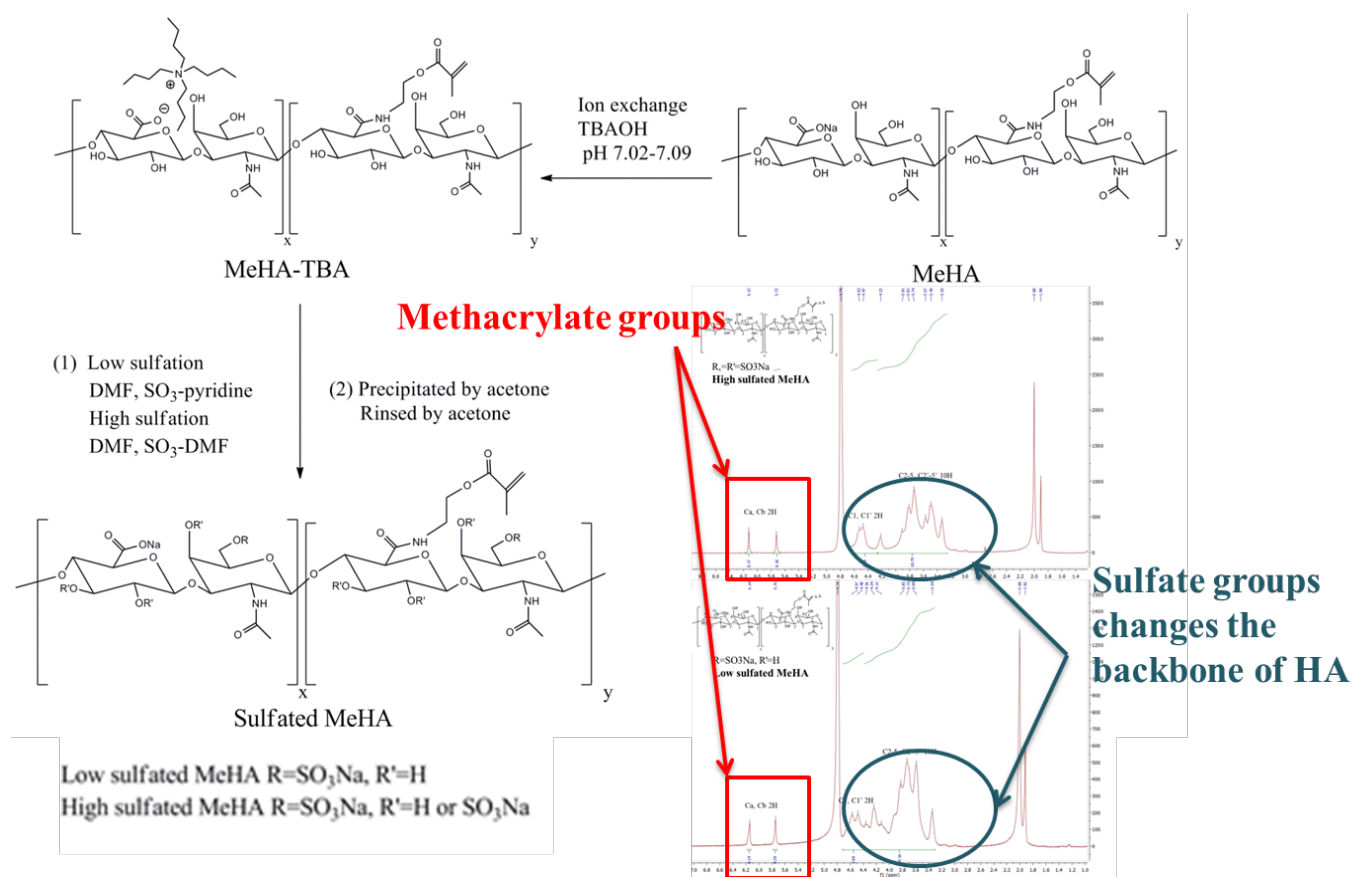


Figure 1. NMR results of the methacrylated HA (MeHA), low-sulfated and high-sulfated MeHA, indicate successful conjugation of methacrylate and sulfate groups to the HA backbone.

Energy Dispersive Spectrometer (EDS)

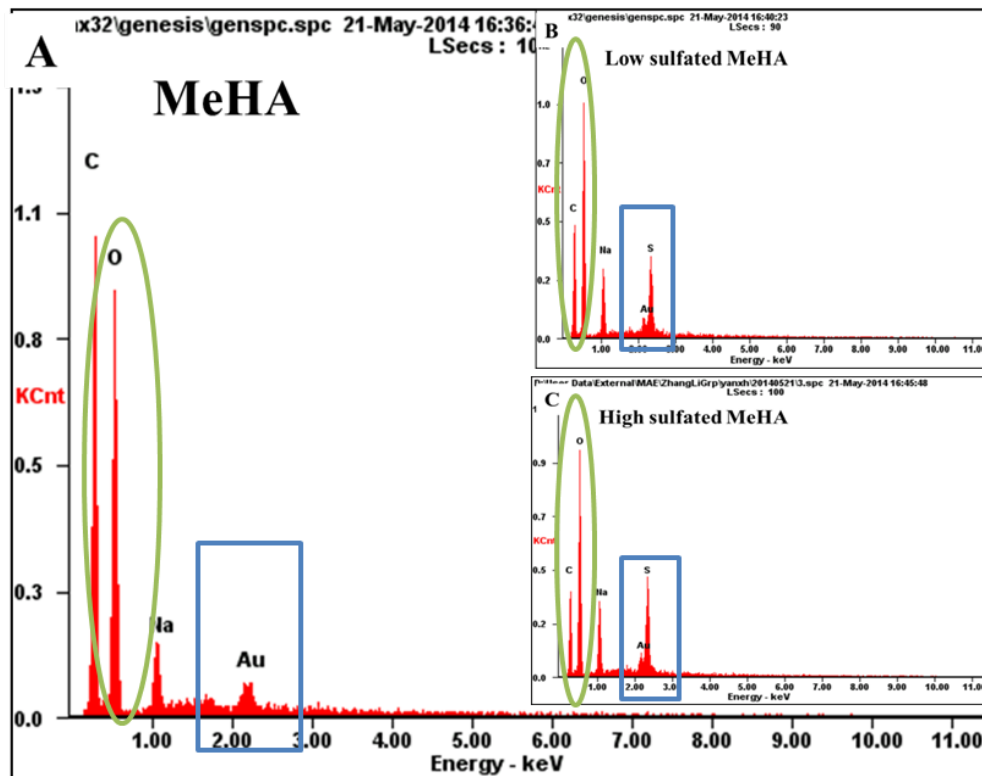


Figure 2. EDS results of the methacrylated HA (MeHA), low-sulfated and high-sulfated MeHA, confirms successful conjugation of different amount of sulfate groups to the HA backbone.

Objective 2: hydrogels have been fabricated using sulfated methacrylated HA (both low and high sulfation MeHA). This demonstrated that the methacrylate groups conjugated are capable of being crosslinked to form hydrogels. DMMB dye staining of the hydrogels confirmed that the different levels of sulfation on the HA molecules are retained in the hydrogels (Figure 3).

Dimethylmethylene blue (DMMB) dye

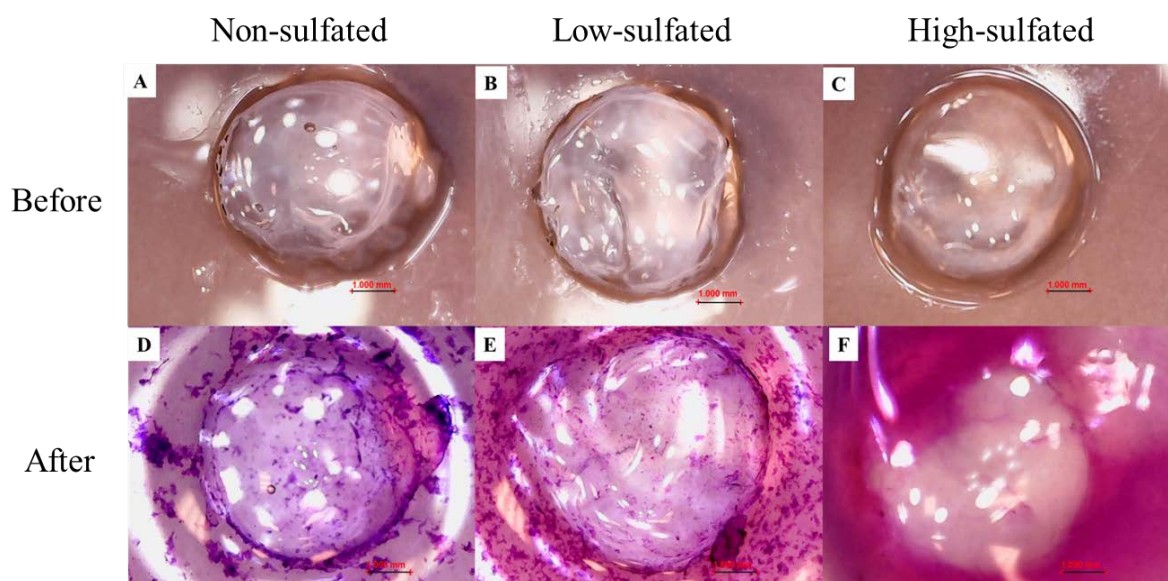


Figure 3. DMMB staining of the fabricated MeHA, low-sulfated and high-sulfated MeHA hydrogels shows more purplish staining in the sulfated hydrogels confirming the presence of sulfate groups.

Objective 3&4: non-sulfated MeHA hydrogels have been evaluated for human mesenchymal stem cells (hMSCs) encapsulation and chondrogenic differentiation. Results show that MeHA hydrogels support chondrogenesis leading to extensive cartilage matrix synthesis by the differentiated stem cells. An in vitro culture model for inducing hypertrophy of the chondrogenically differentiated hMSCs in HA hydrogels has been established (Figure 4). Calcification resulted from stem cell hypertrophy are detected by histology staining. These evaluation and culture protocols will be used to evaluate hMSC differentiation and hypertrophy in the sulfated MeHA hydrogels in the second year.

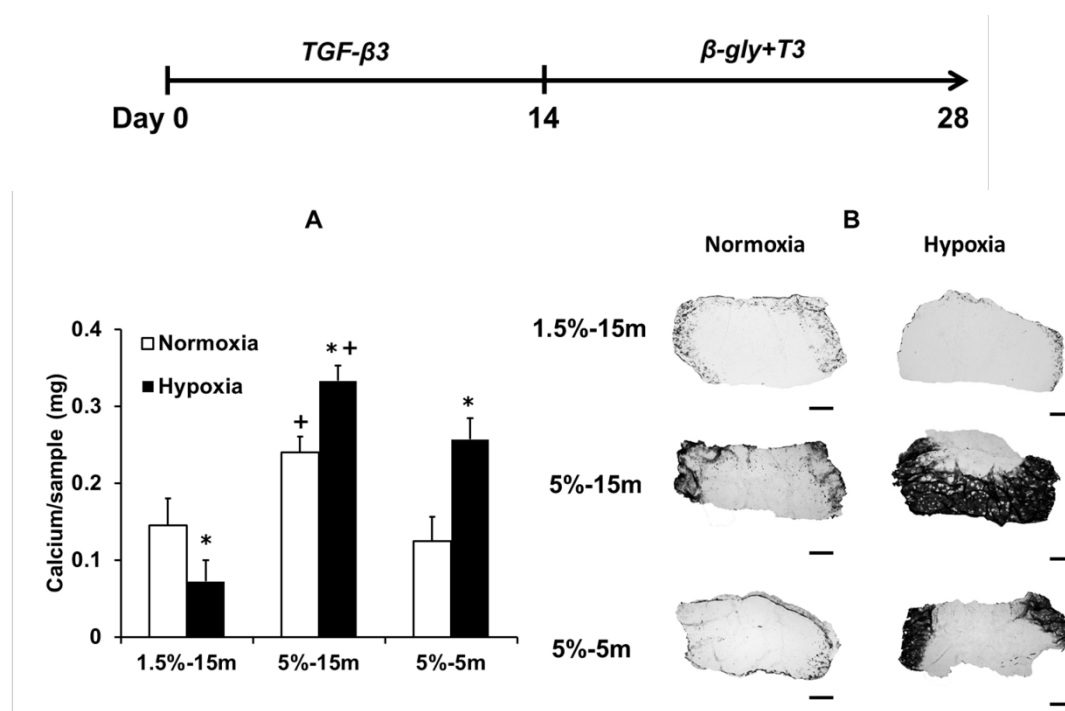


Figure 4. In vitro stem cell hypertrophy protocol has been established and will be used in the next step to investigate the effect of scaffold sulfation on stem cell hypertrophy [1]. Dark staining in the figure shows calcification of the scaffold due to stem cell hypertrophy.

4. PUBLICATION AND AWARDS

(*corresponding author)

[1] Feng, Q.; Zhu, M.; Wei, K.; *Bian, L. Cell-mediated degradation regulates human mesenchymal stem Cell chondrogenesis and hypertrophy in MMP-sensitive hyaluronic acid hydrogels. *PLOS ONE*, accepted for publication, 2014 May (IF=3.73)

[2] Zhu, M.; Feng, Q.; *Bian, L. Differential effect of hypoxia on human mesenchymal stem cell chondrogenesis and hypertrophy in hyaluronic acid hydrogels. *Acta Biomaterialia*, 10(3):1333-40. 2014 Mar. (IF=5.09)

DIELECTROPHORESIS NANO-SEPARATOR FOR PRECISION MANUFACTURING OF POLYMERIC NANOPARTICLES FOR TUMOR-TARGETED DRUG DELIVERY

Principal Investigator: Professor CHEN Shih-Chi ⁽¹⁾
Department of Mechanical and Automation Engineering, CUHK

Co-Investigators:

KUNG Hsiang-Fu ⁽²⁾, LIN Marie ⁽³⁾, LI Wen Jung⁽⁴⁾

Research Team Members:

YANG Shih-Mo ⁽¹⁾, YAO Hong ⁽²⁾, TIAN Yuan ⁽²⁾

⁽¹⁾ Dept. of Mechanical and Automation Engineering, CUHK

⁽²⁾ Stanley Ho Centre for Emerging Infectious Diseases, Faculty of Medicine, CUHK

⁽³⁾ Department of Surgery, Prince of Wales Hospital, CUHK

⁽⁴⁾ Department of Mechanical and Biological Engineering, City University of Hong Kong

Project Start Date: 1 July 2012
Completion Date: 30 June 2014



ABSTRACT

This research aims to develop a dielectrophoresis (DEP)-based high-throughput nanoparticle separation technology that enables precise separation of polymeric nanoparticles for cancer-targeted drug delivery. Studies suggest that precise control of nanoparticles' sizes and surface charges may (1) further improve the effectiveness of the treatment and (2) reduce the related toxicity level. However, due to the solution-based nanoparticle fabrication procedure, to date there has not been any method reported in literature to precisely control the sizes and surface charges of nanoparticles for cancer-targeted treatment. In this project, we have developed multiple DEP-based nano-separators that can collect and separate nanoparticles according to their specific dimensions, e.g. $100\text{nm} \pm 10\text{nm}$, and surface charges. In particular, a new droplet-based microfluidic device was developed not only for particle separation but also automating the nanoparticle synthesis and fabrication processes on-chip, which substantially improve the throughput of nanoparticle preparation time. PEI-CyD-FA mediated polymeric nanoparticles, a promising new cancer-targeting drug developed by our team, were used in the DEP device for separation experiments. We performed a series of *in vitro* experiments on cells as well as *in vivo* experiments on mice. The results proved the on-chip fabricated/separated polymeric nanoparticles possess superior transfection efficiency and reduced cytotoxicity.

1. OBJECTIVES AND SIGNIFICANCE

The overall goal of the proposed research is the development of DEP nano-separator devices that can be used to separate and collect polymeric nanoparticles of various sizes. High-throughput nanoparticle separation has been demonstrated via the new DEP nano-separators, enabling the precision control of nanoparticles size distribution, ranging from 50 nm to 300 nm. We have performed both *in vitro* and *in vivo* studies to validate the efficacy of DEP separated nanoparticles as well as to study the toxicity of DEP treated nanoparticles. The results will be used to guide the development of tumor/cancer-targeted drug delivery for improved performance and reduced toxicity.

Application of the developed DEP-separation technology to nanomedicine and pharmaceutical industry will generate significant impact in the following ways: (1) more precise and specific drug targeting and delivery, (2) reduction in toxicity while improving therapeutic effects, (3) greater control of safety and compatibility, and (4) realization of low cost, high-precision pharmaceutical and medicine manufacturing.

2. RESEARCH METHODOLOGY

1. Model, design and fabricate high-throughput DEP nano-separators optimized for nanoparticle separation.
2. Fabricate and characterize polymer nanoparticle with DEP nano-separator:
 - Prepare the polyplexes of H1/pDNA including H1 synthesis, plasmid expansion and polyplexes formation.
 - DEP separation method: Mix DNA and H1, $N(H1)/P(pcDNA) = 20/1$ in 2.5% glucose solution, standing for 10 min. Let polyplexes pass through DEP chip under four voltage and frequency conditions for nanoparticle collection. Wash DEP chip without electric field and collect the blocked polyplexes from the outlet.
 - Characterization of the quantity, particle size and zeta potential of both the passed and blocked polyplexes.
 - Determine transfection efficiency of the polyplexes on 293T cells by observing the quantity of EGFP positive result in cells after 24 hours.
3. Perform in vivo mice study to investigate the efficacy of the separated polymeric nanoparticles.

3. RESULTS ACHIEVED

3.1. Development of DEP nano-separator and initial results

In the first year, we have designed and fabricated several DEP nano-separators based on our parametric model for polymer nanoparticle (H1/pDNA polyplexes) separation. Figure 1A shows the image of the micro-fabricated DEP device; Fig 1B shows the zoom-in view of the DEP electrodes in the microchannel that generates the AC electric field for particle trapping. Figure 2A shows the results of nanoparticle separation experiments based on the first-generation DEP device. These results indicate that the size of the separated particles was well controlled with a narrow distribution ($\sigma = 10 \sim 50$ nm), which validates that our physical model is correct and the fabricated DEP devices can effectively block both particles of smaller and larger sizes; this is attributed to the combined effects of the nonuniform electric field distribution on the H1/pDNA polyplexes and its interaction with the nonuniform AC electric field generated by the DEP device.

Before the animal experiments, we used the separated polyplexes to treat the cells in vitro in order to verify their effectiveness is not affected by the DEP separation procedure (Transfection dose: $40 \mu\text{L}/\text{well}$ on 293T cells for 24 hours). The results from the cells, shown in Fig 2B, indicate our H1/pDNA polyplexes has improved transfection efficiency after separated by the DEP nano-separator.



Figure 1: (A) First generation DEP nanoparticle sorting chip; (B) Optical image of electrodes and microchannel.

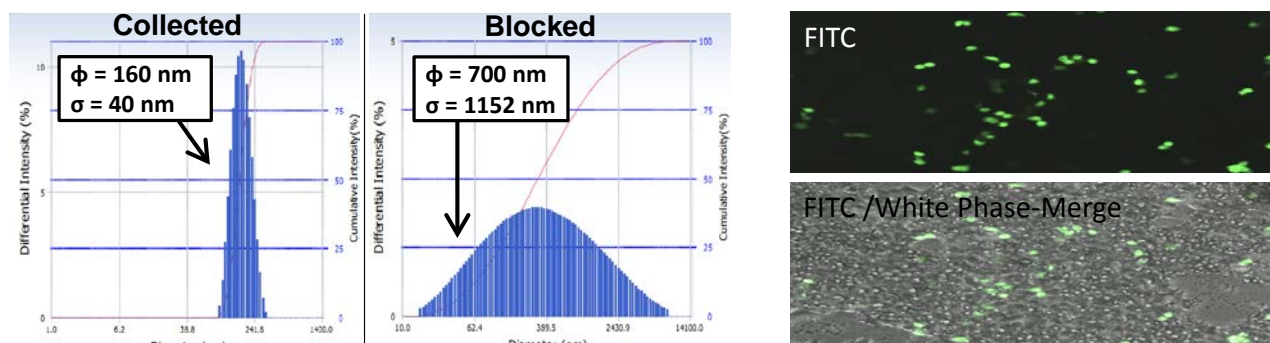


Figure 2: (A) Particle size distribution characterized for both collected and blocked solution; (B) fluorescent image of cells treated with DEP filtered nanoparticle, indicating good transfection efficiency.

3.2. Second generation DEP nano-separator and *in vitro* experimental results

To further improve the effect of particle separation as well as to integrate many time-consuming nanoparticle preparation steps into a single micro-device, a second generation DEP nano-separator was developed based on a novel droplet technique. In a droplet-based system, the H1 and DNA are packaged into a droplet for mixing and assembling (droplets are separated by oils). Since a droplet only has a volume around 1 nanoliter, it intrinsically provides better uniformity and higher reaction speed. After the nanoparticles are fabricated in droplets, they are collected from an on-chip oil-water separation mechanism. The nanoparticles are then sent to the DEP region for finer particle separation. The new microfluidic device that integrates these functions is shown in Fig 3. Specifically, the device automates five critical steps in the nanoparticle fabrication/separation process: (1) formation of H1 and DNA droplets, (2) H1 and DNA mixing, (3) H1 and DNA self-assembling, (4) H1-DNA product extraction, i.e. oil/water separation, and (5) DEP selection for specific particle sizes.

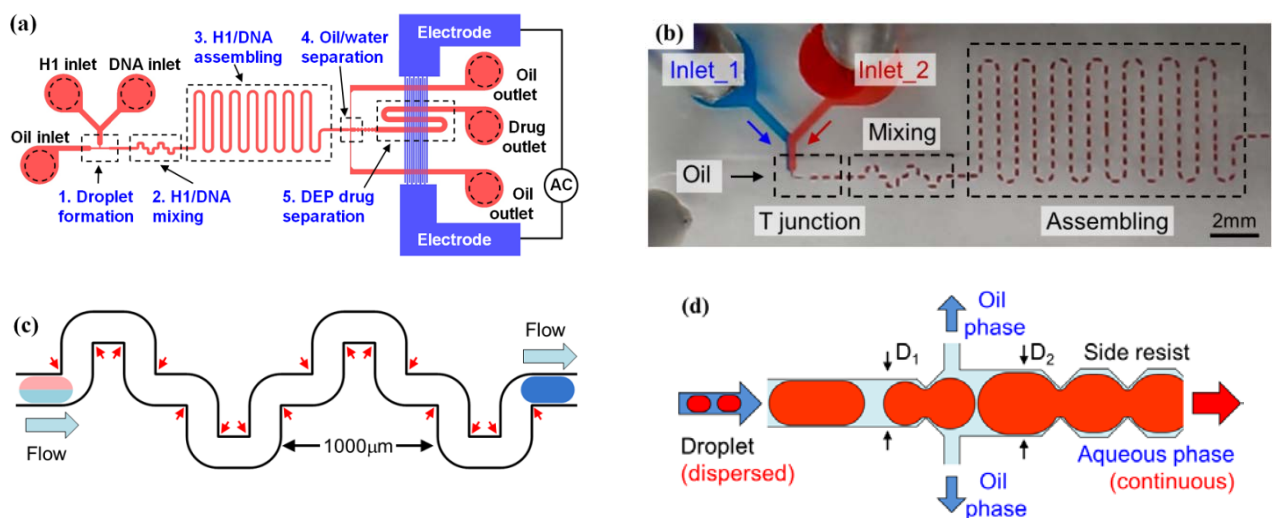


Figure 3: (A) Schematic diagram of the microfluidic chip integrated with droplet-based microfluidic channels and DEP traps via interdigitated metal electrodes. Five regions serve different functions: droplet formation, H1 and DNA mixing and assembling, product extraction and particle separation; (B) Image of the droplet generator, reagent mixing and nanoparticles assembly region on the device; (C) Sixteen right-angled corners, indicated by red arrows, were designed to generate chaotic advection for rapid reagent mixing; (D) Schematic diagram of the passive droplet-oil separator. The expanding channel width and a series of triangular structures assist in reducing the droplet velocity and effective droplet merging. The oil component is automatically expelled to the side microchannels by the compression of two converging droplet surfaces.

For DEP particle separation, we implemented a new electrode design in the device as shown in Fig 4. Compared with the previous design with four electrodes, the new design utilizes 11 electrodes with the microchannel going through the electrode region three times. This design further improves the nanoparticle separation efficiency, as shown Figure 4A and 4B. In addition, finite element analysis was performed to simulate the steady-state electric field for better understanding and predicting the particle separation mechanism. The results are shown in Fig 4C, where the root mean square of an AC electric field (E^2) distribution is shown inside the microchannel. The nanoparticle with negative DEP force passed through the electrodes and was collected at the outlet port for the next step of drug delivery efficiency testing.

To validate the effectiveness of the droplet-based DEP microdevice, we examine the size distributions of nanoparticle under three conditions: (1) manual mixing in Eppendorf, (2) mixing in droplets (on-chip) without DEP and (3) mixing in droplets with DEP. The size distribution of nanoparticles was characterized by the DelsaTM Nano, as shown in Fig 5A- 5C.

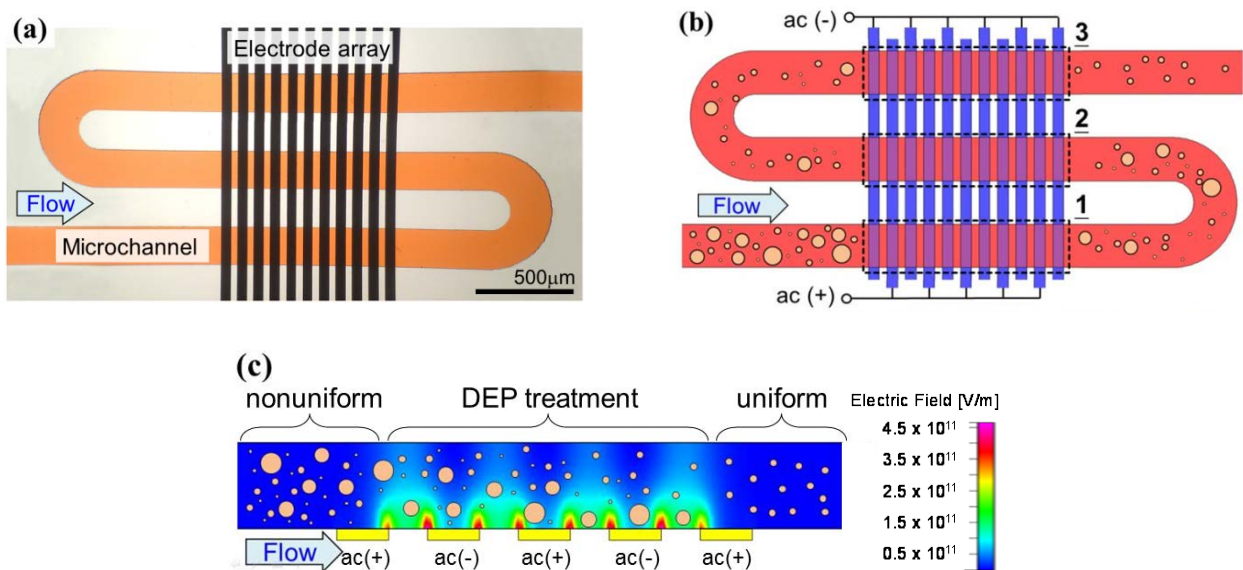


Figure 4: Design of DEP electrodes for particle separation: (A) Image of metal electrodes with a microfluidic channel filled with red dye; (B) Schematic diagram of DEP separation. Nanoparticles are driven by fluidic forces and passed three times through the DEP working regions, indicated by dotted lines; (C) Side view of the flow channel above the electrodes, plotted with the non-uniform AC electric field. Note that the polyplexes of larger sizes are attracted to the bottom electrodes.

For the control group, (i.e., manual mixing), 1 c.c. of H1 and 1 c.c. of DNA solution were mixed in Eppendorf, followed by 10 minutes of static resting for particles assembling, shown in Fig 5A. For the on-chip method without DEP, the H1 and DNA solutions were injected from the inlet ports for self-assembly with a processing time of 1 minute, shown in Fig 5B. Comparing Fig 5A and 5B, the results show that the size of polyplexes assembled in nanoliter volume had a narrower distribution. The peak polyplex diameters in the control group and droplet-based device group were 185.9 nm and 137.2 nm, respectively. These results showed that the mixing efficiency of our droplet-based platform in nano-scale volumes is high (10 times faster) and that the products are more uniform.

Under condition (3), 8Vpp at 20MHz was applied to the electrodes for DEP treatment in the bottom of the microchannel after the polyplexes passed through the water-oil separation region. Polyplexes polarized by positive DEP effect were then attracted to the glass substrate, where the electric field was strong. Nanoparticles that experienced negative DEP force passed through three DEP regions and were collected at the outlet port. The results of the DEP treatment are plotted in Fig 5C, showing an even narrower size distribution that peaked around 116.3 nm and the majority of the larger particles were effectively trapped by the electrodes.

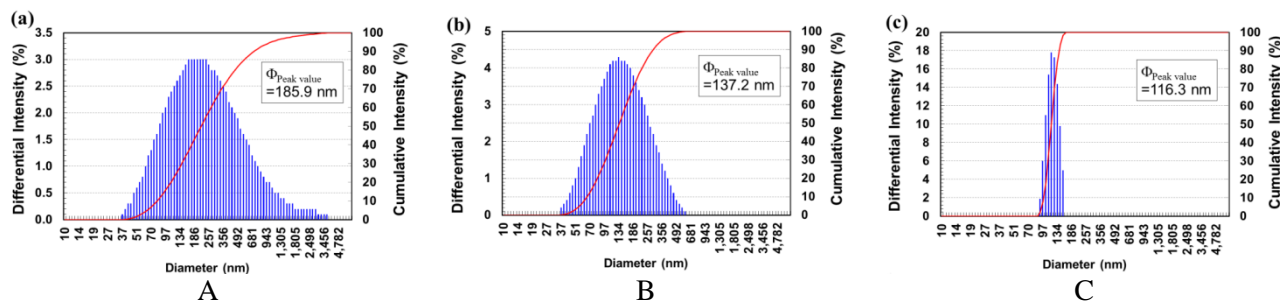


Figure 5: Size distribution for H1-DNA polyplexes: (A) Manual mixing in Eppendorf; (B) On-chip mixing in droplets without DEP; (C) On-chip mixing in droplets with DEP. The results suggest droplet-based method produces more uniform polyplexes and DEP may be used for precise nanomedicine fabrication.

The early results reported in Section 3.1 show DEP separated nanoparticles can improve cell transfection efficiency. For the second generation device, we devised a set of experiments to examine the cell transfection efficiency with various DEP parameters as well as to investigate the toxicity reduction effect with more uniform nanoparticles. A phase control microscope assay of EGFP positive cells was used to evaluate the transfection efficiency of H1/pLuc nanoparticles *in vitro*. Figure 6A shows representative photos of GFP positive cells in hepG2 cells that were transfected under various DEP conditions. The related histogram is presented in Fig 6B, where all DEP treated cases show improved transfection efficiency. Among them, condition 3 (20 MHz, 8Vpp) shows the highest transfection efficiency. Figure 6C presents the cell viability test results of HepG2 cells determined by the MTT assay, which most cases treated with DEP processes show significantly improved cell viability than the non-separated case (NDEP) of the same dose. This indicates the DEP separation technique can reduce the cytotoxicity of H1/pDNA nanoparticles *in vitro*. As condition 3 shows the best result, it is used in all future experiments including *in vivo* experiments on mice. This transfection efficiency experiment also indirectly validated that the smaller-sized polyplexes were effectively collected after DEP treatment. The biological results indicate that the microfluidic design and the concept of DEP nanoparticle separation have potential applications in drug delivery and nanomedicine fabrication.

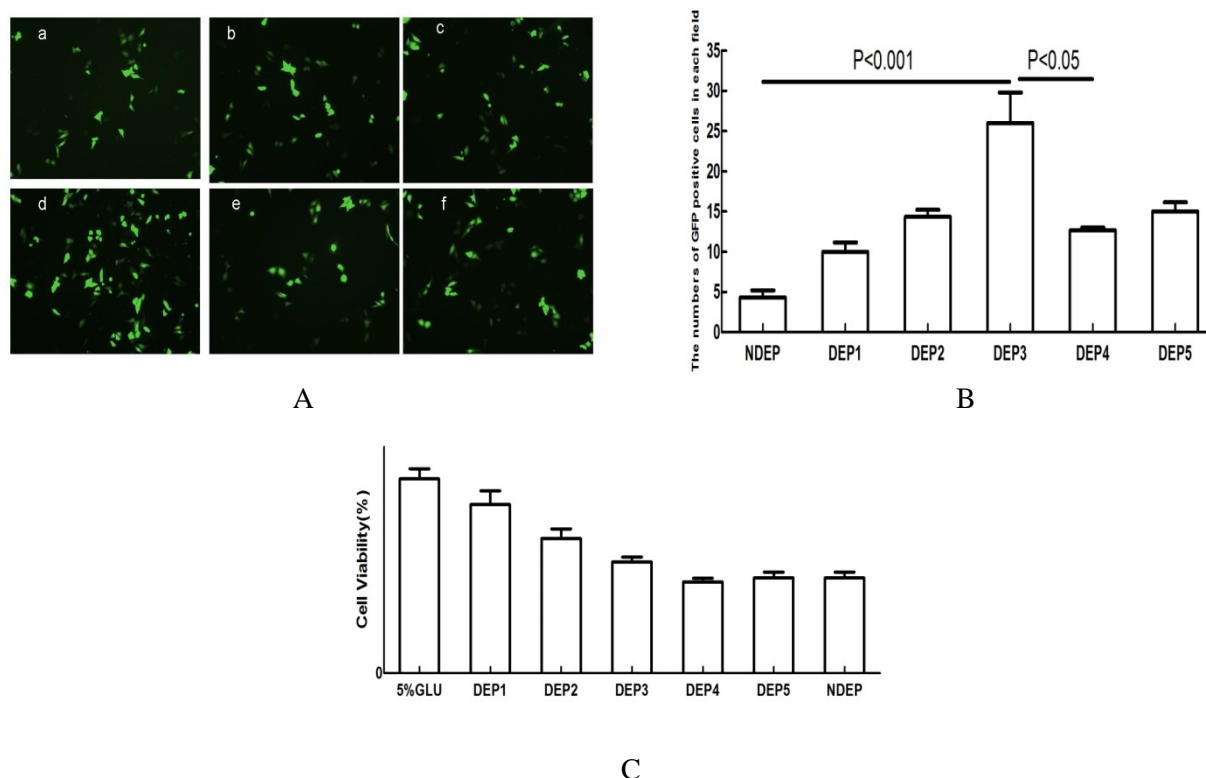


Figure 6: In Vitro experiments of hepG2 cells. (A) Representative photos of GFP positive cells in hepG2 cells under different DEP-separation conditions; (B) Statistical results of GFP positive cells; (C) Statistical results of cell viability determined by MTT assay.

3.3. *In vivo* studies on mouse based on DEP separated polyplexes

With the promising *in vitro* results proving the efficacy of the DEP separation, we devised *in vivo* studies on mice to determine their transfection efficiency. As shown in Fig 7, an *in vivo* imaging technique was used to determine the gene expression level of luciferase transduced by H1/pluciferase nanoparticles in living mice. The bioluminescence signal of luciferin was accumulated

in the upper abdominal section of the mouse via intraperitoneal injection of H1/pLuc nanoparticles, and the efficacy of bioluminescence signaling in mice treated with DEP-separated H1/pLuc nanoparticle was 10 times higher than those treated by non-DEP-separated H1/pLuc nanoparticles. These results suggest that DEP-separated nanoparticles have longer cycling time in mice and can avoid the elimination by the reticuloendothelial system. Accordingly, more nanoparticles can be absorbed by blood vessels in the abdominal cavity, and subsequently circulate to the liver via portal veins, resulting in enhanced transfection efficiency. These results are attributed to the reduced and controlled nanoparticle sizes and enhanced stability through on-chip fabrication and DEP treatment. We will determine the tumor-targeting ability of H1/pDNA nanoparticles in an HCC mouse model in the near future.

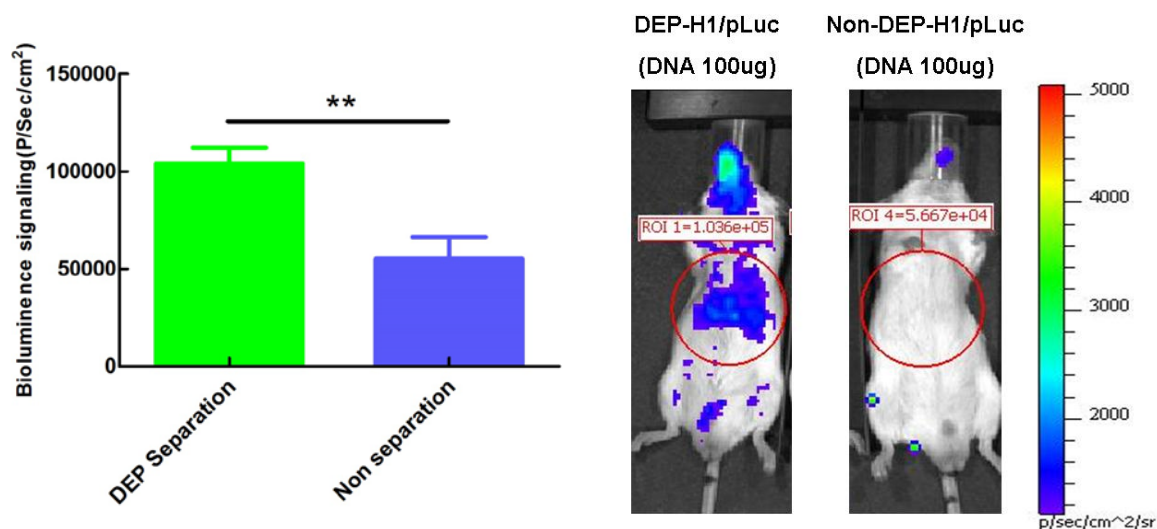


Figure 7: *In vivo* mouse experiments. The gene expression level of DEP-separated H1/pLuc nanoparticles (DNA, 100 μ g) was two times higher than that of non-separated H1/pLuc nanoparticles (DNA, 100 μ g) at 48 hours post intraperitoneal injection in BALB/C mice (n=3, student-t tests, **means: P < 0.05).

4. PUBLICATION AND AWARDS

[1] H. Yao, S.C. Chen, Z. Shen, Y.C. Huang, X. Zhu, X.M. Wang, W. Jiang, Z.F. Wang, X.W. Bian, E.A. Ling, H.F. Kung, and M.C. Lin, "Functional Characterization of a PEI-CyD-FA-coated Adenovirus as Delivery Vector for Gene Therapy," *Current Medicinal Chemistry*, Vol. 20, No. 20, pp. 2601-08, 2013.

[2] S.M. Yang, H. Yao, D. Zhang, W.J. Li, H.F. Kung, and S.C. Chen, "Droplet-based Dielectrophoresis Platform for Polymeric Nanoparticle Separation and Improved Gene Delivery Efficiency," submitted to *Microfluidics and Nanofluidics* in May 2014 (under review).

[3] H. Yao, Y. Tian, H. Zhang, S.M. Yang, H.F. Kung, and S.C. Chen, "DEP-Passed Nanoparticles Enhanced Transfection Efficiency and Reduced Cytotoxicity Both In Vivo and In Vitro", manuscript in preparation to be submitted to *Nature Communication*.

[4] S.M. Yang and S.C. Chen, "A Flow-free Droplet-based Device for High Throughput Polymorphic Crystallization", manuscript in preparation to be submitted to *Lab on a Chip*.

Multimedia Technologies Track

Research Reports In Multimedia Technologies

Continuing Projects

(2014 - 2016) * Managing and Analyzing Big Graph Data

Completed Projects

(2012) * Face Recognition Across Ages Through Binary Tree Learning

The following reports are enclosed in “Research Highlights” printed in June 2014

Completed Projects

- | | |
|--------|---|
| (2011) | <ul style="list-style-type: none">* Semantic Analysis for Image Resizing* Time Critical Applications over a Shared Network* Amplify-and-forward Schemes for Wireless Communications |
|--------|---|

The following reports are enclosed in “Research Highlights” printed in 2013

Completed Projects

- | | |
|--------|---|
| (2010) | <ul style="list-style-type: none">* FADE: Secure Cloud Storage with File Assured Deletion* Security and Detection Protocols for P2P-Live Streaming Systems |
| (2009) | <ul style="list-style-type: none">* An Opportunistic Approach to Capacity Enhancement in Wireless Multimedia Networks* Computer-Aided Second Language Learning through Speech-based Human-Computer Interaction |

The following reports are enclosed in “General Report and Research Highlights 2009-2011” printed in October 2011.

Completed Projects

- | | |
|--------|---|
| (2008) | <ul style="list-style-type: none">* Pattern Computation for Compression and Performance Garment |
| (2007) | <ul style="list-style-type: none">* Real-time Transmission of High Definition (HD) 3D Video and HD Audio in Gigabit-LAN* High Dynamic Range Image Compression and Display* Multimedia Content Distribution over Hybrid Satellite-Terrestrial Communication Networks |
| (2006) | <ul style="list-style-type: none">* Automatic Video Segmentation and Tracking for Real Time Multimedia Services* Information Retrieval from Mixed-Language Spoken Documents* Wireless Networks and Its Potential for Multimedia Applications |

The following reports are enclosed in “Research Highlights 2005-2007” printed in January 2008.

Completed Projects

- | | |
|--------|---|
| (2005) | <ul style="list-style-type: none">* Mobile Wireless Multimedia Communication* An Automatic Multi-layer Video Content Classification Framework* Automatic Multimedia Fission, Categorization and Fusion for Personalized Visualization in Multimedia Information Retrieval |
|--------|---|

MANAGING AND ANALYZING BIG GRAPH DATA

Principal Investigator: Professor James CHENG
Department of Computer Science and Engineering, CUHK

Research Team Members:

Shang Fanhua, Postdoctoral Fellow ⁽¹⁾

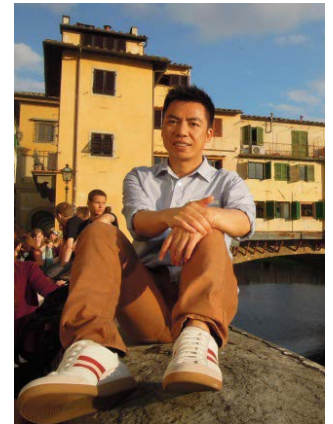
Lu Yi, M.Phil. Student ⁽¹⁾

Huang Yuzhen, Research Assistant (August 2014 to May 2015),

Ph.D. Student (starting from August 2015) ⁽¹⁾

⁽¹⁾ Dept. of Computer Science and Engineering, CUHK

Reporting Period: 1 July 2014 – 30 April 2015



ABSTRACT

This project aims to develop effective and scalable techniques for managing and analyzing big graph data, and to apply them for searching and analyzing multimedia data, especially data from online social networks (e.g., Facebook, Twitter, Google+, LinkedIn) and online shopping platforms (e.g., eBay, Amazon, Taobao). Graph is widely used to model online social network structures, as well as many complicated data types such as images and pictures, videos, and other interactivity contents, etc. We propose to study fundamental issues of big graph data research, including the study of elementary substructures and important properties of massive graphs, the modeling of these graphs for prediction and extrapolation studies, and the applications of big graph data in areas that may create impacts in both industry and academia. The key to big graph data management and analysis is to develop a robust distributed system that provides a general programming framework for implementing all kinds of distributed graph algorithms. Such a system is very useful to many companies for analyzing their data; in particular, we will work with our industrial collaborators such as Taobao to explore the application of our research to manage and analyze massive data collected from their online shopping platform.

1. OBJECTIVES AND SIGNIFICANCE

Objective: The project aims to develop an efficient and scalable system for managing and analyzing big graph data, in particular, massive network data from online social networks and online shopping platforms.

Significance:

1. Impact on academia: The proposed research is a timely study on one of the most important topics in the areas of database and data mining research. The success of this project can significantly advance research in the field of graph data management and graph mining. Techniques developed in this research will also benefit cross-disciplinary research including sociology, physics, biology, ecology, economics, finance, etc., because of the prevalence of graph and network data in their respective domains.
2. Impact on industry: The results obtained in this project will provide deeper insights about the patterns of real-world networks and the behaviors of their users including the communications and relationships among them. Such knowledge can be used by industry such as online social networking companies (e.g., Facebook, Twitter) and telecom operators (e.g., China Mobile, CSL) to better understand user behaviors and their interaction patterns, online auction and shopping platforms (e.g., eBay, Amazon, Taobao) to

analyze shopping trends, airlines and other transportation companies for better logistic and itinerary planning.

2. RESEARCH METHODOLOGY

The first step is to collect massive graphs from various domains including social networks, phone communication networks, web graphs, RDF graphs, and so on. We also use graphs to model multimedia data such as pictures and videos. The graphs in our current collection have up to billions of vertices and edges, which are the largest ones that are publicly available. Some of these graphs are associated with rich attribute information as well as temporal information, which pose significant new challenges as standard techniques cannot be applied.

The proposed research consists of the following four main aspects.

Study of graph structures. Graph structures can reveal many important properties of a graph. However, most graph structures are expensive to compute. For today's big graphs, it is infeasible to even load a graph based on a single-machine setting. Thus, distributed computing becomes necessary. One key challenge of applying distributed computing to solving graph problems is that distributed graph algorithms are often very complicated to design and implement, not to mention complicated issues in a distributed environment such as fault tolerance.

To address the above-mentioned issues, we first propose to develop a general-purpose distributed graph-computing system that provides a user-friendly programming framework for implementing distributed graph algorithms. The system is built on a share-nothing distributed cluster consisting of ordinary PCs or workstations. We adopt Pregel's vertex-centric programming model and users design their algorithms by "thinking like a vertex", while the system automatically handles all complicated issues of distributed computing such as job distribution and scheduling and fault tolerance.

With the general-purpose distributed graph-computing system, we can then develop efficient and scalable distributed algorithms for computing different types of graph structures. We categorize graph structures into two levels: the *micro level* and the *macro level*. At the micro level, small elementary substructures of a graph, such as paths, cycles, triangles, cliques, etc., will be studied. At the macro level, larger components of a graph, such as *k*-cores, *k*-trusses, dense subgraphs, clusters, etc., will be studied.

We will develop algorithms for storing, maintaining, searching, querying, and analyzing various types of micro-level and macro-level structures in massive graphs. In particular, we define a class of algorithms, to be developed based on our general-purpose distributed graph-computing system, with the following properties:

Let n be the total number of vertices in the input graph, $d(v)$ be the number of neighbors of a vertex v in the graph, and p be the number of computing nodes available.

1. *Linear space usage*: each vertex v uses $O(d(v))$ space of storage and each computing node keeps (n/p) vertices.
2. *Linear computation cost*: the amount of work done for processing each vertex v is $O(d(v))$.
3. *Linear communication cost*: the algorithm processes in rounds and at each round, the size of the messages sent/received by each vertex v is $O(d(v))$.
4. *At most logarithmic number of rounds*: the algorithm terminates after $O(\log n)$ rounds.

Properties 1-3 offer good load balancing and linear cost at each round of the parallel computation, while Property 4 controls the total running time. We have identified a long list of fundamental graph problems including *breadth-first search*, *spanning tree*, *Euler tour*, *pre/post-order traversals*, *connected components*, *bi-connected components*, *strongly connected components*, *single-source shortest paths*, *PageRank*, etc., for which there exists a parallel algorithm that satisfies the above defined four properties.

In addition, we will investigate the semantics of various graph structures both individually and collectively, and hence their functions on the evolution of a graph (e.g., a social network) and their correlation with various graph properties. In particular, we are interested in studying the temporal properties of paths in time-varying graphs, for which we define four types of paths, collectively we call them *minimum temporal paths*, as they give the minimum value for different measures:

1. *Earliest-arrival path*: a path that gives earliest arrival time starting from a source s to a target t .
2. *Latest-departure path*: a path that gives latest departure time starting from s in order to reach t by a given time.
3. *Fastest path*: the fastest path to go from s to t .
4. *Shortest path*: the shortest path from s to t .

Both efficient distributed algorithms and scalable indexes will be developed to compute these paths and answer temporal distance queries in real time.

Study of graph properties. We propose to conduct a comprehensive study on the correlation between a series of well-known graph properties such as *density*, *size*, *diameter*, *centrality*, *connectivity*, *sustainability*, etc., as well as to explore new graph properties that may give new insights into the understanding of graphs. We will develop efficient and scalable methods to compute and analyze these properties for big graphs, to categorize them, and to identify their strengths and limitations in various contexts.

Study of graph models. Based on the graph structures and properties, we propose to further explore more accurate models for real-world graphs. Existing models often capture only the more general patterns of a class of graphs while neglecting specific patterns in these graphs. We will study a wide spectrum of real-world graphs, analyze the properties and patterns possessed by these graphs, and propose more specific and accurate graph models. Efficient graph generators will also be developed to generate big graph data for running simulation and extrapolation studies, and for evaluating the performance and scalability of new graph algorithms.

Applications of graphs to multimedia data analysis. We propose to apply the results of our studies to graph structures, graph properties, and graph models to managing and analyzing massive multimedia data on the Web, especially in various online social networks (e.g., Facebook, Twitter, Google+, LinkedIn) and online auction and shopping platforms (e.g., eBay, Amazon, Taobao).

3. RESULTS ACHIEVED SO FAR

The key to this project is the development of a distributed graph-computing system. A new general-purpose, distributed graph-computing system, called Pregel+, has been developed to process different types of graphs and implement different graph algorithms. The results of the research have been accepted and published in Proceedings of the 24th International World Wide Web Conference (WWW 2015), which is the best conference in the area of Web data management.

Pregel+ extends Pregel by supporting two effective message reduction techniques: (1) vertex mirroring and (2) a request-respond paradigm. These techniques not only reduce the total number of messages exchanged through the network, but also bound the number of messages sent/received by any vertex, especially for processing power-law graphs and (relatively) dense graphs. Compared with existing Pregel-like systems, Pregel+ provides simpler programming interface and yet achieves higher computational efficiency.

In another parallel work, we conducted an extensive performance study to evaluate the performance of Pregel+ comparing with the state-of-the-art graph-computing systems. Our results show that Pregel+ is significantly more efficient and more scalable than the most popular system, Apache Giraph, CMU's GraphLab (which includes PowerGraph), and Stanford's GPS, with respect to various graph characteristics, algorithm categories, and various optimization techniques. The results of the research have been accepted and published in PVLDB 2015, which is the best conference in the area of database systems. The details of

the Pregel+ system are documented in Pregel+'s webpage: <http://www.cse.cuhk.edu.hk/pregelplus/>.

In a subsequent work, we also developed another general-purpose distributed graph-computing system, Blogel, which was published in PVLDB 2014. Blogel supports a block-centric programming model, which naturally addresses three adverse graph characteristics that lead to performance bottlenecks in existing graph computing systems such as Pregel: (1) skewed degree distribution, (2) (relatively) high density, and (3) large diameter. Blogel can be even from a few times to an order of magnitude faster than Pregel+. The details of the Blogel system are documented in Blogel's webpage: <http://www.cse.cuhk.edu.hk/blogel/>.

We have also studied the application of Pregel+ to develop graph algorithms in a systematic way. We first identified a set of desirable properties of an efficient Pregel algorithm, such as *linear space, communication and computation cost per iteration*, and *logarithmic number of iterations*. We defined such an algorithm as a *practical Pregel algorithm (PPA)*. We then proposed PPAs for computing *connected components (CCs)*, *biconnected components (BCCs)*, and *strongly connected components (SCCs)*. The PPAs for computing BCCs and SCCs use the PPAs of many fundamental graph problems as building blocks, which are of interest by themselves.

In addition, we also applied the principle of PPA to develop Pregel algorithms that satisfy strict performance guarantees. In particular, we developed a set of useful building blocks that are the PPAs of fundamental graph problems such as *breadth-first search*, *list ranking*, *spanning tree*, *Euler tour*, and *pre/post-order traversal*. As fundamental graph problems, their PPA solutions can also be applied to numerous other graph problems besides BCCs and SCCs considered in our work. Extensive experiments over large real graphs verified that our algorithms have good performance in shared-nothing parallel computing platforms. The results of the research have been accepted and published in PVLDB 2014, which is the best conference in the area of database systems.

4. PUBLICATION AND AWARDS

[1] Y. Liu, F. Shang, W. Fan, J. Cheng, and H. Cheng, "Generalized Higher-Order Orthogonal Iteration for Tensor Decomposition and Completion," *Proceedings of the 27th Annual Conference on Neural Information Processing Systems*, 2014.

[2] Y. Lu, J. Cheng, D. Yan, and H. Wu, "Large-Scale Distributed Graph Computing Systems: An Experimental Evaluation," *PVLDB*, Volume 8, Number 3, Pages 281-292, 2014.

[3] F. Shang, Y. Liu, J. Cheng, and H. Cheng, "Recovering Low-Rank and Sparse Matrices via Robust Bilateral Factorization," *Proceedings of the 14th IEEE International Conference on Data Mining*, 2014.

[4] F. Shang, Y. Liu, J. Cheng, and H. Cheng, "Robust Principal Component Analysis with Missing Data," *Proceedings of the 23rd ACM International Conference on Information and Knowledge Management*, 2014.

[5] D. Yan, J. Cheng, Y. Lu, and W. Ng, "Effective Techniques for Message Reduction and Load Balancing in Distributed Graph Computation," *Proceedings of the 24th International World Wide Web Conference*, 2015.

[6] D. Yan, J. Cheng, Y. Lu, and W. Ng, "Blogel: A Block-Centric Framework for Distributed Computation on Real-World Graphs," *PVLDB*, Volume 7, Number 14, Pages 1981-1992, 2014.

[7] D. Yan, J. Cheng, K. Xing, Y. Lu, W. Ng, and Y. Bu, "Pregel Algorithms for Graph Connectivity Problems with Performance Guarantees," *PVLDB*, Volume 7, Number 14, Pages 1821-1832, 2014.

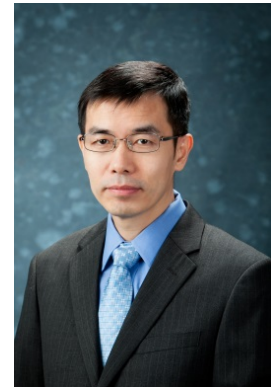
FACE RECOGNITION ACROSS AGES THROUGH BINARY TREE LEARNING

Principal Investigator: Professor : Xiaoou TANG⁽¹⁾
Department of Information Engineering, CUHK

Research Team Member:
Zhifeng LI, Associate Prof. ⁽²⁾

⁽¹⁾ Dept. of Information Engineering, CUHK
⁽²⁾ Shenzhen Institute of Advanced Technology

Project Start Date: 1 July 2012
Completion Date: 31 August 2014



ABSTRACT

Children faces change much faster over time than adult faces, making it much more difficult to process by traditional face recognition algorithms. Unfortunately, researches on age invariant face recognition have been sparse and even the state of the art results are poor on children face recognition across different ages. In this project, we focus on this fundamental research problem. We propose several new face recognition approaches that reduce age variation gap between two age groups. The algorithms developed here can be applied to a wide range of real world applications, including face verification using ID photos with age gaps, digital family photo-album management with photos ranging from childhood until adult years. More importantly, the algorithms developed in this project are critical in meeting a recent urgent need of finding missing children on the internet.

1. OBJECTIVES AND SIGNIFICANCE

In this project, we focus on a fundamental research topic: age invariant face recognition. It has been shown that the recognition tasks for children faces are much harder than for adult faces. This is mainly because children face profiles undergo larger variations over even a short period of time. The state of the art age invariant recognition algorithms achieve only 40% equal error rate on the FGNET database. To address these challenges, we propose several new face recognition algorithms to improve the performance of age invariant face recognition.

The algorithms developed here can be applied to a wide range of tasks. For example, for face verification using ID photo, usually the ID photo is taken long ago (national ID card in China is valid for 20 years), therefore age variation is a significant factor. For digital family photo-album management application, photos may range from childhood until adult years, thus require age invariant face recognition algorithms. This project is also inspired by a recent urgent need of finding missing children on the internet. To address this challenge, we try to apply face recognition technology. However, we found that children faces change rapidly over time and there are few existing algorithms that achieve satisfactory performance on age invariant face recognition for children faces. In this project, we propose several new age invariant face recognition algorithms based on new machine learning algorithms.

2. RESEARCH METHODOLOGY

Traditional cross modality recognition approaches can be categorized into two groups, cross modality modeling based methods and discriminative learning methods. The modeling methods try to reduce cross

modality variation at the preprocessing stage. The discriminative learning methods try to reduce modality gap after the face features are already extracted. Neither approaches work well so far. In this work, unlike the previous works for cross modality face recognition, we propose a new approach called mutual component analysis (MCA) [2] to cross-modality face recognition, which are quite helpful to age invariant face recognition. In the MCA approach, a generative model is first proposed to model the process of generating face images in different modalities, and then an Expectation Maximization (EM) algorithm is designed to iteratively learn the model parameters. The learned generative model is able to infer the mutual components that are associated with the person's identity, thus enabling fast and effective matching for cross-modality face recognition. Our new approach demonstrated the state-of-the-art performance across several public-domain cross-modality face databases.

We also propose two new approaches to directly address age invariant face recognition. In [1], in order to overcome the computational cost and the risk of over-fitting in dense feature extraction, we propose a new approach to dense feature extraction for face recognition, which consists of two steps: first, an encoding scheme is devised that compresses high-dimensional dense features into a compact representation by maximizing the intra-user correlation; and second, we develop an adaptive feature matching algorithm for effective classification. In [3], a new feature descriptor called local patterns selection (LPS) is proposed to improve the performance of age invariant face recognition. The LPS approach is a two-level model. At the first level, it greedily selects low-level discriminant patterns in a way such that intra-user dissimilarity is minimized. At the second level, higher-level visual information is further refined based on the output from the first level. All of these methods have obtained the state-of-the-art results on the largest public-domain face aging database (MORPH Album 2).

In addition, note that age estimation plays a key role in assisting age invariant face recognition. We also conducted extensive research in age estimation problem. In [4], a new feature representation model called age informative embeddings is proposed for age estimation. Specifically, given age-unaware face features X (e.g. dense SIFT or local binary patterns), we convert these features to lower dimensional embeddings via linear projection $Y=WX$, where Y contains enhanced age related information. The embedding matrix W can be learned efficiently via eigen decomposition, and the global optimality is guaranteed. Our new approach obtained the state-of-the-art age estimation performance on three public-domain face aging datasets: FG-NET, MORPH Album 1 and Album 2.

3. RESULTS ACHIEVED SO FAR

We have proposed several new approaches to cross-modality face recognition; age invariant face recognition; and age estimation. Our new approaches obtained the state-of-the-art performance on several public-domain databases. Based on these results, we have already one paper accepted by the top journal (TIP) in this field, and three papers submitted to the top conference and the top journals (ICCV, TIP, ACM TIST) in this field.

4. PUBLICATION AND AWARDS

[1] Zhifeng Li, Dihong Gong, Xuelong Li, and Dacheng Tao, "Learning Compact Feature Descriptor and Adaptive Matching Framework for Face Recognition," Accepted by *IEEE Transactions on Image Processing* (TIP), 2015.

[2] Zhifeng Li, Dihong Gong, Qiang Li, Dacheng Tao, and Xuelong Li, "Mutual Component Analysis for Heterogeneous Face Recognition," submitted to *ACM Transactions on Intelligent Systems and Technology* (under the second round review).

[3] Zhifeng Li, Dihong Gong, Xuelong Li, and Dacheng Tao, "Aging Face Recognition: A Hierarchical Learning Model Based on Local Patterns Selection," submitted to *IEEE Transactions on Image Processing* (under the first round review).

[4] Dihong Gong, Zhifeng Li, and Dacheng Tao, "Learning Age Informative Embeddings for Automatic Age Estimation", submitted to *ICCV 2015* (under review).

Shun Hing Distinguished Lecture Series

To achieve the Institute's mission to promote appreciation of engineering in society through education programs, the Institute has organized a Shun Hing Distinguished Lecture Series. So far, **thirty-nine** distinguished lectures have been presented by renowned scholars. These lectures all were very well received and we will continue to line up and invite outstanding researchers to visit CUHK and to deliver distinguished lectures for the Institute. Here to show the two distinguished lectures between 2014 and June 2015.

Energy Harvesting Communications with Limited Feedback

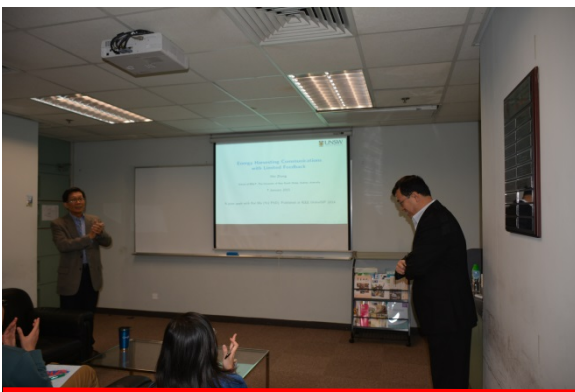
by Professor Wei ZHANG

*Associate Professor, IEEE Fellow
School of Electrical Engineering & Telecommunications
The University of New South Wales, Sydney, Australia*

Date: 7 January 2015 (Wednesday)

Abstracts

In energy harvesting wireless communications, full channel state information at transmitter is generally needed to determine transmission power policy. In this work, we propose online discrete rate and power adaption policies for an energy harvesting communication over Rayleigh fading channels. The receiver periodically sends 1-bit feedback by comparing the channel power gain with a predetermined threshold. The transmitter correspondingly adjusts QAM level and transmission power based on the 1-bit feedback and the available battery energy. To determine the optimal channel threshold, adaptive M-QAM level and corresponding power allocation, we formulate a constrained optimization problem to maximize the throughput within a finite horizon. We show that this problem follows a Markov decision process and can be solved via backward induction method. We further propose an efficient but suboptimal discrete rate and power policy that uses the best effort M-QAM adaption and the channel threshold determined by maximizing the average rate over channel fading and EH processes. Our results show that the performance loss is negligible for the simple M-QAM adaption of the suboptimal policy that is attributed to the optimal choice of channel threshold.



Reaching Asymptotically Efficient Localization Performance Using Squared Measurements in Sensor Networks

by Professor Dominic K. C. HO

*Department of Electrical and Computer Engineering
University of Missouri
USA*

Date: 19 August 2014 (Tuesday)

Abstracts

Localization of an emitting source is a challenging non-linear estimation problem. Exact explicit solution exists by squaring the TOA or TDOA measurements when solving for the location. The squaring operation changes the statistical properties of the measurements and the resulting solution does not reach the CRLB performance and could be quite inaccurate. This talk develops a modified cost function of the squared measurements whose minimum will achieve the CRLB accuracy for Gaussian noise asymptotically. We validate our claim through theoretical analysis and simulation studies. The modified cost function maintains the benefit in which exact solution can be derived. Performance of the developed technique for successive localization of sensor nodes and for acoustic source localization using a network of smart phones will be illustrated.



信興高等工程研究所
Shun Hing Institute of Advanced Engineering

Shun Hing Institute of Advanced Engineering (SHIAE)

The Chinese University of Hong Kong
Shatin, N.T., Hong Kong

Office : Room 702, William M.W. Mong Engineering Building
Tel : (852) 3943 4351
Fax : (852) 3943 4354
Email : info@shiae.cuhk.edu.hk
Website : <http://www.shiae.cuhk.edu.hk>



Shun Hing Institute of Advanced Engineering

